RADC-TDR-64-353
Final Report

RESEARCH IN MATHEMATICAL TARGETING

THE PRACTICAL AND RIGOROUS ADJUSTMENT OF LARGE PHOTOGRAMMETRIC NETS

TECHNICAL DOCUMENTARY REPORT NO. RADC-TDR-64-353

October 1964

Reconnaissance Data Extraction Branch

Rome Air Development Center
Research and Technology Division
Air Force Systems Command
Griffiss Air Force Base, New York

Project No. 5569 , Task No. 556902

(Prepared under Contract No. AF 30(602)-3007 by D. Brown Associates, Inc., P. O. Box 1197, Eau Gallie, Florida, under sub-contractor to Geo Space Corporation, Melbourne, Florida. Authors: Duane C. Brown, Ronald G. Davis and Frederick C. Johnson.)

15550

BLANK PAGES
IN THIS
DOCUMENT
WERE NOT
FILMED

ABSTRACT

The problem of the rigorous simultaneous adjustment of large photogrammetric blocks is reviewed and extensions to an earlier theory are developed. Various matrix iterative approaches to the solution of the very large systems of normal equations characteristic of sizeable photogrammetric nets are investigated. The Method of Block Successive Over Relaxation is found to yield a practical and most satisfactory solution to this problem. Results of an extensive series of numerical simulations are reported. The successful application of the approach to a 23-photo strip of actual photography provides final confirmation of the validity and effectiveness of the solution.

PUBLICATION REVIEW

This report has been reviewed and is approved. For further technical information on this project, contact J. Diello, RADC (EMIRB) x4203.

Approved: Joseph S. Lemone
for ANTHONY DIPENTIMA, Chief
Recon Data Extraction Branch

Approved: Howard Davis
ROBERT J. QUINN, Jr
Colonel, USAF
Chief, Intel & Info Processing Div

FOR THE COMMANDER: Irving J. Gabelman
IRVING J. GABELMAN
Chief, Advanced Studies Group

AIR FORCE, GAFB, N.Y., [illegible]

TABLE OF CONTENTS

Table of Contents (Continued)

PREFACE

The objective of this study is to develop a computationally feasible procedure for the solution of very large systems of normal equations generated in the process of simultaneous adjustment of all observations arising from a large photogrammetric net. Although the theory for forming the normal equations in a systematic and practical manner was developed over six years ago by one of the writers (Brown, 1958 a), it has widely been held that the sheer size of the normal equations for long strips or large blocks of photography would restrict the application of the theory in its full generality to photogrammetric nets of relatively modest dimensions. Consequently, efforts at applying the theory have concentrated largely on piecewise adjustments according to various schemes ranging from cantilever extension using three or more photos per step to extension through adjustment of small blocks. All such solutions are, of course, compromises dictated solely by computational considerations. Few will argue the desirability of simultaneous adjustment of sizeable photogrammetric nets, but many will argue its practicability. We therefore take considerable pride in announcing our success in developing an altogether practical, yet uncompromisingly rigorous solution to the problem of adjusting large photogrammetric nets. Surprisingly, there is evidence that the efficiency of the solution increases with increasing dimensions of the photogrammetric net and is even greater with blocks than with strips. The solution of the normal equations is accomplished through the application of techniques of matrix iterative analysis developed over the past decade by investigators concerned primarily with the solution of large systems of linear equations arising from the numerical solution of systems partial differential equations. A comprehensive treatment of matrix iterative techniques is provided by a recently published book (Varga, 1962).

Our study has been divided into two major parts. Section 1 provides the overall theoretical development essential to the solution. It also incorporates a number of refinements (some previously published, others not) of the original photogrammetric theory

(Brown, 1958 a). In particular, it fully develops the concept of the 'ellipsoidal control point' (previously introduced in Brown, 1959, as a special case of the awkwardly phrased concept of 'relaxation of quasi-observational variances'). The general adjustment is extended to accommodate observations provided by auxiliary external sensors (inertial systems, aircraft tracking systems, etc.). Provisions are made for the calibration of such sensors as an integral part of the overall adjustment.

Section 2 outlines the numerical procedures employed in implementing the solution and presents detailed results of an extensive program of numerical simulation designed to evaluate the effectiveness of the general approach developed in Section 1. Several specific approaches within the framework of the general approach are investigated to determine the particular variant leading to the most effective results.

SECTION 1

THEORETICAL DEVELOPMENT

By
Duane Brown

1.01 INTRODUCTION

In a previous paper (Brown, 1958 a), the writer presented a rigorous least squares solution effecting the simultaneous adjustment of the entire set of original plate measurement arising from a completely general photogrammetric net. It was shown that the development of the general normal equations was an entirely straightforward procedure presenting no difficulties even with a digital computer of relatively small capacity. A direct solution, however, was considered to be impractical for large photogrammetric nets because of the prohibitive dimensions of the normal equations. A practical means was developed to collapse the system of general normal equations to a more tractible system of reduced normal equations whose dimensions were independent of the number of unknown relative control points and were dependent only on the total number of unknown elements of orientation. This version of the solution found immediate application in space geodesy (Brown, 1958 b, 1959, 1960 a) wherein powerful stellar control could be exploited to reduce the number of unknown elements of orientation to three per exposure station (the X, Y, Z of each station). Even rather large geodetic nets (up to 100 stations) were considered to be amenable to this approach for in practice only a handful of stations in the over-all network would observe a given group of flashes thereby making possible the piecewise formation of the partial normal equations generated by relatively small local configurations; the formation of the final system of normal equations would thus reduce to a simple matter of appropriate dissection and subsequent summing of the partial normal equations of individual configurations. In such geodetic applications, the solution of large systems of equations would normally have to be faced only at infrequent intervals and hence would warrant an effort which would otherwise be considered prohibitive.

In Brown (1958 b) the writer outlined an extension of the general adjustment to account for errors in presurveyed locations of exposure stations. This extension was further developed in the Appendix to a later report (Brown, 1959). Here, the solution was modified to cover the case in which any of the elements of orientation and any of the coordinates of control are considered to be measured quantities subject to adjustment. In the original solution, these quantities were considered to be either perfectly known or to be wholly unknown and the entire adjustment was placed on the measured plate coordinates.

In an unpublished, privately circulated paper (Brown, 1960 b) which is referred to by Case (1961), the writer further extended the basic solution to incorporate orbital constraints applicable to a satellite-borne camera. Here it was shown that the entire vector of coordinates of exposure stations for a given orbital pass could be replaced by a 6 x 1 vector of osculating Keplerian elements, these in turn being determined as part of the over-all photogrammetric reduction.

The first unclassified application of the extended form of the writer's solution to aerotriangulation is probably that of Dowdy and McClure (1962). Here, a computer program for the simultaneous adjustment of as many as 12 photographs was developed for the IBM 709 Computer. For long photogrammetric strips, the program employed what might be called a long base cantilever in which six, seven, or eight successive photos were carried in each adjustment. Dowdy and McClure applied the program to the adjustment of 11 sub-blocks of a 50 photo block of actual photography. The solution allowed not only for adjustment of plate coordinates, but also for adjustment of ground control. Although the standard deviations assigned to the ground control ranged typically from 20 to 30 ft., the published adjustment of the ground control turned out to be small fractions of a foot. Dowdy and McClure expressed concern over such unrealistically small corrections but were unable to offer a specific explanation for the result. The present writer, in seeking an explanation for this untoward result, carefully studied the flow charts and program listings published by Dowdy and McClure. Both were found to be in good order and displayed a sound understanding of the method. The difficulty was finally traced to an easily made

blunder in weighting wherein two different unit variances were implicitly carried in the same adjustment; the one for the ground control and the other for the plate measurements. More specifically, the weights assigned to the ground control points were taken as the straight reciprocals of their variances thereby automatically fixing unit variance at unity. Accordingly, the weights of the plate coordinates should also have been taken as the straight reciprocals of their variances. Actually, they were not, for all plate coordinates were assigned unit weight. If onewere to regard the standard deviation of the typical plate coordinate as being $\sigma = 0.025$ mm, the weight of the plate coordinate would then properly become $1/(.025)^2 = 1600$, rather than unity. Accordingly, in Dowdy and McClure's study, all of the plate coordinates were grossly underweighted (by a factor on the order of 1000 to 2000) or, equivalently, all of the ground coordinates were grossly overweighted (again, by a factor on the order of 1000 to 2000). Hence, essentially all of the adjustment was placed on the plate coordinates and practically none was placed on the ground coordinates. For all practical purposes, then, the ground control was actually treated as if it were perfectly known. Within this context, Dowdy and McClure's numerical results may be viewed as being valid.

Dowdy and McClure indicate the IBM 709 running time of the program for a twelve photo adjustment to be slightly more than one half hour per iteration. Inasmuch as computations required for the formation and for the solution of the reduced normal equations increase as the square and cube, respectively, of the number of photos, it follows that between two and four hours would be required per iteration for a twenty four photo adjustment and that between eight and thirty two hours would be required per iteration for a forty eight photo adjustment (this assumes that sufficient memory were available to keep all computations in core). Normally two to three iterative cycles would be required for adequate convergence, thus doubling to tripling the above figures. Small wonder, then, that in recent years enthusiasm has generally waned for the idea of rigorous and simultaneous adjustment of large blocks of photos. Instead, efforts have been directed mostly toward development of compromise solutions such as extension by analytical pairs, triplets or sub-blocks with subsequent adjustment of the model to absolute control (e.g., Mikhail, 1962, 1963; El-Assal, 1963; Schut, 1964; Harris, Tewinkel, Whitten, 1962) or adjustment

of strips or blocks of modest dimensions, typically of 25 photos or less (e.g., Dowdy and McClure, op. cit.; Matos, 1963). A broad review of the development of analytical techniques is given by Doyle (1964).

From the foregoing, it appears that the general impetus towards the implementation of the uncompromisingly rigorous adjustment of large photogrammetric blocks has in great measure died out in favor of suboptimal but more easily implemented analytical approaches. Nonetheless, the desirability of simultaneous adjustment is conceded by virtually all investigators. Because of the general abandonment of the ideal of simultaneous adjustment, o Pandora's box of alternative approaches (most being minor variations of one another) seems to have been opened leading, in the writer's view, to the generally chaotic present state of analytical photogrammetry.

As has already been indicated, the stumbling block to the implementation of rigorous block adjustment has been the solution of the very large systems of normal equations generoted by blocks of even fairly modest dimension. As we indicated, the formation of the normal equations themselves is a relatively minor problem. In all approaches reported to date the solution of the normal equations has been effected by one or another of the numerous variants of Gaussian elimination. This has set a practical limit (on the order of 25 photos) to the size of the photogrammetric net which can be handled, for computational difficulties with Gaussian elimination increase severely with increasing numbers of unknowns.

In 1958, the writer experimented briefly with the Gauss-Seidel iterative technique for the solution of linear equations only to abandon it as utterly impractical upon finding its rate of convergence to be insufferably slow. However, in 1962, the writer's interest in the possibilities of the Gauss-Seidel approach was rekindled upon reading in Faadeva (1959)of an accelerating process developed by Luisternik (1947). It was further aroused upon the writer's discovery that,by means of a scheme of ordering the unknowns of the general normol equations generated by a 'uniform block' (to be defined later), it was possible to obtain a coefficient matrix having highly diagonal characteristics. Indeed, the writer found that with a 'uniform block' it was possible to develop an ordering which

would confine all nonzero elements of the coefficient matrix to a comparatively narrow band about the principal diagonal, the width of the band being completely independent of the photadimensions of the block. Such strong diagonality, it seemed to the writer, might well enhance the prospects of acceptably rapid convergence of an iterative process of solution. In further conjectural development of the renewed possibilities of an iterative approach, the writer conceived of a process for the systematic formation of the normal equations in which an algorithmic scheme of indexing could be employed to bypass the computation of all zero elements of the normal equations, thereby leading to the direct formation of an equivalent 'collapsed' system of far smaller dimensions. This concept of 'collapsed normal equations' further enlarged the possibility of the ultimate development of a practical approach to the problem of the rigorous adjustment of large photogrammetric nets. In December 1962, these ideas were expressed formally in a technical proposal to Rome Air Development Center, resulting subsequently in the award of the present contract to investigate their practicability.

As we shall see, the applicability of the accelerated Gauss-Seidel process turned out to be decidedly marginal. On the other hand, the application of a more powerful iterative technique (that of successive overrelaxation) proved to be successful beyond all expectation. As a result, the rigorous adjustment of blocks of large dimensions may now be said to be entirely practical even though it may entail the simultaneous solution of several thousand equations. Except for the collapsing algorithm, the development of the normal equations for our present solution remains largely the same as in the writer's original papers of 1958 and 1959. However, a number of refinements have been added, foremost of which is a generalized treatment of auxiliary observations which permits the introduction of any desired statistical or functional constraints on the parameters of the adjustment. Before we take up the central problem of the solution of the normal equations, we shall incorporate these refinements into the derivation of the normal equations. Here it is appropriate to note that the extension of the adjustment outlined in Brown (1959) was given without proof, an omission which has led to a number of private requests for clarification. As we shall see in the development to follow, the proof of the extension

is so embarrassingly simple as to be elusive. This is why it was not discovered until shortly after the publication of the original solution. In brief, it involves nothing more than recognition of the fact that the adjusted values of any observations may be carried in the adjustment as unknown parameters.

1.02 THE ELLIPSOIDAL CONTROL POINT

In the formulation of the general photogrammetric adjustment, we shall admit the possibility of correlated observations. Properly exploited, the admissibility of correlated observations provides the investigator with a convenient and flexible means for rigorously implementing any manner of variation in the basic measuring processes without requiring the least alteration of the general adjustment itself. We shall utilize this tool at the very outset to introduce a concept fundamental to our approach, namely that of the 'ellipsoidal control point.' According to this concept, the metric properties of a control point X_j, Y_j, Z_j are fully characterized by its covariance matrix $\ddot{\Lambda}_j$, the elements of which specify, in effect, the relative statistical magnitudes and interactions of the errors in the coordinates. The term ellipsoidal control point stems from the consideration that the following quadratic form

$$(1) \quad q = \Delta_j \ddot{\Lambda}_j^{-1} \Delta_j^T = (X_j - X_j^0 \quad Y_j - Y_j^0 \quad Z_j - Z_j^0) \begin{bmatrix} \sigma_{x_j}^2 & \sigma_{x_j y_j} & \sigma_{x_j z_j} \\ \sigma_{x_j y_j} & \sigma_{y_j}^2 & \sigma_{y_j z_j} \\ \sigma_{x_j z_j} & \sigma_{x_j z_j} & \sigma_{z_j}^2 \end{bmatrix}^{-1} \begin{bmatrix} X_j - X_j^0 \\ Y_j - Y_j^0 \\ Z_j - Z_j^0 \end{bmatrix}$$

defines an ellipsoid centered at the observed point X_j^0, Y_j^0, Z_j^0. By incorporating this quadratic form into the general quadratic form of the adjustment, one

constrains the adjusted rays from the various cameras to a given control point to intersect in probability within the space allowed by the 'error' ellipsoid associated with the point. The concept of the ellipsoidal control point erases the usual distinction between different types of control points. The difference between an absolute control point at the one end of the spectrum and a relative control point at the other becomes merely one of degree. In the case of an absolute control point, the dimensions of the error ellipsoid for a moderate level of probability would be quite small (perhaps on the order of millimeters), whereas, in the case of a relative control point, the dimensions would be comparatively large (perhaps on the order of hundreds of meters). Partially absolute control points are characterized by either extremely flattened (pancake shaped) error ellipsoids for the case when only one of the three coordinates is known accurately, or else by extremely elongated (cigar shaped) error ellipsoids for the case when two of the three coordinates are known accurately.

The ellipsoidal control point provides a particularly convenient means of introducing either absolute or partial control expressed originally in terms of geographic coordinates (ϕ_j , λ_j , h_j) rather than Cartesian coordinates (X_j, Y_j, Z_j). If $\phi_j^0, \lambda_j^0, h_j^0$ denote the 'observed' geographic coordinates, the corresponding Cartesian coordinates X_j^0, Y_j^0, Z_j^0, may be expressed functionally as

$$
\begin{aligned}
X_j^0 &= X_j(\phi_j^0, \lambda_j^0, h_j^0) \ , \\
Y_j^0 &= Y_j(\phi_j^0, \lambda_j^0, h_j^0) \ , \qquad (2) \\
Z_j^0 &= Z_j(\phi_j^0, \lambda_j^0, h_j^0) \ .
\end{aligned}
$$

If the covariance matrix of the geographic coordinates is

$$(3) \qquad T_j = \begin{bmatrix} \sigma^2_{\phi_j} & \sigma_{\phi_j\lambda_j} & \sigma_{\phi_j h_j} \\ \sigma_{\phi_j\lambda_j} & \sigma^2_{\lambda_j} & \sigma_{\lambda_j h_j} \\ \sigma_{\phi_j h_j} & \sigma_{\lambda_j h_j} & \sigma^2_{h_j} \end{bmatrix}$$

that of the derived Cartesian coordinates becomes

$$(4) \qquad \ddot{\Lambda}_j = U_j T_j U_j^T$$

wherein

$$(5) \qquad U_j = \begin{bmatrix} \frac{\partial X^0_j}{\partial \phi^0_j} & \frac{\partial X^0_j}{\partial \lambda^0_j} & \frac{\partial X^0_j}{\partial h^0_j} \\ \frac{\partial Y^0_j}{\partial \phi^0_j} & \frac{\partial Y^0_j}{\partial \lambda^0_j} & \frac{\partial Y^0_j}{\partial h^0_j} \\ \frac{\partial Z^0_j}{\partial \phi^0_j} & \frac{\partial Z^0_j}{\partial \lambda^0_j} & \frac{\partial Z^0_j}{\partial h^0_j} \end{bmatrix}$$

The covariance matrix $\ddot{\Lambda}_j$ contains all of the information pertinent to the error structure of the geographic coordinates. In the event that only one of the three geographic coordinates were known accurately, one could proceed by assigning comfortably large variances to available approximations for the two poorly known coordinates and a realistic variance to the known coordinate. The transformed covariance matrix $\ddot{\Lambda}_j$ would then contain the information that one of the three geographic coordinates is known with worthwhile accuracy while the other two

are known only nominally. The nonzero off-diagonal elements of $\ddot{\Lambda}_j$ are particularly vital to the correctness of the solution for they define the orientation of the error ellipsoid.

By applying the concept of the ellipsoidal control point to geographic coordinates, one circumvents the awkward conventional alternative of forcing rays to intersect with mathematical precision on quadric surfaces, cones and planes. Upon reflection, one begins to appreciate that in the real world absolutely perfect control simply does not exist; all control is subject to error of varying degree. Moreover, there is really no essential distinction between an approximation and an observation, for one can arrive at approximations only through a process of observation, however crude and however indirect. Thus, approximations may be viewed as observations having large and uncertain variances. We shall adopt this view throughout the development of the general photogrammetric adjustment.

1.03 OBSERVATIONAL EQUATIONS GENERATED BY THE PROJECTIVE RELATIONS

As in Brown (1958) we consider the photogrammetric net to involve a total of m exposure stations and a total of n control points. We shall employ the subscript i ($i = 1, 2, \ldots, m$) to denote the i^{th} exposure station and the subscript j ($j = 1, 2, \ldots, n$) to denote the j^{th} control point. When double subscripts are used, the first will refer to the station and the second to the control point. No restrictions are placed on camera orientations or on the nature and distribution of control. We shall proceed at the outset as if every control point were recorded at every station. Later this assumption will be dropped.

The projective equations arising from the j^{th} control point and i^{th} station are shown in Brown (1958a) to be of the form

$$x_{ij} = x_{p_i} + c_i \frac{A_i\lambda_{ij} + B_i\mu_{ij} + C_i\nu_{ij}}{D_i\lambda_{ij} + E_i\mu_{ij} + F_i\nu_{ij}} ,$$

(6)

$$y_{ij} = y_{p_i} + c_i \frac{A'_i\lambda_{ij} + B'_i\mu_{ij} + C'_i\nu_{ij}}{D_i\lambda_{ij} + E_i\mu_{ij} + F_i\nu_{ij}} ,$$

where

(7) x_{ij}, y_{ij} = plate coordinates of j^{th} point on i^{th} photo,

(8) x_{p_i}, y_{p_i} = plate coordinates of principal point of i^{th} photo,

(9) c_i = principal distance of i^{th} photo,

(10) $\begin{bmatrix} A_i & B_i & C_i \\ A'_i & B'_i & C'_i \\ D_i & E_i & F_i \end{bmatrix}$ = orientation matrix of i^{th} photo,

(11) $\begin{bmatrix} \lambda_{ij} \\ \mu_{ij} \\ \nu_{ij} \end{bmatrix} = \frac{1}{R_{ij}} \begin{bmatrix} X_j - X_i^c \\ Y_j - Y_i^c \\ Z_j - Z_i^c \end{bmatrix}$ = direction cosines of ray joining i^{th} exposure station at X_i^c, Y_i^c, Z_i^c and j^{th} control point at X_j, Y_j, Z_j $(R_{ij} = [(X_j - X_i^c)^2 + (Y_j - Y_i^c)^2 + (Z_j - Z_i^c)^2]^{\frac{1}{2}})$.

The elements of the orientation matrix are functions of the three angular elements of orientation α_i, ω_i, κ_i.

All steps leading to the formation and collection of the entire set of linearized observational equations arising from the projective relations will proceed precisely as in our earlier solution. Thus, we let x^0_{ij}, y^0_{ij} denote measured plate coordinates and set

$$
\begin{aligned}
x_{ij} &= x^0_{ij} + v_{x_{ij}} \\
y_{ij} &= y^0_{ij} + v_{y_{ij}} \qquad (i = 1,2,\ldots,m;\ j = 1,2,\ldots,n)
\end{aligned} \tag{12}
$$

where the v's are observational residuals. Similarly, we set

$$
\begin{aligned}
\alpha_i &= \alpha_i^{00} + \delta\alpha_i & x_{p_i} &= x_{p_i}^{00} + \delta x_{p_i} & X_i^c &= (X_i^c)^{00} + \delta X_i^c \\
\omega_i &= \omega_i^{00} + \delta\omega_i & y_{p_i} &= y_{p_i}^{00} + \delta y_{p_i} & Y_i^c &= (Y_i^c)^{00} + \delta Y_i^c \\
\kappa_i &= \kappa_i^{00} + \delta\kappa_i & c_i &= c_i^{00} + \delta c_i & Z_i^c &= (Z_i^c)^{00} + \delta Z_i^c \qquad (i = 1,2,\ldots,m)
\end{aligned} \tag{13}
$$

in which arbitrary approximations are signified by the superscript '00' and the δ's are the appropriate corrections to the approximations. We likewise assume approximations are available for the coordinates of the j^{th} control point and set

$$
\begin{aligned}
X_j &= X_j^{00} + \delta X_j \ , \\
Y_j &= Y_j^{00} + \delta Y_j \ , \\
Z_j &= Z_j^{00} + \delta Z_j \ .
\end{aligned} \tag{14}
$$

The substitution of equations (12), (13), (14) into (6) and subsequent linearization by Taylor's series leads to the observational equations

$$(15) \qquad v_{ij} + \dot{B}_{ij}\,\dot{\delta}_i + \ddot{B}_{ij}\,\ddot{\delta}_j = \epsilon_{ij} \qquad (i = 1,2,\ldots,m;\ j = 1,2,\ldots,n)$$

in which

$$(16) \qquad \underset{(2,1)}{v_{ij}} = \begin{bmatrix} v_{x_{ij}} \\ v_{y_{ij}} \end{bmatrix}, \quad \underset{(2,9)}{\dot{B}_{ij}} = \begin{bmatrix} \frac{\partial x_{ij}}{\partial \alpha_i} & \frac{\partial x_{ij}}{\partial \omega_i} & \cdots \frac{\partial x_{ij}}{\partial Z_i^c} \\ \frac{\partial y_{ij}}{\partial \alpha_i} & \frac{\partial y_{ij}}{\partial \omega_i} & \cdots \frac{\partial y_{ij}}{\partial Z_i^c} \end{bmatrix}, \quad \underset{(9,1)}{\dot{\delta}_i} = \begin{bmatrix} \delta\alpha_i \\ \delta\omega_i \\ \delta\kappa_i \\ \vdots \\ \delta Z_i^c \end{bmatrix},$$

$$(17) \qquad \underset{(2,3)}{\ddot{B}_{ij}} = \begin{bmatrix} \frac{\partial x_{ij}}{\partial X_j} & \frac{\partial x_{ij}}{\partial Y_j} & \frac{\partial x_{ij}}{\partial Z_j} \\ \frac{\partial y_{ij}}{\partial X_j} & \frac{\partial y_{ij}}{\partial Y_j} & \frac{\partial y_{ij}}{\partial Z_j} \end{bmatrix}, \quad \underset{(3,1)}{\ddot{\delta}_j} = \begin{bmatrix} \delta X_j \\ \delta Y_j \\ \delta Z_j \end{bmatrix}, \quad \underset{(2,1)}{\epsilon_j} = \begin{bmatrix} x_{ij}^0 - x_{ij}^{00} \\ y_{ij}^0 - y_{ij}^{00} \end{bmatrix}.$$

The partial derivatives in $\dot{B}_{ij}$ and $\ddot{B}_{ij}$ are evaluated at the approximations α_i^{00}, ω_i^{00}, etc. The quantities x_{ij}^{00}, y_{ij}^{00} in ϵ_{ij} denote the values resulting when the right hand sides of equations (6) are evaluated using the approximations. Detailed expressions for the partial derivatives are given in our earlier paper (Brown 1958) and need not be repeated here.

At this point a comment on notation is appropriate. Throughout the paper we shall continue the practice (already begun) of affixing the superscript '0' to quantities which are considered to be observed and the superscript '00' to quantities which are considered to be approximations or the result of approximations (as, for example, in the quantities x_{ij}^{00}, y_{ij}^{00} which denote the plate coordinates computed from approximate elements of orientation and approximate coordinates of control).

We shall denote the covariance matrix of the plate coordinates x^0_{ij}, y^0_{ij} by

$$(18) \qquad \Lambda_{ij} = \begin{bmatrix} \sigma^2_{x_{ij}} & \sigma_{x_{ij}y_{ij}} \\ \sigma_{x_{ij}y_{ij}} & \sigma^2_{y_{ij}} \end{bmatrix}$$

and shall define the weight matrix of x^0_{ij}, y^0_{ij} to be

$$(19) \qquad W_{ij} = \Lambda^{-1}_{ij} \ .$$

By allowing the plate coordinates for a given point to be correlated, we admit a variety of possible plate measuring techniques (e.g., goniometric, polar coordinate) in addition to those which directly produce Cartesian coordinates. We also thereby admit the possibility of employing cameras which do not have flat fields (e.g., panoramic cameras, meteor cameras, Baker Nunn Satellite Tracking Cameras, CZR cameras), for here the plate coordinates to be carried in the adjustment would be those derived from the appropriate transformation (usually from cylindrical to plane coordinates) of the original film measurements. In general, if ξ^0_{ij}, η^0_{ij} denote the measured coordinates of an image in whatever coordinate system is appropriate to the camera or measuring method and if

$$(20) \qquad \begin{aligned} x^0_{ij} &= x(\xi^0_{ij}, \eta^0_{ij}) \ , \\ y^0_{ij} &= y(\xi^0_{ij}, \eta^0_{ij}) \ , \end{aligned}$$

define the transformation to Cartesian coordinates, the covariance matrix of the derived plate coordinates is given by

$$(21) \qquad \Lambda_{ij} = C_{ij} \, \hat{\Lambda}_{ij} \, C^T_{ij} \ ,$$

where

$$(22)\qquad C_{ij} = \begin{bmatrix} \frac{\partial x}{\partial \xi_{ij}} & \frac{\partial x}{\partial \eta_{ij}} \\ \frac{\partial y}{\partial \xi_{ij}} & \frac{\partial y}{\partial \eta_{ij}} \end{bmatrix}, \qquad \hat{\Lambda}_{ij} = \begin{bmatrix} \sigma^2_{\xi_{ij}} & \sigma_{\xi_{ij}\eta_{ij}} \\ \sigma_{\xi_{ij}\eta_{ij}} & \sigma^2_{\eta_{ij}} \end{bmatrix}.$$

By employing the full covariance matrix Λ_{ij} in conjunction with the derived plate coordinates, we correctly propagate and preserve the informational content of the original observations throughout the entire photogrammetric adjustment.

Returning now to the linearized projective equations (15), we may express the entire set of such equations generated by all m exposure stations as

$$(23)\qquad v_j + \dot{B}_j \dot{\delta} + \ddot{B}_j \ddot{\delta}_j = \epsilon_j$$

where

$$(24)\qquad \underset{(2m,1)}{v_j} = \begin{bmatrix} v_{1j} \\ v_{2j} \\ \vdots \\ v_{mj} \end{bmatrix}, \quad \underset{(2m,9m)}{\dot{B}_j} = \begin{bmatrix} \dot{B}_{1j} & 0 & \cdots & 0 \\ 0 & \dot{B}_{2j} & \cdots & 0 \\ \vdots & \vdots & & \vdots \\ 0 & 0 & \cdots & \dot{B}_{mj} \end{bmatrix}, \quad \underset{(9m,1)}{\dot{\delta}} = \begin{bmatrix} \dot{\delta}_1 \\ \dot{\delta}_2 \\ \vdots \\ \dot{\delta}_m \end{bmatrix}, \quad \underset{(2m,3)}{\ddot{B}_j} = \begin{bmatrix} \ddot{B}_{1j} \\ \ddot{B}_{2j} \\ \vdots \\ \ddot{B}_{mj} \end{bmatrix}, \quad \underset{(2m,1)}{\epsilon_j} = \begin{bmatrix} \epsilon_{1j} \\ \epsilon_{2j} \\ \vdots \\ \epsilon_{mj} \end{bmatrix}$$

Inasmuch as we shall assume independence of plate coordinates of different images, we may express the covariance and weight matrices for the composite observational vector for the j^{th} point as

$$(25)\qquad \underset{(2m,2m)}{\Lambda_j} = \begin{bmatrix} \Lambda_{1j} & 0 & \cdots & 0 \\ 0 & \Lambda_{2j} & \cdots & 0 \\ \vdots & \vdots & & \vdots \\ 0 & 0 & \cdots & \Lambda_{mj} \end{bmatrix}, \quad W_j = \begin{bmatrix} W_{1j} & 0 & \cdots & 0 \\ 0 & W_{2j} & \cdots & 0 \\ \vdots & \vdots & & \vdots \\ 0 & 0 & \cdots & W_{mj} \end{bmatrix}$$

If next we collect all equations generated by all control points, we shall arrive at the system

$$(26) \qquad v + \dot{B}\dot{\delta} + \ddot{B}\ddot{\delta} = \epsilon$$

in which

$$(27) \qquad \underset{(2mn,1)}{v} = \begin{bmatrix} v_1 \\ v_2 \\ \vdots \\ v_n \end{bmatrix}, \quad \underset{(2mn,9n)}{\dot{B}} = \begin{bmatrix} \dot{B}_1 & & & \\ & \dot{B}_2 & & \\ & & \ddots & \\ & & & \dot{B}_n \end{bmatrix}, \quad \underset{(2mn,3n)}{\ddot{B}} = \begin{bmatrix} \ddot{B}_1 & 0 & \cdots & 0 \\ 0 & \ddot{B}_2 & \cdots & 0 \\ \vdots & \vdots & & \vdots \\ 0 & 0 & \cdots & \ddot{B}_n \end{bmatrix}, \quad \underset{(3n,1)}{\ddot{\delta}} = \begin{bmatrix} \ddot{\delta}_1 \\ \ddot{\delta}_2 \\ \vdots \\ \ddot{\delta}_n \end{bmatrix}, \quad \underset{(2mn,1)}{\epsilon} = \begin{bmatrix} \epsilon_1 \\ \epsilon_2 \\ \vdots \\ \epsilon_n \end{bmatrix}.$$

The corresponding covariance and weight matrices are

$$(28) \qquad \underset{(2mn,2mn)}{\Lambda} = \begin{bmatrix} \Lambda_1 & 0 & \cdots & 0 \\ 0 & \Lambda_2 & \cdots & 0 \\ \vdots & \vdots & & \vdots \\ 0 & 0 & \cdots & \Lambda_n \end{bmatrix}, \quad \underset{(2mn,2mn)}{W} = \begin{bmatrix} W_1 & 0 & \cdots & 0 \\ 0 & W_2 & \cdots & 0 \\ \vdots & \vdots & & \vdots \\ 0 & 0 & \cdots & W_n \end{bmatrix}.$$

Equations (26) and (28) contain the entire store of information provided by the projective equations. Our original treatment of the adjustment of a photogrammetric net (Brown, 1958a) was based entirely on these equations.

1.04 OBSERVATIONAL EQUATIONS GENERATED BY ELLIPSOIDAL CONTROL POINTS

We shall now turn to other possible sources of information. If we regard the coordinates of the j^{th} control point as also being available from independent external observations, we may write

$$
\begin{aligned}
X_j &= X_j^0 + v_{X_j} \quad , \\
Y_j &= Y_j^0 + v_{Y_j} \quad , \\
Z_j &= Z_j^0 + v_{Z_j} \quad .
\end{aligned}
\tag{29}
$$

Here, as before, X_j, Y_j, Z_j denote the adjusted coordinates. The observed coordinates are X_j^0, Y_j^0, Z_j^0 and their observational residuals are v_{X_j}, v_{Y_j}, v_{Z_j}. The covariance matrix of the observed coordinates is $\ddot{A}_j$ and the weight matrix is $\ddot{W}_j$. As we saw in our discussion of the ellipsoidal control point, by permitting the covariance matrix $\ddot{A}_j$ to be filled, we gain a new measure of observational flexibility. Equations (29), simple though they are, constitute the observational equations arising from externally observed control points. By employing the expressions in (14) for the adjusted coordinates, we may replace (29) by the equivalent relations

$$
\begin{aligned}
X_j^{00} + \delta X_j &= X_j^0 + v_{X_j} \\
Y_j^{00} + \delta Y_j &= Y_j^0 + v_{Y_j} \\
Z_j^{00} + \delta Z_j &= Z_j^0 + v_{Z_j}
\end{aligned}
\tag{30}
$$

or

$$
\begin{aligned}
v_{X_j} - \delta X_j &= \epsilon_{X_j} \ , \\
v_{Y_j} - \delta Y_j &= \epsilon_{Y_j} \ , \\
v_{Z_j} - \delta Z_j &= \epsilon_{Z_j} \ ,
\end{aligned} \tag{31}
$$

where

$$
\epsilon_{X_j} = X_j^{00} - X_j^0 \ , \quad \epsilon_{Y_j} = Y_j^{00} - Y_j^0 \ , \quad \epsilon_{Z_j} = Z_j^{00} - Z_j^0 \tag{32}
$$

We shall express (31) in matrix form as

$$
\ddot{v}_j - \ddot{\delta}_j = \ddot{\epsilon}_j \ . \tag{33}
$$

The observational equations arising from independently obtained coordinates of all n control points are then given by

$$
\ddot{v} - \ddot{\delta} = \ddot{\epsilon} \ , \tag{34}
$$

where

$$
\underset{(3n,1)}{\ddot{v}} = \begin{bmatrix} \ddot{v}_1 \\ \ddot{v}_2 \\ \vdots \\ \ddot{v}_n \end{bmatrix} \ , \quad \underset{(3n,1)}{\ddot{\delta}} = \begin{bmatrix} \ddot{\delta}_1 \\ \ddot{\delta}_2 \\ \vdots \\ \ddot{\delta}_n \end{bmatrix} \ , \quad \underset{(3n,1)}{\ddot{\epsilon}} = \begin{bmatrix} \ddot{\epsilon}_1 \\ \ddot{\epsilon}_2 \\ \vdots \\ \ddot{\epsilon}_n \end{bmatrix} \tag{35}
$$

If we were to assume that the coordinates of different points are independent of each other, the covariance and weight matrices associated with the observational vector of (34) would assume the forms

$$(36)\qquad \underset{(3n,3n)}{\ddot{\Lambda}} = \begin{bmatrix} \ddot{\Lambda}_1 & 0 & \dots & 0 \\ 0 & \ddot{\Lambda}_2 & \dots & 0 \\ \vdots & \vdots & & \vdots \\ 0 & 0 & \dots & \ddot{\Lambda}_n \end{bmatrix}, \qquad \underset{(3n,3n)}{\ddot{W}} = \begin{bmatrix} \ddot{W}_1 & 0 & \dots & 0 \\ 0 & \ddot{W}_2 & \dots & 0 \\ \vdots & \vdots & & \vdots \\ 0 & 0 & \dots & \ddot{W}_n \end{bmatrix}$$

1.05 OBSERVATIONAL EQUATIONS GENERATED BY ELEMENTS OF ORIENTATION

It is clear that we could proceed as in the preceding section to introduce any independent observations which may be available for elements of orientation. We shall assume initially that independent observations are available for all elements of orientation for all exposure stations. If α_i^0, ω_i, ... denote observed elements, we may write the observational equations for the i^{th} station:

$$(37)\qquad \begin{aligned} \alpha_i &= \alpha_i^0 + v_{\alpha_i}, & x_{p_i} &= x_{p_i}^0 + v_{x_{p_i}}, & X_i^c &= (X_i^c)^0 + v_{X_i^c}, \\ \omega_i &= \omega_i^0 + v_{\omega_i}, & y_{p_i} &= y_{p_i}^0 + v_{y_{p_i}}, & Y_i^c &= (Y_i^c)^0 + v_{Y_i^c}, \\ \kappa_i &= \kappa_i^0 + v_{\kappa_i}, & c_i &= c_i^0 + v_{c_i}, & Z_i^c &= (Z_i^c)^0 + v_{Z_i^c}, \end{aligned}$$

where the v's are observational residuals. If we eliminate the adjusted observations from equations (13) and (37), we shall arrive at the equivalent set of observational equations:

$$
\begin{aligned}
v_{\alpha_i} - \delta\alpha_i &= \alpha_i^{00} - \alpha_i^{0} = \epsilon_{\alpha_i} \\
v_{\omega_i} - \delta\omega_i &= \omega_i^{00} - \omega_i^{0} = \epsilon_{\omega_i} \qquad (38) \\
&\vdots \\
v_{Z_i^c} - \delta Z_i^c &= (Z_i^c)^{00} - (Z_i^c)^{0} = \epsilon_{Z_i^c}
\end{aligned}
$$

With obvious notation we may represent these in matrix form as

$$\dot{v}_i - \dot{\delta}_i = \dot{\epsilon}_i \quad . \qquad (39)$$

The observational equations for all m stations are then

$$\dot{v} - \dot{\delta} = \dot{\epsilon} \qquad (40)$$

where

$$\underset{(9m,1)}{\dot{v}} = \begin{bmatrix} \dot{v}_1 \\ \dot{v}_2 \\ \vdots \\ \dot{v}_m \end{bmatrix}, \quad \underset{(9m,1)}{\dot{\delta}} = \begin{bmatrix} \dot{\delta}_1 \\ \dot{\delta}_2 \\ \vdots \\ \dot{\delta}_m \end{bmatrix}, \quad \underset{(9m,1)}{\dot{\epsilon}} = \begin{bmatrix} \dot{\epsilon}_1 \\ \dot{\epsilon}_2 \\ \vdots \\ \dot{\epsilon}_m \end{bmatrix} \quad . \qquad (41)$$

We shall let $\dot{\Lambda}_i$ denote the covariance matrix of the observations of the elements of orientation for the i^{th} station and shall let $\dot{W}_i = \dot{\Lambda}_i^{-1}$ denote the corresponding weight matrix. We shall not require that these matrices necessarily be diagonal. We shall assume, for the time being, that the observations of elements of orientation are independent from one station to another. Then the covariance and weight matrices for the observed elements of orientation can be written

$$(42) \quad \underset{(9m,9m)}{\dot{\Lambda}} = \begin{bmatrix} \dot{\Lambda}_1 & 0 & \dots & 0 \\ 0 & \dot{\Lambda}_2 & \dots & 0 \\ \vdots & \vdots & & \vdots \\ 0 & 0 & \dots & \dot{\Lambda}_m \end{bmatrix}, \quad \underset{(9m,9m)}{\dot{W}} = \begin{bmatrix} \dot{W}_1 & 0 & \dots & 0 \\ 0 & \dot{W}_2 & \dots & 0 \\ \vdots & \vdots & & \vdots \\ 0 & 0 & \dots & \dot{W}_m \end{bmatrix}$$

We shall ultimately allow $\dot{\Lambda}$ and $\dot{W}$ to be completely filled matrices.

1.06 NORMAL EQUATIONS IN THE ABSENCE OF DATA FROM EXTERNAL SENSORS

We now have developed the observational equations arising from

(a) measured plate coordinates,
(b) ellipsoidal control points,
(c) independently determined elements of orientation.

We have yet to consider still another potential source of information which may be applicable to the photogrammetric adjustment: namely, external sensors and, in particular, external sensors which may themselves be significantly biased and which may, therefore, need to be calibrated as part of the overall photogrammetric adjustment in order that their potential accuracies might be fully realized. Before we turn to such considerations, we shall pause briefly to consider the form of the

normal equations generated by the observational equations developed thus far. The three sets of observatianal equations, namely,

$$
\begin{array}{lllll}
 & v + \dot{B}\dot{\delta} + \ddot{B}\ddot{\delta} = \epsilon & \text{(linearized projective equations)} \\
(43) & \dot{v} - \dot{\delta} = \dot{\epsilon} & \text{(constraints on elements of orientation)} \\
 & \ddot{v} - \ddot{\delta} = \ddot{\epsilon} & \text{(constraints from ellipsoidal control points)}
\end{array}
$$

may be merged into the single matrix equatian

$$
(44) \qquad \begin{bmatrix} v \\ \dot{v} \\ \ddot{v} \end{bmatrix} + \begin{bmatrix} \dot{B} & \ddot{B} \\ -I & 0 \\ 0 & -I \end{bmatrix} \begin{bmatrix} \dot{\delta} \\ \ddot{\delta} \end{bmatrix} = \begin{bmatrix} \epsilon \\ \dot{\epsilon} \\ \ddot{\epsilon} \end{bmatrix} ,
$$

and this in turn may be reduced to

$$
(45) \qquad \bar{v} + \bar{B}\delta = \bar{\epsilon}
$$

where, with obvious notation

$$
(46) \quad \underset{(n_0, n_0)}{\bar{v}} = \begin{bmatrix} v \\ \dot{v} \\ \ddot{v} \end{bmatrix} , \quad \underset{(n_0, 1)}{\bar{B}} = \begin{bmatrix} \dot{B} & \ddot{B} \\ -I & 0 \\ 0 & -I \end{bmatrix} , \quad \underset{(p_0, 1)}{\delta} = \begin{bmatrix} \dot{\delta} \\ \ddot{\delta} \end{bmatrix} , \quad \underset{(n_0, 1)}{\bar{\epsilon}} = \begin{bmatrix} \epsilon \\ \dot{\epsilon} \\ \ddot{\epsilon} \end{bmatrix}
$$

where $n_0 = 2mn + 9m + 3n$, $p_0 = 9m + 3n$.

In a similar manner we may merge the covariance matrices and weight matrices of the three basic observational vectors into the single composite matrices $\bar{\Lambda}$ and $\bar{W}$ where

$$(47)\qquad \underset{(n_0,n_0)}{\bar{\Lambda}} = \begin{bmatrix} \underset{(2mn,2mn)}{\Lambda} & 0 & 0 \\ 0 & \underset{(9m,9m)}{\dot{\Lambda}} & 0 \\ 0 & 0 & \underset{(3n,3n)}{\ddot{\Lambda}} \end{bmatrix}, \quad \underset{(n_0,n_0)}{\bar{W}} = \underset{(n_0,n_0)}{\bar{\Lambda}^{-1}} = \begin{bmatrix} \underset{(2mn,2mn)}{W} & 0 & 0 \\ 0 & \underset{(9m,9m)}{\dot{W}} & 0 \\ 0 & 0 & \underset{(3n,3n)}{\ddot{W}} \end{bmatrix}.$$

The normal equations leading to the determination of that pair of vectors $\bar{v}$, δ which satisfy (45) while simultaneously leading to the minimization of the quadratic form of the residuals

$$(48)\qquad s = \bar{v}^T \bar{W} \bar{v}$$

is shown in Brown (1955) to consist of

$$(49)\qquad (\bar{B}^T \bar{W} \bar{B})\,\delta = \bar{B}^T \bar{W} \epsilon \ .$$

By virtue of (46) and (47) the normal equations may be written

$$(50)\qquad \begin{bmatrix} \dot{B}^T & -I & 0 \\ \ddot{B}^T & 0 & -I \end{bmatrix} \begin{bmatrix} W & 0 & 0 \\ 0 & \dot{W} & 0 \\ 0 & 0 & \ddot{W} \end{bmatrix} \begin{bmatrix} \dot{B} & \ddot{B} \\ -I & 0 \\ 0 & -I \end{bmatrix} \begin{bmatrix} \dot{\delta} \\ \ddot{\delta} \end{bmatrix} \qquad \begin{bmatrix} \dot{B}^T & -I & 0 \\ \ddot{B}^T & 0 & -I \end{bmatrix} \begin{bmatrix} W & 0 & 0 \\ 0 & \dot{W} & 0 \\ 0 & 0 & \ddot{W} \end{bmatrix} \begin{bmatrix} \epsilon \\ \dot{\epsilon} \\ \ddot{\epsilon} \end{bmatrix},$$

which, upon reduction, become

$$(51)\qquad \begin{bmatrix} \dot{N} + \dot{W} & \bar{N} \\ \bar{N}^T & \ddot{N} + \ddot{W} \end{bmatrix} \begin{bmatrix} \dot{\delta} \\ \ddot{\delta} \end{bmatrix} = \begin{bmatrix} \dot{c} - \dot{W}\epsilon \\ \ddot{c} - \ddot{W}\epsilon \end{bmatrix},$$

wherein

$$
\underset{(9m,9m)}{\dot{N}} = \underset{(9m,2mn)}{\dot{B}^T}\ \underset{(2mn,2mn)}{W}\ \underset{(2mn,9m)}{\dot{B}}\,, \qquad \underset{(9m,1)}{\dot{c}} = \underset{(9m,2mn)}{\dot{B}^T}\ \underset{(2mn,2mn)}{W}\ \underset{(2mn,1)}{\epsilon}\,,
$$

$$
\underset{(9m,3n)}{\bar{N}} = \underset{(9m,2mn)}{\dot{B}^T}\ \underset{(2mn,2mn)}{W}\ \underset{(2mn,3n)}{\ddot{B}}\,, \tag{52}
$$

$$
\underset{(3n,3n)}{\ddot{N}} = \underset{(3n,2mn)}{\ddot{B}^T}\ \underset{(2mn,2mn)}{W}\ \underset{(2mn,3n)}{\ddot{B}}\,, \qquad \underset{(3n,1)}{\ddot{c}} = \underset{(3n,2mn)}{\ddot{B}^T}\ \underset{(2mn,2mn)}{W}\ \underset{(2mn,1)}{\epsilon}\,.
$$

The normal equations (51) are of the form described in our earlier paper (Brown, 1959). We shall temporarily defer the further treatment of the normal equations until Subsection (1.12) and, in the next three subsections, shall consider the extension of the basic solution to incorporate information from external sensors.

1.07 OBSERVATIONAL EQUATIONS GENERATED BY AUXILIARY EXTERNAL SENSORS

For the sake of complete generality, we shall now consider the possibility that there may be certain auxiliary measurements interrelating elements of orientation and coordinates of control. For instance, the distances between certain pairs of exposure stations may be known, or distances between certain pairs of control points, or even distances between certain exposure stations and certain control points. It is altogether likely in the near future that the relative positions of successive aerial exposure stations will be measured with worthwhile accuracy by inertial sensors. Conceivably, the effectiveness and accuracy of such sensors could be increased if certain parameters peculiar to the sensors were carried as unknowns in an appropriate modification of the photogrammetric adjustment. To enlarge on this, let us consider an inertial system in somewhat greater detail. The output of an inertial navigational system of high quality has a very low random component, but is subject to a cumulative time varying error upon which may be superimposed a sinusoidal type of error having the Schuler period P (approximately 84 minutes near the earth's surface). Strictly for purposes of discussion, let us assume that the following equations adequately describe the nature of the errors in the navigational output for the latitude ϕ_i and longitude λ_i of the i^{th} exposure of a photogrammetric strip:

$$\underset{\text{(true)}}{\phi_i} - \underset{\text{(measured)}}{\phi_i^0} = \underset{\text{(random error)}}{\epsilon_{\phi_i}} + a_0 + a_1(t_i - t_{00}) + a_2 \sin\frac{2\pi}{P}(t_i - t_{00}) + a_3 \cos\frac{2\pi}{P}(t_i - t_{00}) + \text{higher order terms, (assumed negligible)} \tag{53}$$

$$\underset{\text{(true)}}{\lambda_i} - \underset{\text{(measured)}}{\lambda_i^0} = \underset{\text{(random error)}}{\epsilon_{\lambda_i}} + b_0 + b_1(t_i - t_{00}) + b_2 \sin\frac{2\pi}{P}(t_i - t_{00}) + b_3 \cos\frac{2\pi}{P}(t_i - t_{00}) + \text{higher order terms . (assumed negligible)}$$

In these equations

t_i = time of i^{th} exposure,

t_{00} = arbitrary time of reference which would normally be selected to correspond to a time near the center of the strip,

$a_0 + a_3$, $b_0 + b_3$ = zeroing errors at time $t_i = t_{00}$ (ordinarily $a_0 >> a_3$, $b_0 >> b_3$),

a_1, b_1 = coefficients of first order secular drift,

a_2, a_3, b_2, b_3 = coefficients of first order periodic drift.

Let us further suppose that the aititude of the aircraft is measured by means of a precise pressure altimeter and that a nominally constant altitude is flown. Aside from zeroing, the systematic errors in pressure altitude are primarily attributable to the slowly changing departure of the isobaric surface at flying height from the spheroid of reference. If s_i were to denote the distance along the flight path of the i^{th} exposure station ($s=0$ when $t=t_{00}$), a suitable error model for measured pressure altitudes might well be of the form

$$(54) \qquad \underbrace{h_i - h_i^0}_{\text{(true) (measured)}} = \underbrace{\epsilon_{h_i}}_{\text{(random error)}} + \underbrace{c_0 + c_1 s_i + c_2 s_i^2 + c_3 s_i^3 + \dots}_{\text{equations defining isobaric departure along flight line from reference spheroid.}}$$

If the velocity of the aircraft were nearly constant, one could replace s_i in this equation by $s_i = v(t_i - t_{00})$ where v denotes the average velocity along the flight interval. By means of appropriate transformations the above equations for ϕ_i, λ_i, h_i could be expressed in terms of Cartesian coordinates. Thus, we may write functionally

$$
\begin{aligned}
X_i^c &= f_{1i}(\phi_i^0 + \epsilon_{\phi_i}, \lambda_i^0 + \epsilon_{\lambda_i}, h_i^0 + \epsilon_{h_i}, a_0, a_1, \ldots; b_0, b_1, \ldots; c_0, c_1, \ldots; t_i) , \\
Y_i^c &= f_{2i}(\phi_i^0 + \epsilon_{\phi_i}, \lambda_i^0 + \epsilon_{\lambda_i}, h_i^0 + \epsilon_{h_i}, a_0, a_1, \ldots; b_0, b_1, \ldots; c_0, c_1, \ldots; t_i) , \\
Z_i^c &= f_{3i}(\phi_i^0 + \epsilon_{\phi_i}, \lambda_i^0 + \epsilon_{\lambda_i}, h_i^0 + \epsilon_{h_i}, a_0, a_1, \ldots; b_0, b_1, \ldots; c_0, c_1, \ldots; t_i) .
\end{aligned} \tag{55}
$$

Here we have expressed the adjusted Cartesian coordinates for the i^{th} exposure station in terms of independently determined geographic coordinates together with a set of unknown error coefficients necessary for their calibration. Equations (55) may therefore be considered to constitute another set of observational equations involving not only parameters heretofore considered (X_i^c, Y_i^c, Z_i^c) but also a new set of parameters (a_i, b_i, c_i) independent of the parameters of the photogrammetric model proper. Nothing in principle prevents us from incorporating such observational equations into the photogrammetric adjustment. By doing so, we may possibly strengthen the photogrammetric adjustment to a worthwhile degree and, in the process, calibrate the external sensors over the flight interval employed.

The above discussion is intended to provide a heuristic introduction to the next phase of our formulation of the general photogrammetric adjustment, namely the incorporation of observational equations arising from external sensors. We postulate the existence of a general observational vector

$$
\theta^T = (\theta_1^0 \quad \theta_2^0 \quad \ldots \quad \theta_p^0) \tag{56}
$$

provided by an unspecified combination of unspecified external sensors. We shall assume that the adjusted values $\theta_k = \theta_k^0 + v_{\theta_k}$ of the external observations must satisfy a set of r equations of the general functional form

$$(57) \qquad f_k(\theta_1, \theta_2, \ldots, \theta_p;\ \dot{u}_1, \dot{u}_2, \ldots, \dot{u}_{9m};\ \ddot{u}_1, \ddot{u}_2, \ldots, \ddot{u}_{3n};\ \dddot{u}_1, \dddot{u}_2, \ldots, \dddot{u}_q) = 0$$

in which

$\dot{u}_1, \dot{u}_2, \ldots, \dot{u}_{9m}$ = elements of orientation (e.g., $u_1 = \alpha_1$, $u_2 = \omega_1$, etc.)

$\ddot{u}_1, \ddot{u}_2, \ldots, \ddot{u}_{3n}$ = coordinates of control (e.g., $u_1 = X_1$, $u_2 = Y_1$, etc.)

$\dddot{u}_1, \dddot{u}_2, \ldots, \dddot{u}_q$ = unknown parameters peculiar to the external sensors.

To linearize equations (57), we set

$$(58) \qquad \begin{aligned} \dot{u}_i &= \dot{u}_i^{00} + \delta\dot{u}_i, \quad i = 1,2,\ldots,9m, \\ \ddot{u}_j &= \ddot{u}_j^{00} + \delta\ddot{u}_j, \quad j = 1,2,\ldots,3n, \\ \dddot{u}_k &= \dddot{u}_k^{00} + \delta\dddot{u}_k, \quad k = 1,2,\ldots,q, \end{aligned}$$

in which the approximations for the elements of orientation $\dot{u}_i^{00}$ and coordinates of control $\ddot{u}_j^{00}$ are the same values as were used in the linearization of the projective equations. The substitution of these expressions together with the expressions $\theta_k = \theta_k^0 + v_{\theta_k}$ into equations (57) and subsequent linearization by Taylor's series yields

$$(59)\quad a_{1g}v_{\theta_1} + a_{2g}v_{\theta_2} + \ldots + a_{pg}v_{\theta_p} + \dot{f}_{1g}\delta\dot{v}_1 + \dot{f}_{2g}\delta\dot{v}_2 + \ldots + \dot{f}_{9m,g}\delta\dot{v}_{9m}$$
$$+ \ddot{f}_{1g}\delta\ddot{v}_1 + \ddot{f}_{2g}\delta\ddot{v}_2 + \ldots + \ddot{f}_{3n,g}\delta\ddot{v}_{3n}$$
$$+ \dddot{f}_{1g}\delta\dddot{v}_1 + \dddot{f}_{2g}\delta\dddot{v}_2 + \ldots + \dddot{f}_{q,g}\delta\dddot{v}_q = \epsilon_{\theta_g}$$

where

$$(60)\quad a_{gh} = \left.\frac{\partial f_g}{\partial \theta_h}\right|_0, \quad \dot{f}_{gh} = \left.\frac{\partial f_g}{\partial \dot{v}_h}\right|_0, \quad \ddot{f}_{gh} = \left.\frac{\partial f_g}{\partial \ddot{v}_h}\right|_0, \quad \dddot{f}_{gh} = \left.\frac{\partial f_g}{\partial \dddot{v}_h}\right|_0,$$

$$(61)\quad \epsilon_{\theta_g} = f_g(\theta_1^0, \theta_2^0, \ldots, \theta_p^0; \dot{v}_1^{00}, \dot{v}_2^{00}, \ldots, \dot{v}_{9m}^{00}; \ddot{v}_1^{00}, \ddot{v}_2^{00}, \ldots, \ddot{v}_{3n}^{00}; \dddot{v}_1^{00}, \dddot{v}_2^{00}, \ldots, \dddot{v}_q^{00}).$$

Equations (59) may be expressed in matrix form as

$$(62)\quad A_\theta v_\theta + \dot{B}_\theta \dot{\delta} + \ddot{B}_\theta \ddot{\delta} + \dddot{B} \dddot{\delta} = \epsilon_\theta$$

where $\dot{\delta}$ and $\ddot{\delta}$ are the same as in (24) and (27) respectively and

$$(63)\quad \underset{(r,p)}{A_\theta} = \begin{bmatrix} a_{11} & a_{12} & \cdots & a_{1p} \\ a_{21} & a_{22} & \cdots & a_{2p} \\ \vdots & \vdots & & \vdots \\ a_{r1} & a_{r2} & \cdots & a_{rp} \end{bmatrix}, \quad \underset{(p,1)}{v_\theta} = \begin{bmatrix} v_{\theta_1} \\ v_{\theta_2} \\ \vdots \\ v_{\theta_p} \end{bmatrix}, \quad \underset{(r,9m)}{\dot{B}_\theta} = \begin{bmatrix} \dot{f}_{11} & \dot{f}_{12} & \cdots & \dot{f}_{1,9m} \\ \dot{f}_{21} & \dot{f}_{22} & \cdots & \dot{f}_{2,9m} \\ \vdots & \vdots & & \vdots \\ \dot{f}_{r1} & \dot{f}_{r2} & \cdots & \dot{f}_{r,9m} \end{bmatrix}$$

$$(64)\qquad \underset{(r,3n)}{\overset{\cdot\cdot}{B}_\theta} = \begin{bmatrix} \overset{\cdot\cdot}{f}_{11} & \overset{\cdot\cdot}{f}_{12} & \cdots & \overset{\cdot\cdot}{f}_{1,3n} \\ \overset{\cdot\cdot}{f}_{21} & \overset{\cdot\cdot}{f}_{22} & \cdots & \overset{\cdot\cdot}{f}_{2,3n} \\ \vdots & \vdots & & \vdots \\ \overset{\cdot\cdot}{f}_{r1} & \overset{\cdot\cdot}{f}_{r2} & \cdots & \overset{\cdot\cdot}{f}_{r,3n} \end{bmatrix}, \quad \underset{(r,q)}{\overset{\cdot\cdot\cdot}{B}} = \begin{bmatrix} \overset{\cdot\cdot\cdot}{f}_{11} & \overset{\cdot\cdot\cdot}{f}_{12} & \cdots & \overset{\cdot\cdot\cdot}{f}_{1,q} \\ \overset{\cdot\cdot\cdot}{f}_{21} & \overset{\cdot\cdot\cdot}{f}_{22} & \cdots & \overset{\cdot\cdot\cdot}{f}_{2,q} \\ \vdots & \vdots & & \vdots \\ \overset{\cdot\cdot\cdot}{f}_{r1} & \overset{\cdot\cdot\cdot}{f}_{r2} & \cdots & \overset{\cdot\cdot\cdot}{f}_{rq} \end{bmatrix}, \quad \underset{(r,1)}{\epsilon_\theta} = \begin{bmatrix} \epsilon_{\theta_1} \\ \epsilon_{\theta_2} \\ \vdots \\ \epsilon_{\theta_r} \end{bmatrix},$$

$$(65)\qquad \underset{(q,1)}{\overset{\cdot\cdot\cdot}{\delta}} = (\overset{\cdot\cdot\cdot}{\delta u_1}\ \overset{\cdot\cdot\cdot}{\delta u_2}\ \cdots\ \overset{\cdot\cdot\cdot}{\delta u_q})^T .$$

We shall let the covariance and weight matrices of the observational vector θ be denoted by Λ_θ and $W_\theta = \Lambda_\theta^{-1}$.

By means of equations (62) we can introduce into the photogrammetric adjustment any pertinent information available from independent sources. For example, in the special case considered at the beginning of this section, the matrices A_θ and $\dot{B}_\theta$ would assume the forms

$$(66)\qquad \underset{(3m,3m)}{A_\theta} = \begin{bmatrix} A_{11} & 0 & \cdots & 0 \\ 0 & A_{22} & \cdots & 0 \\ \vdots & \vdots & & \vdots \\ 0 & 0 & \cdots & A_{mm} \end{bmatrix}, \text{ where } \underset{(3,3)}{A_{11}} = \begin{bmatrix} a_{31-2,31-2} & a_{31-2,31-1} & a_{31-2,31} \\ a_{31-1,31-2} & a_{31-1,31-1} & a_{31-1,31} \\ a_{31,31-2} & a_{31,31-1} & a_{31,31} \end{bmatrix},$$

$$(67)\qquad \underset{(3m,9m)}{\dot{B}_\theta} = \begin{bmatrix} \dot{F}_{11} & 0 & \cdots & 0 \\ 0 & \dot{F}_{22} & \cdots & 0 \\ \vdots & \vdots & & \vdots \\ 0 & 0 & \cdots & \dot{F}_{mm} \end{bmatrix} \qquad \text{where } \underset{(3,9)}{\dot{F}_{ii}} = \begin{bmatrix} 0 & 0 & 0 \\ 0 & 0 & 0 \\ 0 & 0 & 0 \\ 0 & 0 & 0 \\ 0 & 0 & 0 \\ 0 & 0 & 0 \\ \dot{f}_{3i-2,9i-2} & \dot{f}_{3i-1,9i-2} & \dot{f}_{3i,9i-2} \\ \dot{f}_{3i-2,9i-1} & \dot{f}_{3i-1,9i-1} & \dot{f}_{3i,9i-1} \\ \dot{f}_{3i-2,9i} & \dot{f}_{3i-1,9i} & \dot{f}_{3i,9i} \end{bmatrix}^T$$

Because no control points are involved in equations (55), the matrix $\ddot{B}_\theta$ would be a zero matrix. Since the $\ddot{u}$'s (the a_i, b_i, c_i in the present case) are common to all equations, the matrix $\dddot{B}_\theta$ would be a completely filled 3m by q matrix, where q would equal 12 if four parameters were carried in each of the error models of (53) and (54).

Inasmuch as different strips of a block may be flown on different occasions, it may be necessary to employ fresh coefficients in the error models for each strip or subgroup of strips. This situation is easily accommodated by a reinterpretation of (62), (65), (66), and (67). We now attach a subscript i to the matrices defined in (64), (65), (66) to signify that they arise from the i^{th} strip or i^{th} group of strips for which the i^{th} set of error coefficients apply. If we postulate that the block is subdivided into a total of s subblocks, each having a re-initialized error model for the external sensors, the matrices in (62) assume the forms

$$(68)\qquad A_\theta = \begin{bmatrix} A_{\theta_1} & 0 & \cdots & 0 \\ 0 & A_{\theta_2} & \cdots & 0 \\ \vdots & \vdots & & \vdots \\ 0 & 0 & \cdots & A_{\theta_s} \end{bmatrix}, \quad v_\theta = \begin{bmatrix} v_{\theta_1} \\ v_{\theta_2} \\ \vdots \\ v_{\theta_s} \end{bmatrix}, \quad \dot{B}_\theta = \begin{bmatrix} \dot{B}_{\theta_1} \\ \dot{B}_{\theta_2} \\ \vdots \\ \dot{B}_{\theta_s} \end{bmatrix},$$

$$(69)\qquad \dddot{B} = \begin{bmatrix} \dddot{B}_1 & 0 & \cdots & 0 \\ 0 & \dddot{B}_2 & \cdots & 0 \\ \vdots & \vdots & & \vdots \\ 0 & 0 & \cdots & \dddot{B}_s \end{bmatrix}, \quad \dddot{\delta} = \begin{bmatrix} \dddot{\delta}_1 \\ \dddot{\delta}_2 \\ \vdots \\ \dddot{\delta}_s \end{bmatrix}, \quad \epsilon_\theta = \begin{bmatrix} \epsilon_{\theta_1} \\ \epsilon_{\theta_2} \\ \vdots \\ \epsilon_{\theta_s} \end{bmatrix}.$$

Here $\dddot{\delta}_i$ refers to the corrections to the i^{th} set of error coefficients (these apply only to the i^{th} sub-block). In the present application the elements v_{θ_i}, ϵ_{θ_i} of the vectors v_θ, ϵ_θ are themselves vectors (applying to the i^{th} sub-block) and are not to be confused with the scalars v_{θ_i}, ϵ_{θ_i} appearing in (57) (these should now be redefined as $v_{\theta_{ij}}$, $\epsilon_{\theta_{ik}}$ to refer, respectively, to the j^{th} residual and k^{th} discrepancy term arising from the i^{th} sub-block).

From the foregoing example it should be clear that equations (62) may be interpreted with sufficient generality to accommodate any available auxiliary data pertaining, however remotely, to any of the elements of orientation or to any coordinates of control.

1.08 OBSERVATIONAL EQUATIONS GENERATED BY APRIORI KNOWLEDGE OF PARAMETERS OF ERROR MODELS

Our final set of observational equations is intended to exploit any information that may be available concerning the admissible variation of the coefficients of error models of external sensors. We assume that the parameter $\overset{\cdots}{u}_k$ is itself subject to observation and write

$$(70) \qquad \overset{\cdots}{u}_k = \overset{\cdots}{u}{}^0_k + \overset{\cdots}{v}_k , \quad k = 1,2,\ldots,q.$$

Upon eliminating $\overset{\cdots}{u}_k$ from equations (58) and (70) we get

$$(71) \qquad \overset{\cdots}{v}_k - \delta\overset{\cdots}{u}_k = \overset{\cdots}{u}{}^{00}_k - \overset{\cdots}{u}{}^0_k = \overset{\cdots}{\epsilon}_k$$

which may be expressed in matrix form as

$$(72) \qquad \underset{(q,1)}{\overset{\cdots}{v}} - \underset{(q,1)}{\overset{\cdots}{\delta}} = \underset{(q,1)}{\overset{\cdots}{\epsilon}} .$$

We shall let $\underset{(q,q)}{\overset{\cdots}{\Lambda}}$ and $\underset{(q,q)}{\overset{\cdots}{W}} = \underset{(q,q)}{\overset{\cdots}{\Lambda}{}^{-1}}$ denote the covariance and weight matrices of the a priori values of the error coefficients. In the event no a priori constraints were to be placed on the error coefficients, $\overset{\cdots}{W}$ would become zero. By the same token, if no constraints were to be placed on a particular error coefficient, the rows and columns of $\overset{\cdots}{W}$ corresponding to that coefficient would consist of zero elements.

1.09 THE MERGED OBSERVATIONAL EQUATIONS

Bringing together the various sets of observational equations which may apply to the adjustment of a general photogrammetric net, we have

$$
\begin{aligned}
& v + \dot{B}\dot{\delta} + \ddot{B}\ddot{\delta} = \epsilon && \text{(See Section (1.03))} \\
& A_\theta v_\theta + \dot{B}_\theta \dot{\delta} + \ddot{B}_\theta \ddot{\delta} + \dddot{B}_\theta \dddot{\delta} = \epsilon_\theta && \text{(See Section (1.07))} \\
& \dot{v} - \dot{\delta} = \dot{\epsilon} && \text{(See Section (1.05))} \\
& \ddot{v} - \ddot{\delta} = \ddot{\epsilon} && \text{(See Section (1.04))} \\
& \dddot{v} - \dddot{\delta} = \dddot{\epsilon} && \text{(See Section (1.08))}
\end{aligned} \tag{73}
$$

These may be written

$$
\begin{bmatrix} 1 & 0 & 0 & 0 & 0 \\ 0 & A_\theta & 0 & 0 & 0 \\ 0 & 0 & 1 & 0 & 0 \\ 0 & 0 & 0 & 1 & 0 \\ 0 & 0 & 0 & 0 & 1 \end{bmatrix} \begin{bmatrix} v \\ v_\theta \\ \dot{v} \\ \ddot{v} \\ \dddot{v} \end{bmatrix} + \begin{bmatrix} \dot{B} & \ddot{B} & 0 \\ \dot{B}_\theta & \ddot{B}_\theta & \dddot{B}_\theta \\ -1 & 0 & 0 \\ 0 & -1 & 0 \\ 0 & 0 & -1 \end{bmatrix} \begin{bmatrix} \dot{\delta} \\ \ddot{\delta} \\ \dddot{\delta} \end{bmatrix} = \begin{bmatrix} \epsilon \\ \epsilon_\theta \\ \dot{\epsilon} \\ \ddot{\epsilon} \\ \dddot{\epsilon} \end{bmatrix}, \tag{74}
$$

which may be represented more compactly as

$$
\bar{A}\,\bar{v} + \bar{B}\,\bar{\delta} = \bar{\epsilon} \tag{75}
$$

The covariance and weight matrices corresponding to the combined observational vectors is

$$(76)\qquad \bar{\Lambda} = \begin{bmatrix} \Lambda & 0 & 0 & 0 & 0 \\ 0 & \Lambda_\theta & 0 & 0 & 0 \\ 0 & 0 & \dot{\Lambda} & 0 & 0 \\ 0 & 0 & 0 & \ddot{\Lambda} & 0 \\ 0 & 0 & 0 & 0 & \dddot{\Lambda} \end{bmatrix} , \quad \bar{W} = \bar{\Lambda}^{-1} = \begin{bmatrix} W & 0 & 0 & 0 & 0 \\ 0 & W_\theta & 0 & 0 & 0 \\ 0 & 0 & \dot{W} & 0 & 0 \\ 0 & 0 & 0 & \ddot{W} & 0 \\ 0 & 0 & 0 & 0 & \dddot{W} \end{bmatrix} .$$

All of the information pertinent to the adjustment is contained in equations (75) and (76).

1.10 THE GENERAL NORMAL EQUATIONS

The normal equations for the minimum variance adjustment are obtained from the particular pair of vectors $\bar{v}$, $\bar{\delta}$ which simultaneously satisfy the specified observational equations while minimizing the quadratic form

$$(77)\qquad s = \bar{v}^T \bar{W} \bar{v} .$$

The writer has shown (Brown, 1955) that the solution to this problem leads to a set of normal equations of the form

$$(78)\qquad N \bar{\delta} = c ,$$

in which

$$N = \bar{B}^T(\bar{A}\bar{\Lambda}\bar{A}^T)^{-1}\bar{B} , \tag{79}$$

$$c = \bar{B}^T(\bar{A}\bar{\Lambda}\bar{A}^T)^{-1}\bar{\epsilon} . \tag{80}$$

If we set

$$G = (A_\theta \Lambda_\theta A_\theta^T)^{-1} , \tag{81}$$

we can express the matrix $(\bar{A}\bar{\Lambda}\bar{A}^T)^{-1}$ as

$$(\bar{A}\bar{\Lambda}\bar{A}^T)^{-1} = \begin{bmatrix} W & 0 & 0 & 0 & 0 \\ 0 & G & 0 & 0 & 0 \\ 0 & 0 & \dot{W} & 0 & 0 \\ 0 & 0 & 0 & \ddot{W} & 0 \\ 0 & 0 & 0 & 0 & \dddot{W} \end{bmatrix} . \tag{82}$$

From this and from the implicit partitioning of $\bar{B}$ in (75) we may express the coefficient matrix N as

$$N = \begin{bmatrix} \dot{B}^T & \dot{B}_\theta^T & -I & 0 & 0 \\ \ddot{B}^T & \ddot{B}_\theta^T & 0 & -I & 0 \\ 0 & \ddot{B}_\theta^T & 0 & 0 & -I \end{bmatrix} \begin{bmatrix} W & 0 & 0 & 0 & 0 \\ 0 & G & 0 & 0 & 0 \\ 0 & 0 & \dot{W} & 0 & 0 \\ 0 & 0 & 0 & \ddot{W} & 0 \\ 0 & 0 & 0 & 0 & \dddot{W} \end{bmatrix} \begin{bmatrix} \dot{B} & \ddot{B} & 0 \\ \dot{B}_\theta & \ddot{B}_\theta & \dddot{B}_\theta \\ -I & 0 & 0 \\ 0 & -I & 0 \\ 0 & 0 & -I \end{bmatrix} \tag{83}$$

which reduces to

$$(84)\qquad N = \begin{bmatrix} \dot{B}^T W \dot{B} + \dot{B}_\theta^T G \dot{B}_\theta + \dot{W} & \dot{B}^T W \ddot{B} + \dot{B}_\theta^T G \ddot{B}_\theta & \dot{B}_\theta^T G \dddot{B}_\theta \\ \ddot{B}^T W \dot{B} + \ddot{B}_\theta^T G \dot{B}_\theta & \ddot{B}^T W \ddot{B} + \ddot{B}_\theta^T G \ddot{B}_\theta + \ddot{W} & \ddot{B}_\theta^T G \dddot{B}_\theta \\ \dddot{B}_\theta^T G \dot{B}_\theta & \dddot{B}_\theta^T G \ddot{B}_\theta & \dddot{B}_\theta^T G \dddot{B}_\theta + \dddot{W} \end{bmatrix} .$$

Similarly we may show that c is of the form

$$(85)\qquad c = \begin{bmatrix} \dot{B}^T W \epsilon + \dot{B}_\theta^T G \epsilon_\theta - \dot{W}\dot{\epsilon} \\ \ddot{B}^T W \epsilon + \ddot{B}_\theta^T G \epsilon_\theta - \ddot{W}\ddot{\epsilon} \\ \dddot{B}_\theta^T G \epsilon_\theta - \dddot{W}\dddot{\epsilon} \end{bmatrix} .$$

From (84) and (85) we see that the general normal equations (78) can be expressed as the sum of the following two sets of normal equations:

$$(86)\qquad \begin{bmatrix} \dot{N} + \dot{W} & \ddot{N} & 0 \\ \ddot{N}^T & \ddot{N} + \ddot{W} & 0 \\ 0 & 0 & 0 \end{bmatrix} \begin{bmatrix} \dot{\delta} \\ \ddot{\delta} \\ \dddot{\delta} \end{bmatrix} = \begin{bmatrix} \dot{c} - \dot{W}\dot{\epsilon} \\ \ddot{c} - \ddot{W}\ddot{\epsilon} \\ 0 \end{bmatrix}$$

$$(87)\qquad \begin{bmatrix} \dot{N}_\theta & \ddot{N}_\theta & \tilde{N}_\theta \\ \ddot{N}_\theta^T & \ddot{N}_\theta & \hat{N}_\theta \\ \tilde{N}_\theta^T & \hat{N}_\theta^T & \dddot{N}_\theta + W \end{bmatrix} \begin{bmatrix} \dot{\delta} \\ \ddot{\delta} \\ \dddot{\delta} \end{bmatrix} = \begin{bmatrix} \dot{c}_\theta \\ \ddot{c}_\theta \\ \dddot{c}_\theta - \dddot{W}\epsilon \end{bmatrix}$$

in which

$$
\begin{aligned}
&\dot{N} = \dot{B}^T W \dot{B}\,, \qquad \dot{N}_\theta = \dot{B}_\theta^T G \dot{B}_\theta\,, \qquad \tilde{N}_\theta = \dot{B}_\theta^T G \dddot{B}_\theta\,,\\
&\bar{N} = \dot{B}^T W \ddot{B}\,, \qquad \bar{N}_\theta = \dot{B}_\theta^T G \ddot{B}_\theta\,, \qquad \hat{N}_\theta = \ddot{B}_\theta^T G \dddot{B}_\theta\,,\\
(88)\quad &\ddot{N} = \ddot{B}^T W \ddot{B}\,, \qquad \ddot{N}_\theta = \ddot{B}_\theta^T G \ddot{B}_\theta\,, \qquad \dddot{N}_\theta = \ddot{B}_\theta^T G \dddot{B}_\theta\,.\\
&\dot{c} = \dot{B}^T W \epsilon\,, \qquad \dot{c}_\theta = \dot{B}_\theta^T G \epsilon_\theta\,,\\
&\ddot{c} = \ddot{B}^T W \epsilon\,, \qquad \ddot{c}_\theta = \ddot{B}_\theta^T G \epsilon_\theta\,,\\
&\qquad\qquad \dddot{c}_\theta = \dddot{B}_\theta^T G \epsilon_\theta\,,
\end{aligned}
$$

We recognize equations (86) as being those derived in 1.06 and in our earlier papers (Brown 1958a, 1959); they arise from the projective relations and from constraints placed directly on the elements of orientation and coordinates of control. Equations (87) reflect the combined contribution of those external sensors not involved in the generation of the constraining matrices $\dot{W}$ and $\ddot{W}$. In the case of the Air Force USQ-28 system, for example, such sensors would include: a precise inertial system (Hypernas II) providing accurate measurements (σ = 10 arc sec.) of the direction of the camera axis relative to the local vertical, together with measurements of heading (σ = 40 arc sec.) and of relative position (ϕ,λ); a precise ranging system (SHIRAN) providing simultaneous measurements (σ = 3 ft.) of the distances of the aircraft from up to four ground stations; a Terrain Profile Recorder providing a continuous measure (σ = 10 ft.) of the distance to the nadir of the aircraft; a precise pressure altimeter monitoring the altitude of the aircraft relative to an isobaric profile. Equations (87) are sufficiently general to encompass all of the sensors of the present USQ-28 system plus any other sensors which might later be added to the system.

1.11 DETAILED STRUCTURE OF THE NORMAL EQUATIONS

To proceed further we shall confine our consideration to normal equations of the form (86). From the partitioning of (27), (28), (35), (36), and (41) we can show that the normal equations (86) (with the third rows and columns dropped) are of the form

$$
(89)\qquad
\left[\begin{array}{c|ccc}
(\sum_{j=1}^{n} \dot{N}_j) + \dot{W} & \bar{N}_1 & \bar{N}_2 & \cdots \; \bar{N}_n \\
\hline
\bar{N}_1^T & \ddot{N}_1 + \ddot{W}_1 & & \cdots \; 0 \\
\bar{N}_2^T & & \ddot{N}_2 + \ddot{W}_2 & \cdots \; 0 \\
\vdots & \vdots & \vdots & \vdots \\
\bar{N}_n^T & 0 & 0 & \cdots \; \ddot{N}_n + \ddot{W}_n
\end{array}\right]
\left[\begin{array}{c} \dot{\delta} \\ \hline \ddot{\delta}_1 \\ \ddot{\delta}_2 \\ \vdots \\ \ddot{\delta}_n \end{array}\right]
=
\left[\begin{array}{c} (\sum_{j=1}^{n} \dot{c}_j) - \dot{W}\dot{\epsilon} \\ \hline \ddot{c}_1 - \ddot{W}_1 \ddot{\epsilon}_1 \\ \ddot{c}_2 - \ddot{W}_2 \ddot{\epsilon}_2 \\ \vdots \\ \ddot{c}_n - \ddot{W}_n \ddot{\epsilon}_n \end{array}\right]
\qquad (91
$$

in which

$$
\begin{aligned}
\dot{N}_j &= \dot{B}_j^T \dot{W}_j \dot{B}_j \;, & \dot{c}_j &= \dot{B}_j^T \dot{W}_j \dot{\epsilon}_j \;, \\
(90)\qquad \bar{N}_j &= \dot{B}_j^T \dot{W}_j \ddot{B}_j \;, & \ddot{c}_j &= \ddot{B}_j \dot{W}_j \ddot{\epsilon}_j \;. \\
\ddot{N}_j &= \ddot{B}_j^T \ddot{W}_j \ddot{B}_j \;,
\end{aligned}
$$

From the further partitioning of (24), (25), and (42) we can expand (89) to the form

(91)

$$\left[\begin{array}{cccc|ccccc}
\dot{N}_{11}+\dot{W}_1 & 0 & \cdots & 0 & \bar{N}_{11} & \bar{N}_{12} & \cdots & \bar{N}_{1n} \\
0 & \dot{N}_{22}+\dot{W}_2 & \cdots & 0 & \bar{N}_{21} & \bar{N}_{22} & \cdots & \bar{N}_{2n} \\
\vdots & \vdots & & \vdots & \vdots & \vdots & & \vdots \\
0 & 0 & \cdots & \dot{N}_{mm}+\dot{W}_m & \bar{N}_{m1} & \bar{N}_{m2} & \cdots & \bar{N}_{mn} \\
\hline
\bar{N}_{11}^T & \bar{N}_{21}^T & \cdots & \bar{N}_{m1}^T & \ddot{N}_1+\ddot{W}_1 & 0 & \cdots & 0 \\
\bar{N}_{12}^T & \bar{N}_{22}^T & \cdots & \bar{N}_{m2}^T & 0 & \ddot{N}_2+\ddot{W}_2 & \cdots & 0 \\
\vdots & \vdots & & \vdots & \vdots & \vdots & & \vdots \\
\bar{N}_{1n}^T & \bar{N}_{2n}^T & \cdots & \bar{N}_{mn}^T & 0 & 0 & \cdots & \ddot{N}_n+\ddot{W}_n
\end{array}\right]
\left[\begin{array}{c}
\dot{\delta}_1 \\ \dot{\delta}_2 \\ \vdots \\ \dot{\delta}_m \\ \hline \ddot{\delta}_1 \\ \ddot{\delta}_2 \\ \vdots \\ \ddot{\delta}_n
\end{array}\right]
=
\left[\begin{array}{c}
\dot{c}_{11}-\dot{W}_1\dot{\epsilon}_1 \\ \dot{c}_{22}-\dot{W}_2\dot{\epsilon}_2 \\ \vdots \\ \dot{c}_{mm}-\dot{W}_m\dot{\epsilon}_m \\ \hline \ddot{c}_1-\ddot{W}_1\ddot{\epsilon}_1 \\ \ddot{c}_2-\ddot{W}_2\ddot{\epsilon}_2 \\ \vdots \\ \ddot{c}_n-\ddot{W}_n\ddot{\epsilon}_n
\end{array}\right]$$

in which

$$\dot{N}_{ii} = \sum_{j=1}^{n} \dot{B}_{ij}^T \dot{W}_{ij} \dot{B}_{ij} , \qquad \dot{c}_{ii} = \sum_{j=1}^{n} \dot{B}_{ij}^T \dot{W}_{ij} \dot{\epsilon}_{ij} ,$$

(92) $$\bar{N}_{ij} = \dot{B}_{ij}^T \dot{W}_{ij} \ddot{B}_{ij} ,$$

$$\ddot{N}_i = \sum_{j=1}^{n} \ddot{B}_{ij}^T \ddot{W}_{ij} \ddot{B}_{ij} , \qquad \ddot{c} = \sum_{j=1}^{n} \ddot{B}_{ij}^T \ddot{W}_{ij} \ddot{\epsilon}_{ij} .$$

The upper left hand portion of the normal equations consists of m diagonally arranged 9x9 blocks of elements, each such block corresponding to the elements of orientation for a particular exposure station. When the elements of interior orientation are rigidly enforced to precalibrated values (as would normally be the case in aerial photogrammetry), the 9x9 blocks reduce to 6x6 blocks. In general, any parameter of the normal equations

may be enforced at the value employed in the linearization of the projective relations by simply deleting the rows and columns of the normal equations corresponding to the parameters. This is equivalent to the operation of letting the a priori weight (in the $\dot{W}$ or $\ddot{W}$ matrix) of the parameter approach infinity. By so doing one forces the solution for the given parameter to assume the value of zero, which, when substituted in the remaining equations, eliminates the parameter from the overall system.

The lower right hand portion of the normal equations consists of n diagonally arranged 3x3 blocks of elements, each such block corresponding to the coordinates of a particular control point. B, making the appropriate diagonal element of the $\ddot{W}$ matrix for a given point sufficiently large, one can force the adjustment to reproduce a pre-established value of any coordinate of the point to within any desired tolerance. One could, of course, rigidly enforce a given control point by striking out the rows and columns of the normal equations corresponding to the point. Again, this would be tantamount to giving the point infinite weight.

1.12 THE REDUCED NORMAL EQUATIONS

When the number of unknown elements of orientation is not excessively large, it becomes practical to reduce the general normal equations (91) to a system of lower order by a process of inversion of a partitioned system. The practicability of this approach depends on the fact that, by virtue of diagonality, the inversion of the lower right hand matrix of the normal equations $(\ddot{N}+\ddot{W})$ consists merely of the inversion of n individual 3x3 matrices (the $\ddot{N}_j+\ddot{W}_j$) and, hence, can be accomplished no matter how great the number of control points. As shown in our earlier paper (Brown, 1958a), inversion by partitioning leads to the following expressions for $\dot{\delta}$ and $\ddot{\delta}$:

$$(93) \qquad \dot{\delta} = \dot{M}(c - W\epsilon) + \bar{M}(\ddot{c} - \ddot{W}\epsilon) \ .$$

$$(94) \qquad \ddot{\delta} = \bar{M}^T(\dot{c} - \dot{W}\epsilon) + \ddot{M}(\ddot{c} - \ddot{W}\epsilon) \ .$$

in which

$$(95) \qquad \dot{M} = [\ \dot{N} + \dot{W} - \bar{N}(\ddot{N}+\ddot{W})^{-1}\bar{N}^T\ ]^{-1} \ ,$$

$$(96) \qquad \ddot{M} = (\ddot{N}+\ddot{W})^{-1} + (\ddot{N}+\ddot{W})^{-1}\bar{N}^T\dot{M}\bar{N}(\ddot{N}+\ddot{W})^{-1} \ .$$

$$(97) \qquad \bar{M} = -\dot{M}\bar{N}(\ddot{N}+\ddot{W})^{-1} \ .$$

If we set

$$(98) \qquad Q = (\ddot{N}+\ddot{W})^{-1}\bar{N}^T \ .$$

and note that $\bar{M}$ in (97) then can be written

$$(99) \qquad \bar{M} = -\dot{M}Q^T \ ,$$

the expression (93) for $\dot{\delta}$ may be put into the form

$$(100) \qquad \dot{\delta} = \dot{M}[\ \dot{c} - \dot{W}\epsilon - Q^T(\ddot{c} - \ddot{W}\epsilon)\ ] \ .$$

We shall refer to (100) as the reduced system of normal equations. A more convenient alternative expression for $\ddot{\delta}$ can be derived from (94) by first using (98) to express $\ddot{M}$ in (96) as

$$(101) \qquad \ddot{M} = (\ddot{N}+\ddot{W})^{-1} + Q\dot{M}Q^T$$

and then substituting this together with (99) into (94), getting, upon collecting terms

$$(102) \quad \ddot{\delta} = (\ddot{N}+\ddot{W})^{-1}(\ddot{c}-\ddot{W}\ddot{\epsilon}) - Q M [\dot{c} - \dot{W}\dot{\epsilon} - Q^T(\ddot{c}-\ddot{W}\ddot{\epsilon})]$$

in which, by virtue of (100), the postmultiplier of Q in the second term may be replaced by $\dot{\delta}$, thus reducing the expression for $\ddot{\delta}$ to simply

$$(103) \quad \ddot{\delta} = (\ddot{N}+\ddot{W})^{-1}(\ddot{c}-\ddot{W}\ddot{\epsilon}) - Q\dot{\delta} \quad .$$

This expression for $\ddot{\delta}$ differs from that in our earlier paper (Brown, 1958a) in that the approximations for control are not required necessarily to be precomputed in a manner forcing $\ddot{c} - \ddot{W}\ddot{\epsilon}$ to zero.

The partitioning employed in the formation of the normal equations can be exploited to derive a convenient cumulative process for forming the reduced normal equations(100). From the data generated by the j^{th} control point, one would compute the intermediate matrices

$$(104) \quad Q_j = (\ddot{N}_j + \ddot{W}_j)^{-1} \bar{N}_j^T$$

$$(105) \quad R_j = \bar{N}_j Q_j$$

$$(106) \quad S_j = \dot{N}_j - R_j$$

$$(107) \quad \bar{c}_j = \dot{c}_j - Q_j^T (\ddot{c}_j - \ddot{W}_j \ddot{\epsilon}_j) \quad .$$

As S_j and $\bar{c}_j$ are formed they are cumulatively added to their predecessors yielding, after the final control point has thus been processed,

(108) $S = S_1 + S_2 + \ldots + S_n$

(109) $\bar{c} = \bar{c}_1 + \bar{c}_2 + \ldots + \bar{c}_n$

In terms of these the solution for $\dot{\delta}$ becomes

(110) $\dot{\delta} = (S + \dot{W})^{-1}(\bar{c} - \dot{W}\dot{\epsilon})$.

Once $\dot{\delta}$ has thus been determined, the solution for each control point can be computed in turn from

(11') $\ddot{\delta}_j = (\ddot{N}_j + \ddot{W}_j)^{-1} - Q_j \dot{\delta}$,

which is a direct consequence of the partitioning of (103).

The reduction based on equations (104) through (111) has a number of attractive properties:

(a) the order of the largest matrix to be formed, inverted or otherwise operated on, is equal to the total number of unknown elements of orientation and is completely unaffected by the number of control points involved in the reduction;

(b) the computations are so arranged that data arising from a given control point are processed independently of the data from any other control point up to the stage of the cumulative formation of the reduced normal equations (this means that the internal storage required of the computer depends almost exclusively on m and is essentially independent of n);

(c) for $n >> m$ the total number of computations is essentially proportional to $m^2 n$ rather than to m^3 as would have been the case had the coefficient matrix of the normal equations been completely filled with nonzero elements.

1.13 THE PROCESS OF ITERATION

Before the final residuals are computed, it may be necessary to iterate the adjustment a number of times in order to reduce the effects of higher order terms to insignificance. For this reason we rewrite equations (110) and (111) to reflect the solutions resulting from the $\imath^{th}$ iteration of the adjustment:

$$(112) \quad \dot{\delta}^{(\imath)} = (S^{(\imath)} + \dot{W})^{-1} (c^{(\imath)} - \dot{W}\, \dot{\epsilon}^{(\imath)}) ,$$

$$(113) \quad \ddot{\delta}_j^{(\imath)} = (\ddot{N}_j^{(\imath)} + \ddot{W}_j)^{-1} (\ddot{c}_j^{(\imath)} - \ddot{W}_j\, \ddot{\epsilon}_j^{(\imath)}) .$$

The initial solution corresponds to the case $\imath = 0$, and each subsequent solution results from the relinearization of the original observational equations about the values resulting from the preceding solution. The process of iteration should be continued until a sufficiently stable solution is obtained.

Inasmuch as initial approximations are essentially arbitrary, nothing would have prevented us from letting the a priori observations of elements of orientation and coordinates of control serve as initial approximations for the linearization of the observational equations. By thus setting

$$
\begin{aligned}
\alpha_i^{00} &= \alpha_i^0 & X_j^{00} &= X_j^0 \,, \\
\omega_i^{00} &= \omega_i^0 & Y_j^{00} &= Y_j^0 \,, \\
&\vdots & Z_j^{00} &= Z_j^0 \,. \\
(Z_i^c)^{00} &= (Z_i^c)^0
\end{aligned}
\tag{114}
$$

we would have reduced the initial discrepancy vectors $\dot{\epsilon}^{(0)}$ and $\ddot{\epsilon}^{(0)}$ to zero vectors. As a result, the discrepancy vectors to be used for the first iteration of the adjustment would have become

$$
\begin{aligned}
\dot{\epsilon}^{(1)} &= \dot{\epsilon}^{(0)} + \dot{\delta}^{(0)} = \dot{\delta}^{(0)} \,, \\
\ddot{\epsilon}^{(1)} &= \ddot{\epsilon}^{(0)} + \ddot{\delta}^{(0)} = \ddot{\delta}^{(0)} \,,
\end{aligned}
\tag{115}
$$

and in general

$$
\begin{aligned}
\dot{\epsilon}^{(i)} &= \dot{\epsilon}^{(i-1)} + \dot{\delta}^{(i-1)} = \dot{\delta}^{(0)} + \dot{\delta}^{(1)} + \ldots + \dot{\delta}^{(i-1)} \,, \\
\ddot{\epsilon}^{(i)} &= \ddot{\epsilon}^{(i-1)} + \ddot{\delta}^{(i-1)} = \ddot{\delta}^{(0)} + \ddot{\delta}^{(1)} + \ldots + \ddot{\delta}^{(i-1)} \,.
\end{aligned}
\tag{116}
$$

We see then that, although initial discrepancy vectors for $\dot{\epsilon}$ and $\ddot{\epsilon}$ can be made equal to zero by the natural and perfectly valid equating of initial approximations and a priori observations, this does not mean that subsequent discrepancy vectors $\dot{\epsilon}$ and $\ddot{\epsilon}$ arising from the process of iteration are equal to zero. Indeed as (115) shows, discrepancy vectors for $\dot{\epsilon}$ and $\ddot{\epsilon}$ subsequent to zero initial vectors are no longer arbitrary, but are equal to the sum of all preceding adjustments of the parameters. It is because this fact could have been so easily overlooked that we chose to give prominence to the vectors $\dot{\epsilon}$ and $\ddot{\epsilon}$ by avoiding the natural choice for initial approximations which would have rendered $\dot{\epsilon}$ and $\ddot{\epsilon}$ equal to zero.

1.14 ERROR PROPAGATION

After the final iteration of the solution, equations (26), (34), and (40) can be solved for the final vectors of residuals, giving

$$
\begin{aligned}
v &= \epsilon - B\delta - \overset{\bullet\bullet}{B}\overset{\bullet\bullet}{\delta} - \overset{\bullet\bullet\bullet\bullet}{B}\overset{\bullet\bullet\bullet\bullet}{\delta} \\
\overset{\bullet}{v} &= \overset{\bullet}{\epsilon} - \overset{\bullet}{\delta} \quad , \qquad (117) \\
\overset{\bullet\bullet}{v} &= \overset{\bullet\bullet}{\epsilon} - \overset{\bullet\bullet}{\delta} \quad .
\end{aligned}
$$

If the process of iteration were carried to the point where the final vectors $\overset{\bullet}{\delta}$, $\overset{\bullet\bullet}{\delta}$ were reduced to insignificance, equations (117) would reduce to

$$
\begin{aligned}
v &= \epsilon \quad , \\
\overset{\bullet}{v} &= \overset{\bullet}{\epsilon} \quad , \qquad (118) \\
\overset{\bullet\bullet}{v} &= \overset{\bullet\bullet}{\epsilon} \quad ,
\end{aligned}
$$

in which the discrepancy vectors are those resulting from the substitution of the final parameters into the original observational equations.

The quadratic form of the residuals arising from the adjustment is

$$
(119) \qquad s = \bar{v}^T \bar{W} \bar{v} = v^T W v + \overset{\bullet}{v}^T \overset{\bullet}{W} \overset{\bullet}{v} + \overset{\bullet\bullet}{v}^T \overset{\bullet\bullet}{W} \overset{\bullet\bullet}{v} \quad .
$$

The degrees of freedom associated with the quadratic form is equal to the number of observations in excess of the minimum required for a unique solution. In the case where all control points were to appear on all plates and where a priori values were available for all elements of orientation, the total number of observations n_0 would be equal to $2mn+9m+3n$ and the degrees of freedom

would become $f = n_0 - (9m+3n) = 2mn$. In most cases of interest, however, only a relatively few of the total number of control points will appear on a given plate. This situation is readily handled by assigning dummy observations having zero weights to those control points not appearing on a given plate. In this manner the theory can be made to hold for any observational situation and total number of observations n_0 becomes equal to the number of nonzero diagonal elements in the composite weight matrix $\overline{W}$. With n_0 thus reckoned, the degrees of freedom for the adjustment becomes, in general,

$$f = n_0 - (9m + 3n). \tag{120}$$

If a total of $\hat{m}$ of the 9m elements of orientation were rigidly enforced (thereby reducing the order of the normal equations), the term 9m in (120) should be replaced by $9m-\hat{m}$. Similarly, if $\hat{n}$ of the 3n coordinates of control actually were to consist of relative control for which the assigned variances of the approximations were grossly relaxed, the term 3n in (120) should be replaced by $3n-\hat{n}$. On the other hand, if the assigned variances of the approximations employed for relative control were considered to be fairly realistic, the term 3n would be better left unaltered.

If the observational vector has the multivariate normal distribution, the statistic

$$\chi_0^2 = s \tag{121}$$

will have the chi square distribution with f degrees of freedom. This may be exploited in statistical testing of the adequacy of the adjustment. The estimate of unit variance arising from the adjustment is given by

$$\sigma_0^2 = s/f\,. \tag{122}$$

Ideally, σ_0^2 should be equal to unity. From the chi square test one can determine whether or not the departure of σ_0^2 from unity is statistically significant.

The covariance matrix of the adjusted parameters is provided by the inverse of the coefficient matrix of the normal equations. In particular, the covariance matrix of the adjusted elements of orientation is

$$(123) \quad \dot{\Sigma} = (S + \dot{W})^{-1} = \dot{M}$$

and that of the adjusted vector of coordinates of control is

$$(124) \quad \ddot{\Sigma} = \ddot{M} = (\ddot{N} + \ddot{W})^{-1} + Q \dot{M} Q^T .$$

The submatrix of $\ddot{\Sigma}$ corresponding to the j^{th} control point can be shown to be

$$(125) \quad \ddot{\Sigma}_j = (\ddot{N}_j + \ddot{W}_j)^{-1} + Q_j \dot{M} Q_j^T .$$

The first term of this equation $(\ddot{N}_j + \ddot{W}_j)^{-1}$ represents the covariance matrix of the adjusted coordinates of control under the assumption that the elements of orientation are error free. The second term $Q_j \dot{M}_j Q_j^T$ represents the contribution to the error in triangulation of errors remaining in the adjusted elements of orientation. With a sufficiently strong photogrammetric net, one could hope to suppress the contribution of the second term to insignificance relative to the first. This is generally the case with a ballistic camera net where abundant stellar control can be exploited to reduce the errors in the calibrated elements of orientation to insignificance. On the other hand, with aerial photography the effects of residual error in adjusted elements of orientation are difficult to suppress sufficiently when absolute control is minimal.

7.15 COMPARISON WITH OTHER THEORIES

An alternative treatment of the problem of adjusting the observed coordinates of control points merits consideration. Let us first rewrite the observational equations arising from the projective equations and from the coordinates of control. These are

$$(126)\qquad \begin{aligned} v + \dot{B}\dot{\delta} + \ddot{B}\ddot{\delta} &= \epsilon\,, \\ \ddot{v} - \ddot{\delta} &= \ddot{\epsilon}\,. \end{aligned}$$

As discussed earlier, we are at perfect liberty to choose the approximations for the coordinates of control to be equal to their observed values, thereby rendering $\ddot{\epsilon} = 0$. Assuming this to be done, we may write $\ddot{v} = \ddot{\delta}$ and then eliminate the parametric vector $\ddot{\delta}$ from the first of the above pair of equations, thus getting

$$(127)\qquad v + \ddot{B}\ddot{v} + \dot{B}\dot{\delta} = \epsilon\,.$$

We may rewrite this as

$$(128)\qquad A\bar{v} + \dot{B}\dot{\delta} = \epsilon$$

where A and $\bar{v}$ are now defined as

$$(129)\qquad \underset{(2mn,b)}{A} = \underset{(2mn,2mn)(2mn,3n)}{(\ I \qquad \ddot{B}\ )}, \qquad \underset{(b,1)}{\bar{v}} = \begin{bmatrix} \underset{(2mn,1)}{v} \\ \\ \underset{(3n,1)}{\ddot{v}} \end{bmatrix}$$

where $b = 2mn + 3n$. By virtue of the elimination of the parametric vector $\ddot{\delta}$ from the linearized projective equations, we have reduced the number of unknown param-

eters and, hence, the arder af the general normal equatiors from 9m + 3n to simply 9m. The normal equations for the present approach are

$$(130) \qquad [\dot{B}^T (A \bar{\Lambda} A^T)^{-1} \dot{B}] \dot{\delta} = \dot{B}^T (A \bar{\Lambda} A^T)^{-1} \epsilon$$

where $\bar{\Lambda}$ is now defined as

$$(131) \quad \underset{(b,b)}{\bar{\Lambda}} = \begin{bmatrix} \underset{(2mn,2mn)}{\Lambda} & 0 \\ 0 & \underset{(3n,3n)}{\ddot{\Lambda}} \end{bmatrix}$$

The formation af the normal equations is thusseen to entail the formation and inversion of the intermediate matrix

$$(132) \qquad \underset{(2mn,2mn)}{G} = \underset{(2mn,b)}{A} \underset{(b,b)}{\bar{\Lambda}} \underset{(b,2mn)}{A^T} \quad .$$

By virtue of (129) and (131) this may be written

$$(133) \qquad G = \begin{bmatrix} I & \ddot{B} \end{bmatrix} \begin{bmatrix} \Lambda & 0 \\ 0 & \ddot{\Lambda} \end{bmatrix} \begin{bmatrix} I \\ \ddot{B}^T \end{bmatrix} = \Lambda + \ddot{B} \ddot{\Lambda} \ddot{B}^T \quad .$$

From the partitioning of B and $\ddot{\Lambda}$ indicated in (27) and (36) we may write

$$(134) \quad \ddot{B} \ddot{\Lambda} \ddot{B}^T \begin{bmatrix} \ddot{B}_1 & 0 & \dots & 0 \\ 0 & \ddot{B}_2 & \dots & 0 \\ \vdots & \vdots & & \\ 0 & 0 & \dots & \ddot{B}_n \end{bmatrix} \begin{bmatrix} \ddot{\Lambda}_1 & 0 & \dots & 0 \\ 0 & \ddot{\Lambda}_2 & \dots & 0 \\ \vdots & \vdots & & \vdots \\ 0 & 0 & \dots & \ddot{\Lambda}_n \end{bmatrix} \begin{bmatrix} \ddot{B}_1^T & 0 & \dots & 0 \\ 0 & \ddot{B}_2^T & \dots & 0 \\ \vdots & \vdots & & \vdots \\ 0 & 0 & \dots & \ddot{B}_n^T \end{bmatrix}$$

which reduces to

$$(135)\qquad \overset{\cdot\cdot}{B}\,\overset{\cdot\cdot}{\Lambda}\,\overset{\cdot\cdot}{B}^{T} = \begin{bmatrix} \overset{\cdot\cdot}{B}_1\overset{\cdot\cdot}{\Lambda}_1\overset{\cdot\cdot}{B}_1^{T} & 0 & \cdots & 0 \\ 0 & \overset{\cdot\cdot}{B}_2\overset{\cdot\cdot}{\Lambda}_2\overset{\cdot\cdot}{B}_2^{T} & \cdots & 0 \\ \vdots & \vdots & & \vdots \\ 0 & 0 & \cdots & \overset{\cdot\cdot}{B}_n\overset{\cdot\cdot}{\Lambda}_n\overset{\cdot\cdot}{B}_n^{T} \end{bmatrix} .$$

This is a diagonal matrix of n matrices of dimension 2m by 2m. Inasmuch as Λ is a diagonal matrix of mn matrices of dimension 2x2, it follows that the required inversion of G breaks down to the inversion of n individual matrices of dimension 2m x 2m. On the other hand, in the approach we developed in Subsection 1.12 the reduction of the normal equations to an equivalent 9m x 9m system was accomplished through the inversion of n intermediate matrices of order 3x3 (the $\overset{\cdot\cdot}{N}_j$). It follows that the approach of the present section, though mathematically equivalent to that developed earlier, entails grossly more computation for large m; in fact, only in the case of the single photo (m=1) does the present approach entail less computation (for this case it provides a practical solution to the problem of photogrammetric resection of a single camera when the given control is subject to significant error).

Schmid (1959) published a solution similar in many respects to that of Brown (1958a). One major difference is in Schmid's treatment of errors in control points. For the general case in which all n points appear on all m photos, Schmid employs an approach wherein the coordinates of each ground control point are adjusted independently for each photograph. Within the framework of the present subsection, we can reconstruct the essentials of Schmid's solution as follows. The typical 2m x 2m submatrix $\overset{\cdot\cdot}{B}_j\,\overset{\cdot\cdot}{\Lambda}_j\,\overset{\cdot\cdot}{B}_j^{T}$ appearing in (135) may, by the partitioning of (24), be expanded to

$$(136)\quad \ddot{B}_j \ddot{\Lambda}_j \ddot{B}_j^T = \begin{bmatrix} \ddot{B}_{1j} \\ \ddot{B}_{2j} \\ \vdots \\ \ddot{B}_{mj} \end{bmatrix} \ddot{\Lambda}_j \begin{bmatrix} \ddot{B}_{1j}^T & \ddot{B}_{2j}^T & \cdots & \ddot{B}_{mj}^T \end{bmatrix}$$

$$(137)\quad \ddot{B}_j \ddot{\Lambda}_j \ddot{B}_j^T \qquad \begin{bmatrix} \ddot{B}_{1j} \ddot{\Lambda}_j \ddot{B}_{1j}^T & \ddot{B}_{1j} \ddot{\Lambda}_j \ddot{B}_{2j}^T & \cdots & \ddot{B}_{1j} \ddot{\Lambda}_j \ddot{B}_{mj}^T \\ \ddot{B}_{2j} \ddot{\Lambda}_j \ddot{B}_{1j}^T & \ddot{B}_{2j} \ddot{\Lambda}_j \ddot{B}_{2j}^T & \cdots & \ddot{B}_{2j} \ddot{\Lambda}_j \ddot{B}_{mj}^T \\ \vdots & \vdots & & \vdots \\ \ddot{B}_{mj} \ddot{\Lambda}_j \ddot{B}_{1j}^T & \ddot{B}_{mj} \ddot{\Lambda}_j \ddot{B}_{2j}^T & \cdots & \ddot{B}_{mj} \ddot{\Lambda}_j \ddot{B}_{mj}^T \end{bmatrix}$$

This is a filled nxm matrix of matrices of dimensions 2x2. In Schmid's treatment only the diagonal elements of above matrix are actually formed. This is equivalent to setting

$$(138)\quad \ddot{B}_{kj} \ddot{\Lambda}_j \ddot{B}_{\ell j}^T = 0 \quad \text{for all } k \neq \ell \,.$$

In this manner, the matrices $\ddot{B}_j \ddot{\Lambda}_j \ddot{B}_j^T$ in (137) are all reduced to diagonal matrices of m 2x2 matrices and this in turn reduces $\ddot{B} \ddot{\Lambda} \ddot{B}^T$ (and, hence, also $A \bar{\Lambda} A^T$ which, in Schmid's solution, is termed $A P^{-1} A^T$) to a diagonal matrix of mn 2x2 matrices. Thus the inversion of $A \bar{\Lambda} A^T$ becomes the equivalent of the simple inversion of mn 2x2 matrices in place of the far more formidable inversion of n 2mx2m matrices as in the rigorous development.

The effect of unlocking the $B_j \ddot{A}_j B_j'$ matrices by the arbitrary imposition of (138) can be theoretically justified only if the coordinates of the control points were somehow to shift randomly about their true positions from one exposure to the next. Inasmuch as the world is not made of jelly, such an approach is unsound in our opinion. Moreover, because the coordinates of a given absolute control point are free to shift independently for each plate, they will tend to compensate unduly for errors in the measured plate coordinates and will, thus, lead to attractively small, but spurious, plate residuals. This consequence may also be viewed as stemming from the fact that the degrees of freedom for the adjustment are, in effect, grossly increased from the correct value of $f = 2mn + \hat{m} - 9m$ (for the case where all control is considered to be subject to adjustment and appears on all photos) to $f = 2mn + 3mn + \hat{m} - 9m - 3n$.

Schmid (1959, p. 38) discusses the possibility of modifying the adjustment so that control points subject to error are adjusted only once within a given photogrammetric net, but, instead of developing the approach fully, he advocates (because of computational difficulties) an alternative two step approach in which

(1) the adjustment is performed first with all absolute control treated as purely relative control except for the minimum control needed for a unique solution (this leads to a photogrammetric model that is approximately correctly translated, rotated and scaled);

(2) coordinates of the resulting model are subsequently further refined by means of a seven parameter transformation (three translations, three rotations, and change of scale) determined in a second adjustment by the minimization of the sum of the squares of the residual distances between the model coordinates and the known coordinates of the withheld absolute control.

Schmid suggests that the above means of circumventing the computational difficulties inherent in the strictly correct adjustment of control subject to error is "from the theoretical standpoint sufficiently rigorous." Our results and experience would seem to contradict this. If, for example, one were to withhold all but minimal control from the adjustment of a long strip that is affected only by random errors of measurement, the typical result would be a sinuous deformation of the model because of unfavorable propagation of random error (systematic error would contribute a secular component to such deformation). When only minimal absolute control is exercised in the simultaneous adjustment of all photos in the strip, the build-up of quasi-systematic deformation is not prevented, although the degree of such deformation is not as severe as in the case of a photo-by-photo cantilever extension. With a sufficiently long strip, the overall deformation is characterized by several slowly changing cycles of positive and negative departure. It follows that when the model is subjected to a rigid transformation (three translations and three rotations) coupled with a uniform stretch, only a small part of the total deformation will be removed, for such a transformation can accommodate, at best, only one-half cycle of quasi-systematic error over the length of the strip. The end results of such an approach will ordinarily bear little resemblance to the results one would obtain from exercising all available control in the original adjustment of the strip. The effect of utilizing control in this manner is to 'pinch' the build-up of quasi-systematic error to zero (very nearly) in the vicinity of each absolute control point. For the limiting case of absolute control of unrestricted abundance, one can suppress the build-up of quasi-systematic error to complete insignificance, provided the control is actually exercised in the photogrammetric adjustment. On the other hand, if it is for the most part withheld, as suggested by Schmid, such control can do nothing to squelch the inevitable build-up of significant, sequentially correlated deformation of low spatial frequency.

Aside from ultimate considerations of accuracy, there is another cogent reason why available absolute control should be exercised in the adjustment rather than being withheld for subsequent determination of a 'corrective' transformation of one kind or another (e.g., the rigid transformation advocated by Schmid or more complex polynomial transformations advocated by Schut (1964), Harris, Tewinkel, Whitten (1962), and others). As will presently be demonstrated, we have found that the rate of convergence of the recommended iterative solution of the normal equations is accelerated by the introduction of absolute control. Once a certain critical level of control is attained, convergence can be speeded by as much as an order of magnitude. For a long strip, the critical level appears, on the average, to be a pair of fresh absolute control points per four to five photos.

As we demonstrated in Subsections 1.06 and 1.11, the rigorous adjustment of absolute control subject to significant error is computationally very simple within the framework of the concept of the ellipsoidal control point, for such control can be treated precisely in the same manner as relative control, the only distinction being in the lower magnitudes of the elements of the covariance matrices (the $\ddot{\Lambda}_j$) of the absolute control. In view of this and in view of the foregoing discussion, we most strongly advocate that the entire store of available observational material be utilized in the simultaneous adjustment of a photogrammetric net. The general theory developed in this paper is sufficiently comprehensive to accommodate virtually any conceivable type of information that might be applicable to the photogrammetric problem.

Before we leave this subsection to take up the problem of the solution of the normal equations for large photogrammetric nets, it is appropriate to review the few remaining differences of consequence between the writer's earlier solution (Brown, 1958a, 1958b, 1959) and that of Schmid (1959). For the introduction of partial absolute control expressed in terms of latitude ϕ, longitude λ, and height h, Schmid

employs an approach similar to that of Dodge (1959). A partial control point given by h, for instance, is considered to define a spheroidal surface on which the rays are forced to intersect through the introduction of the appropriate observational equation. By the same token, appropriate observational equations defining specific cones and planes are imposed for partial control given in terms of ϕ and λ. In the approach of Brown (1959), partial control expressed in terms of ϕ, λ and/or h is treated as in Subsection 1.06 of the present report (in the earlier report, the terminology 'relaxation of quasi-observational variances' was employed in place of the 'ellipsoidal control point' of the present report). Here, instead of forcing rays to intersect on various mathematical surfaces (or intersection thereof), one constrains the rays to intersect as closely as possible to the center of an appropriately defined ellipsoid of probability. By virtue of this concept, all essential distinction between various types of control points is erased; all possibilities are embraced by the ellipsoidal control point.

The extended solution outlined in Brown (1959) provided the first (and, to this point, the only) treatment of the problem of adjusting any of the elements of orientation considered to be observed quantities subject to random errors. This opened up the possibility of the rigorous incorporation of auxiliary data gathered by those external sensors which could be considered to be sensibly unbiased (information from unbiased sensors can be fully absorbed by the matrices W and ϵ). The primary theoretical innovation of the present report is the extension of the solution to apply to auxiliary sensors whose observations may be biased to a significant degree. The primary practical innovation is the demonstration of the feasibility of certain of the iterative procedures for the solution of the enormous systems of normal equations generated by large photogrammetric nets.

Aside from the differences outlined above between the solutions of Schmid (1959) and of Brown (1958a, 1959), there are virtually no further differences of consequence between the two insofar as the fundamental photogrammetric adjustment

is concerned. In our comparative analysis we have concentrated mainly on Schmid's theory because, in our view, it is, in spite of a few lapses in rigor, the only competing theory which aspires to the simultaneous adjustment of a general photogrammetric net with comparable theoretical and statistical soundness. Also, the precise relationship between the two theories has not, we feel, generally been appreciated by the photogrammetric community.

1.16 THE PROBLEM OF ADJUSTING LARGE BLOCKS OF AERIAL PHOTOGRAPHY

The reduction of the normal equations developed in Subsection 1.12 has proven effective in geodetic applications and in applications to small to medium blocks of aerial photography (on the order of 20 to 30 photos). However, problems of rounding error and computing time ultimately render this approach impractical for relatively large blocks (on the order of 40 photos or more). This means that, if large blocks of photography are to be successfully adjusted as organic units, an effective alternative to the reduction of the normal equations must be developed. The development of such an alternative is actually the primary objective of this investigation. Toward this end, we have concentrated mainly on the problem of adjusting large blocks of aerial photography having fairly consistent patterns of forward and side overlap. Our original approach was based on the following considerations:

(1) the coefficient matrix of the general normal equations for an aerial block is both highly patterned and highly sparse (i.e., consists predominantly of zero elements);

(2) by means of an appropriate indexing algorithm, it is possible to collapse the full coefficient matrix of the normal equations to a far more compact matrix containing few zero elements;

(3) this 'collapsed system' of normal equations can be computed directly, thus by-passing the unnecessary computation of zero elements;

(4) a computing algorithm can be formulated to exploit the collapsed system of normal equations to effect, if practical, the solution by means of recently developed iterative procedures which are vast improvements on the classical Gauss-Seidel method;

(5) the computing algorithm can be designed to operate on natural blocks of elements of the normal equations, rather than on a single row at a time;

(6) through a process called "intertwining," it is possible to rearrange the coefficient matrix of the general normal equations in such a manner as to achieve a highly diagonal form which could conceivably be conducive to the more rapid convergence of the iterative process.

The rationale of our approach is perhaps best presented in terms of concrete examples. Let us begin with consideration of the form of the general normal equations arising from what we shall term a 'uniform block.' A uniform photogrammetric block is one which has a consistent, self-reproducing pattern of control and overlap. A specific illustration of a uniform block four photos wide and five photos long is presented in Figure 1.1. Each photo in the block has a consistent nine point pattern of control (we use the term 'control' here in the broad sense to denote anything from a relative control point (pass point) to an absolute control point; all are ellipsoidal control points). The forward overlap is sixty per cent and side overlap is twenty per cent. Except where boundary conditions prevail, each triple overlap area and each sextuple overlap area contains one and only one control point. In practice, of course, it is most unlikely that one will obtain blocks of photography displaying such uniform characteristics of overlap. On the contrary, it is not unusual for there to be gaps in the side overlap and for there to be different numbers of photos in contiguous strips, thus rendering the strips 'out of phase' insofar as the uniform block is concerned. In some instances, such difficulties could be rectified by the twofold expedients of (a) inserting dummy observations having zero weight matrices, (b) inserting both dummy observations having zero weight matrices and appropriate dummy photos having nonzero weight matrices. Thus, for example, if a control point for a certain position were to be missing on one

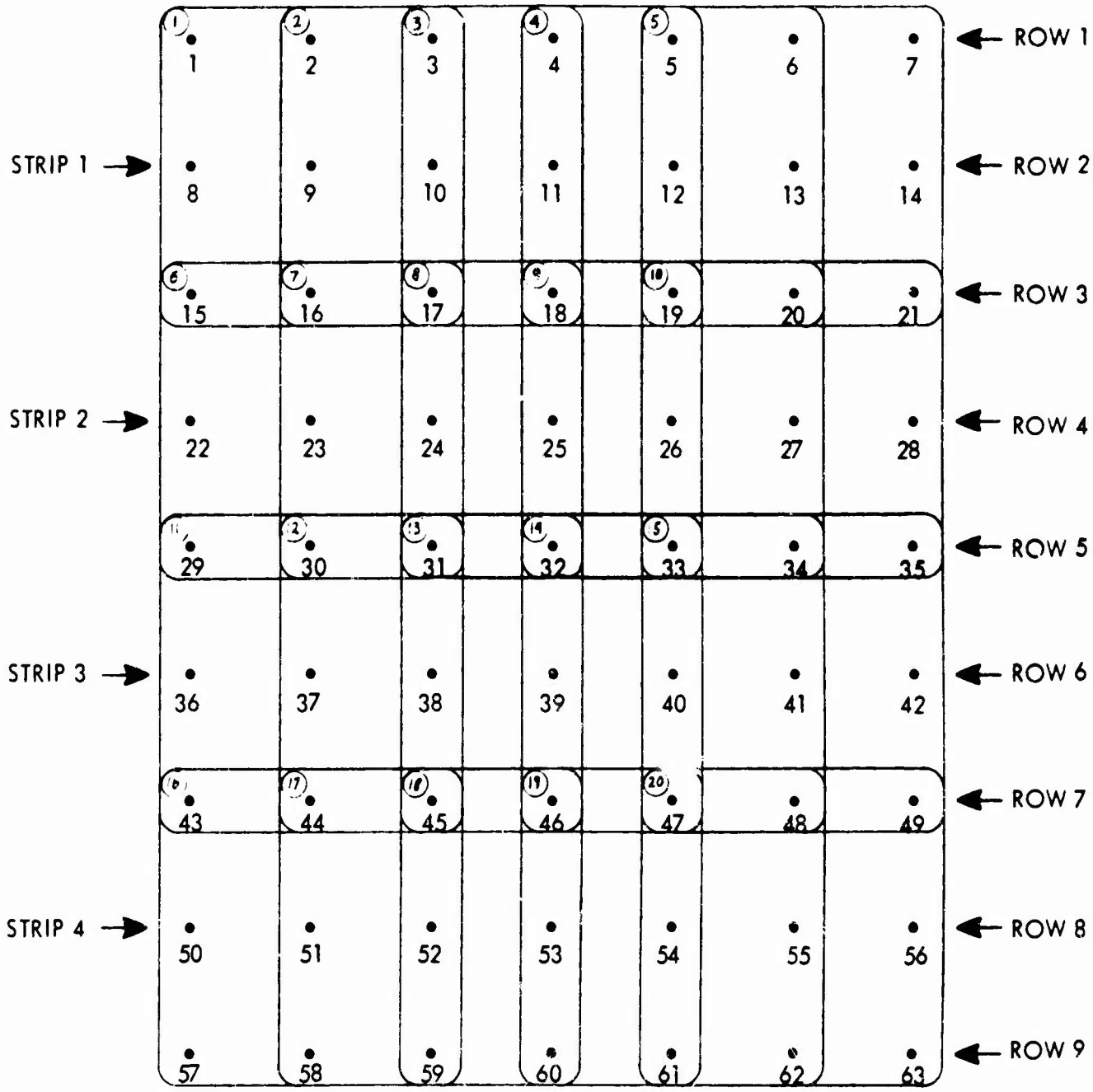

Figure 1.1 Illustrating Uniform Block of Dimensions 4x5. Numbering of Control Points and Photos is According to Rows.

or more photos (as might easily happen if sidelap were to fall outside of tolerance), one could assign dummy plate coordinates, say (0,0), to the missing image and assign zero weights to these plate coordinates. By virtue of such weighting, the dummy coordinates will in no way affect the final results. In a similar manner, complete gaps in the photography or phasing discrepancies of strips can often be rectified through the insertion of dummy photos having dummy images. To avoid indeterminacy, the assigned elements of orientation of dummy photos must be given finite weights. When introduced in this manner, dummy photos have no effect on the end results, but yet do contribute to the complete predictability of the data flow. This is of great value in the exploratory formulation of simple indexing algorithms for the collapsing and subsequent implicit reconstruction of the coefficient matrix of the normal equations. For this reason, at the outset of our investigation we confined our consideration to uniform blocks. Once the effectiveness of our proposed approach had been demonstrated, we abandoned the stipulation that a uniform block be employed for, even with the aid of dummy observations and dummy photos, the transformation of an actual block into a uniform block can prove to be cumbersome, except for the case of the isolated strip.

With the understanding, then, that our consideration of the uniform block is strictly for exploratory purposes, we may proceed to investigate the character of the normal equations of the form (91) as generated by the adjustment of the sample block of Figure 1.1. The form of this coefficient matrix is indicated in Figure 1.2a. The solid and shaded areas of the figure correspond to nonzero elements; all other areas are filled by zero elements. The most striking characteristics of the coefficient matrix are

(a) the regularity of the pattern,

(b) the predominance of zero elements.

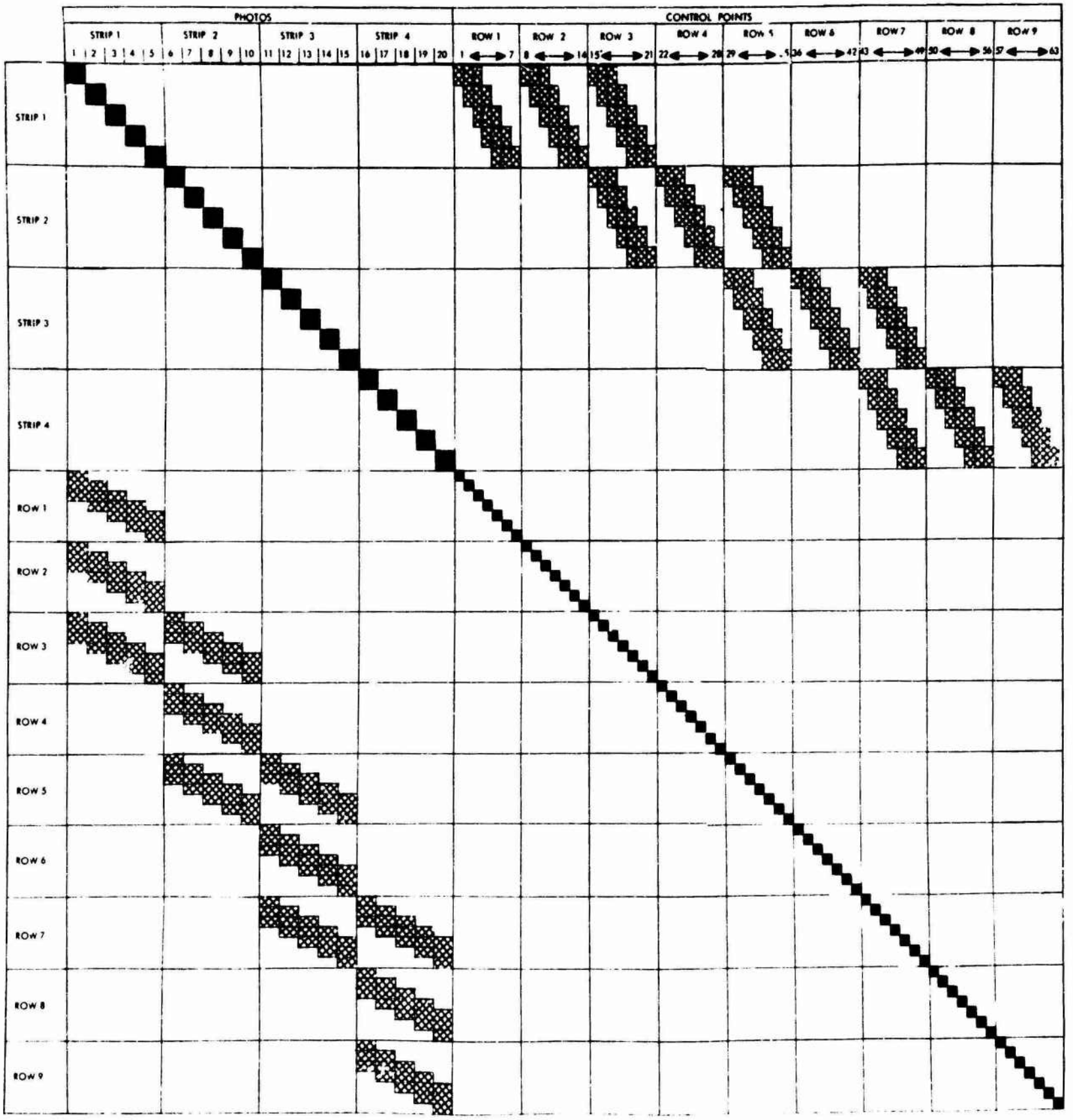

FIGURE 1.2a. FORM OF COEFFICIENT MATRIX GENERATED BY UNIFORM BLOCK WITH POINTS AND PHOTOS NUMBERED AS IN FIG. 1.1. EACH SMALL SQUARE REPRESENTS A 3x3 BLOCK OF ELEMENTS; ORDER OF FULL MATRIX IS 309x309.

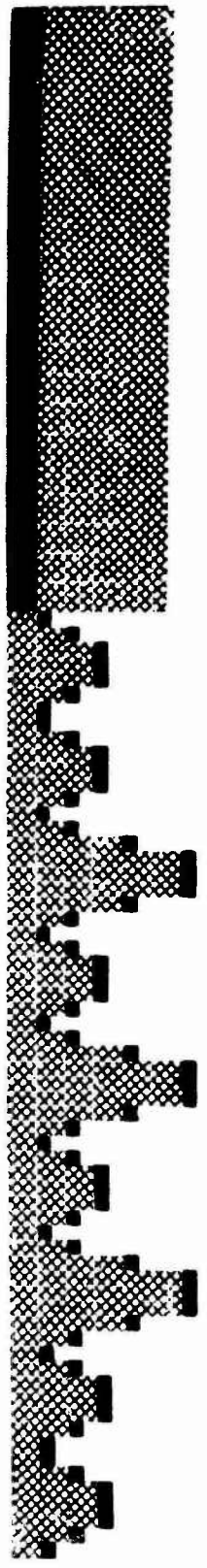

FIGURE 1.2b. COLLAPSED FORM OF COEFFICIENT MATRIX OF FIG. 1.2a.

The submatrices $\bar{N}_{ij}$ of the $\bar{N}$ portion of the normal equations are nonzero matrices only when the j^{th} point appears on the i^{th} photograph, in which case the $\bar{N}_{ij}$ interlocks the corresponding $\dot{N}_{ii}$ and $\ddot{N}_{j}$ portions of the normal equations. The portion of the matrix corresponding to $\bar{N}$ may be described as consisting of four 'landings' of 'staircase' matrices with three parallel staircases to a landing. Each individual staircase is generated by a particular row of control points; the longer the row the longer the staircase. Each landing is generated by a particular strip; the number of landings is equal to the number of strips. The number of staircases per landing is equal to the number of rows of control points per strip. The last staircase in each landing lies directly over the first staircase in the next landing. This is a consequence of the control in the side overlap (were there no control in the side overlap, the normal equations for the block would degenerate into separable sets of independent normal equations for strips). From the foregoing considerations, it becomes a simple matter to generalize the pattern of the normal equations in Figure 1.2a to apply to a uniform block of any dimensions, as long as the basic nine point pattern of control is maintained and the numbering of photos and control points corresponds to that of Figure 1.1. For instance, if the block were 4x50 instead of 4x5, the staircases would merely become lengthened to 50 steps instead of 5 steps. The $\dot{N}+\dot{W}$ portion of the matrix would consist of 200 diagonally arranged, nonoverlapping 6x6 matrices instead of 20, and the $\ddot{N}+\ddot{W}$ portion would be increased from 63 diagonally arranged, nonoverlapping 3x3 matrices to 378. In general, the number of control points in a uniform block of the type of Figure 1.1 is $(2s+1)x(p+2)$ where s denotes the number of strips and p is the number of photos per strip. If the 4x50 block were now increased, to, say, a 10x50, the effect on the $\bar{N}$ portion of the matrix would be merely to increase the number of staircase landings from 4 to 10 with each landing consisting of 3 parallel staircases 50 steps high, the first staircase in each landing being directly below the last staircase in the landing above. The $\dot{N}+\dot{W}$ and $\ddot{N}+\ddot{W}$ matrices would increase to 500 diagonally arranged 6x6 matrices and to 1092 diagonally arranged 3x3 matrices, respectively. The order of the general normal equations would thus become $6x500 + 3x1092 = 6276$.

As a uniform block becomes larger and larger, the ratio of the number of nonzero elements to the total number of elements in N (the coefficient matrix) decreases drastically. For the type of block of Figure 1.1 this ratio is

$$\frac{\text{number of nonzero elements in N}}{\text{total number of elements in N}} = \frac{9\,(42sp + 4s + p + 2)}{9\,(4sp + 4s + p + 2)^2}$$

$$\cong \frac{2.6}{sp} \quad \text{for large s and p.}$$

Thus, in a 4x5 block about 1 element in 12 is nonzero, in a 4x50 black the ratio is about 1 in 76, and in a 10x50 block it is abaut 1 in 194. The fact that the normal equations are so highly patterned with such a small portion of the elements being nonzero suggests

(a) that the normal equations be formed in such a manner that only the nonzero elements are actually generated,

(b) that an alternative representation of the normal equations be developed to exploit to the fullest the patterned characteristics of the equations and to render the system as compact as possible,

(c) that the solution of the normal equations be effected by a suitable iterative process designed to operate only on the blocks of nonzero elements.

With regard to (a) there is no particular problem. The logic of generating only the nonzero constituents of the normal equations is fairly simple and straightforward. With regard to (b) there is again no particular problem, for the coefficient matrix of the general normal equations can be 'callapsed' to the compact scheme indicated in Figure 1.2b. Here all zero blocks of elements have been 'squeezed' out of the original normal equations by sliding each nonzero sub-block to the left as far as possible. The solid blocks in Figure 1.2b correspond to the diagonal blocks of the original normal equations. We

see that the collapsed normal equations are also highly patterned. It is clearly possible to establish a set of rules or algorithms by means of which the elements of the collapsed matrix can be related to their counterparts in the original matrix. Inasmuch as the collapsed system in conjunction with a small set of algorithms is sufficient to reconstruct the original system, there is really no need to generate the original system in the first place. It is sufficient to generate the collapsed system directly. Not only can this be done, but it can be done on a relatively small digital computer such as the IBM 1620 (not that we necessarily recommend this). This is true no matter what the dimensions of the block, for the maximum number of columns in the collapsed system can never exceed 39 (this again assumes the 9 point pattern of control of Figure 1.1). The only effect of increasing the length or width of the block is to lengthen the collapsed matrix of normal equations; it can never be widened. Thus the computer can be programmed in such a manner as to generate the collapsed normal equations row by row or, more naturally, horizontal block by horizontal block. The total computational time in setting up the collapsed system will thus increase only linearly with the number of photos in the block. It is this fact that makes the use of a small computer feasible for this stage of the reduction.

With regard to point (c) above, it is a relatively simple matter to set up an iterative solution that will operate only on the nonzero blocks of elements. The pivotal question is whether or not a prohibitive number of iterations will be required for adequate convergence. Unfortunately, this question cannot be answered in advance on the basis of purely theoretical considerations. The answer is to be obtained only by actual trial through numerical simulation of various typical operational situations of particular interest. The great bulk of our effort in the present investigation has been directed toward this end. Details of the numerical processes employed and of the results obtained are given in Section 2. We shall confine our attention in the remainder of this section to further development of the general approach and to a brief discussion of the high points of our numerical results.

1.17 ALTERNATIVE ARRANGEMENTS OF THE NORMAL EQUATIONS

Let us take the block of Figure 1.1, but, instead of numbering the photos and control points according to rows, let us number them according to columns as in Figure 1.3. The general normal equations then assume the alternative form indicated in Figure 1.4a, the collapsed form of which is indicated in Figure 1.4b. The $\bar{N}$ portion of this system is somewhat simpler than in our earlier system of Figure 1.2a. This raises the question of whether one arrangement offers any practical advantage over the other with regard to rapidity of convergence of the iterative process. It also raises the broader question of the role played by the arrangement of the normal equations in general. Is there some optimal arrangement offering significant advantages?

In our further investigation of arrangements of the normal equations, we were able to devise orderings of the unknowns which would confine all nonzero blocks of elements to lie with a limited band about the diagonal. The normal equations for one such arrangement are indicated in Figure 1.5a and, in collapsed form, in Figure 1.5b. Here, the numbering of photos and points is according to columns as in Figure 1.3. However, the vector of unknowns has been rearranged according to the following scheme in which successive sub-vectors of the solution vector are listed horizontally:

$\ddot{\delta}_1, \dot{\delta}_1, \ddot{\delta}_2, \ddot{\delta}_3, \dot{\delta}_2, \ddot{\delta}_4, \ddot{\delta}_5, \dot{\delta}_3, \ddot{\delta}_6, \ddot{\delta}_7, \dot{\delta}_4, \ddot{\delta}_8, \ddot{\delta}_9$	1st column of photos and points
$\ddot{\delta}_{10}, \dot{\delta}_5, \ddot{\delta}_{11}, \ddot{\delta}_{12}, \dot{\delta}_6, \ddot{\delta}_{13}, \ddot{\delta}_{14}, \dot{\delta}_7, \ddot{\delta}_{15}, \ddot{\delta}_{16}, \dot{\delta}_8, \ddot{\delta}_{17}, \ddot{\delta}_{18}$	2nd column of photos and points
$\ddot{\delta}_{19}, \dot{\delta}_9, \ddot{\delta}_{20}, \ddot{\delta}_{21}, \dot{\delta}_{10}, \ddot{\delta}_{22}, \ddot{\delta}_{23}, \dot{\delta}_{11}, \ddot{\delta}_{24}, \ddot{\delta}_{25}, \dot{\delta}_{12}, \ddot{\delta}_{26}, \ddot{\delta}_{27}$	3rd column of photos and points

etc.

The control point vectors δ_{46} through δ_{63} generated by the last two columns of control terminate the sequence of unknowns. This system of normal equations may be said to be dominated by elements on and near the diagonal. All nonzero elements are confined to a diagonal band 225 elements in width; moreover, within this band one can define five narrower bands (each 21 elements in width) which contain all nonzero elements except those generated by the last two columns of control. An attractive feature of this

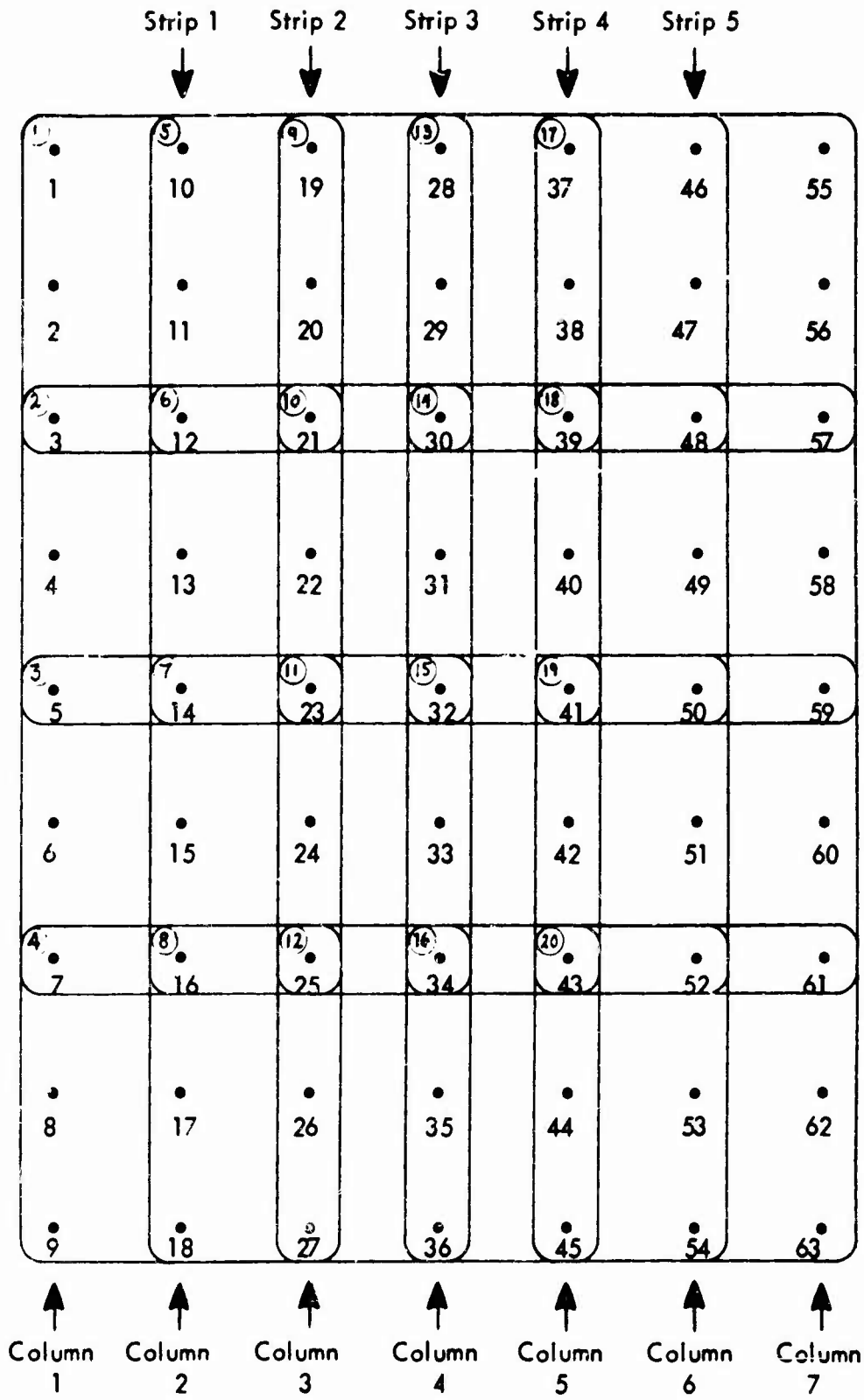

Figure 1.3 Illustrating Uniform Block of Dimensions 4x5. Numbering of Control Points and Photos is According to Columns. Strips are Considered to Run Vertically.

arrangement of the normal equations is that the width of the diagonal band confining all nonzero elements is independent of either the length or the width of the block of photos. In this sense, then, as the dimensions of the block increase, so does the relative diagonality of the normal equations. In the case of a 10x50 block, for instance, the diagonal band containing all nonzero elements will comprise only about three per cent of the matrix.

We have employed the term 'intertwining' to describe the process of reordering the unknowns for the purpose of achieving relatively strong diagonality. The guiding principle of the process of intertwining is the devising of an arrangement of the normal equations such that the coefficients of the unknowns corresponding to a given control point are as close in the matrix as possible to those photos on which the points appear.

At the outset of the investigation the writer's collaborators devised two other schemes of intertwining of greater compactness and efficiency than that of Figure 1.5a. These are illustrated in Figures 2.21 and 2.22 of Section 2. During the course of the investigation we learned that our initial enthusiasm for the prospective effectiveness of intertwining as a means for accelerating the convergence of the iterative solution of the normal equations was unwarranted, for the simpler and more prosaic orderings of Figures 1.2 and 1.4 actually turned out to be more effective in this regard. As we shall see in Section 2, the failure of intertwining to live up to expectations, though a blow to our intuition, is hardly to be regarded as an untoward result, particularly in view of the relative complexity of the collapsing algorithms associated with the process. Moreover, since future investigators may profit from our negative finding by avoiding the duplication of this particular approach, we feel our discussions of the concept of intertwining are justified.

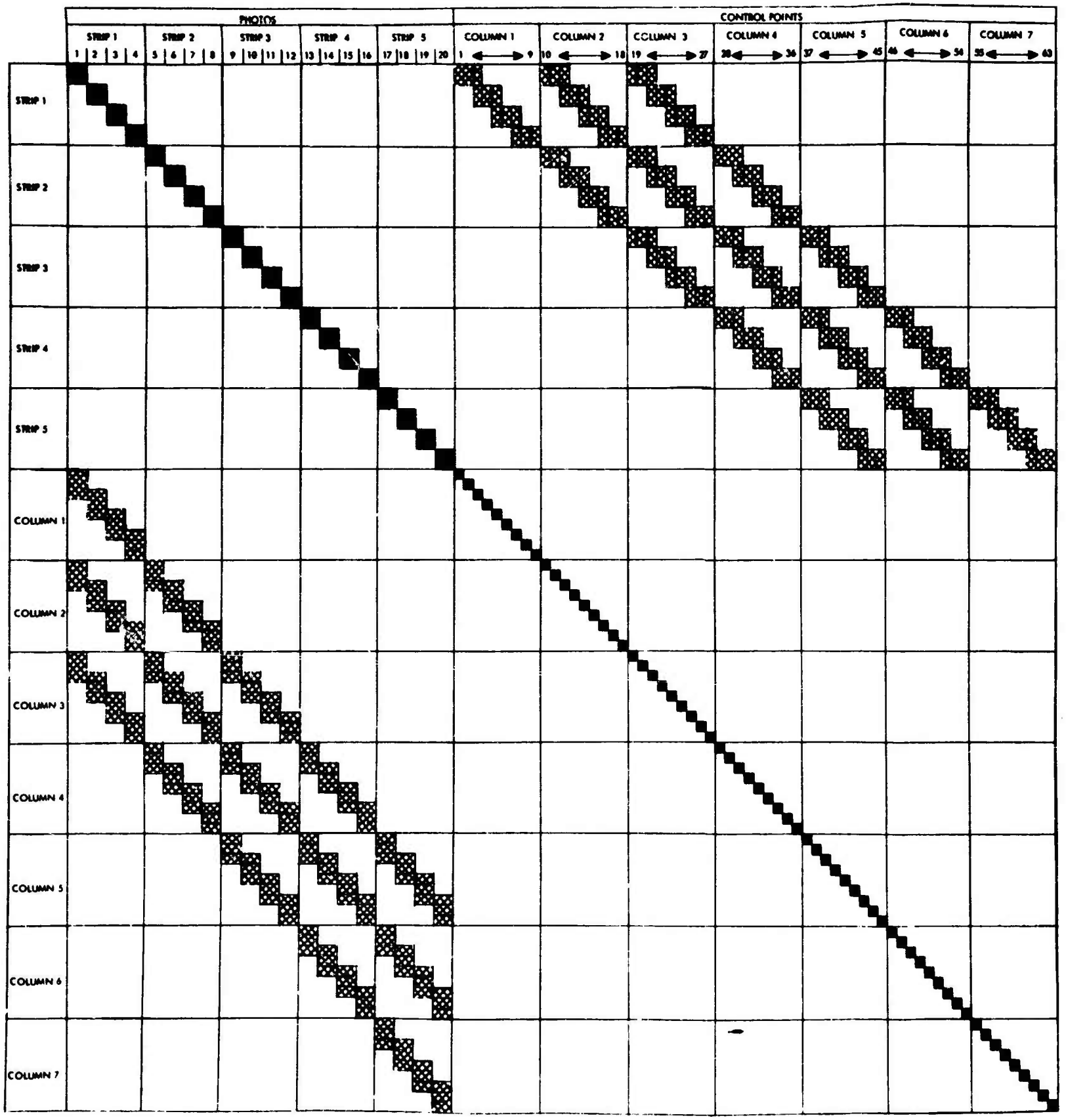

FIGURE 1.4a. FORM OF COEFFICIENT MATRIX GENERATED BY UNIFORM BLOCK WITH POINTS AND PHOTOS NUMBERED AS IN FIGURE 1.3. THE FIVE STRIPS OF THIS BLOCK ARE CONSIDERED TO BE VERTICAL STRIPS RATHER THAN HORIZONTAL STRIPS AS IN FIGURE 1.1.

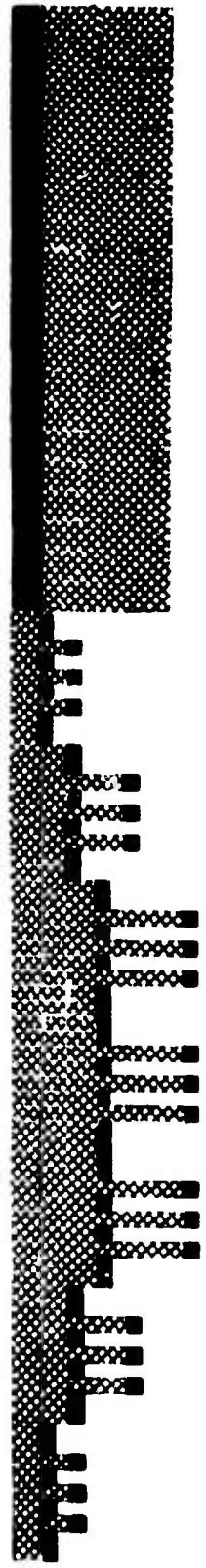

FIGURE 1.4b. COLLAPSED FORM OF COEFFICIENT MATRIX OF FIG. 1.4a.

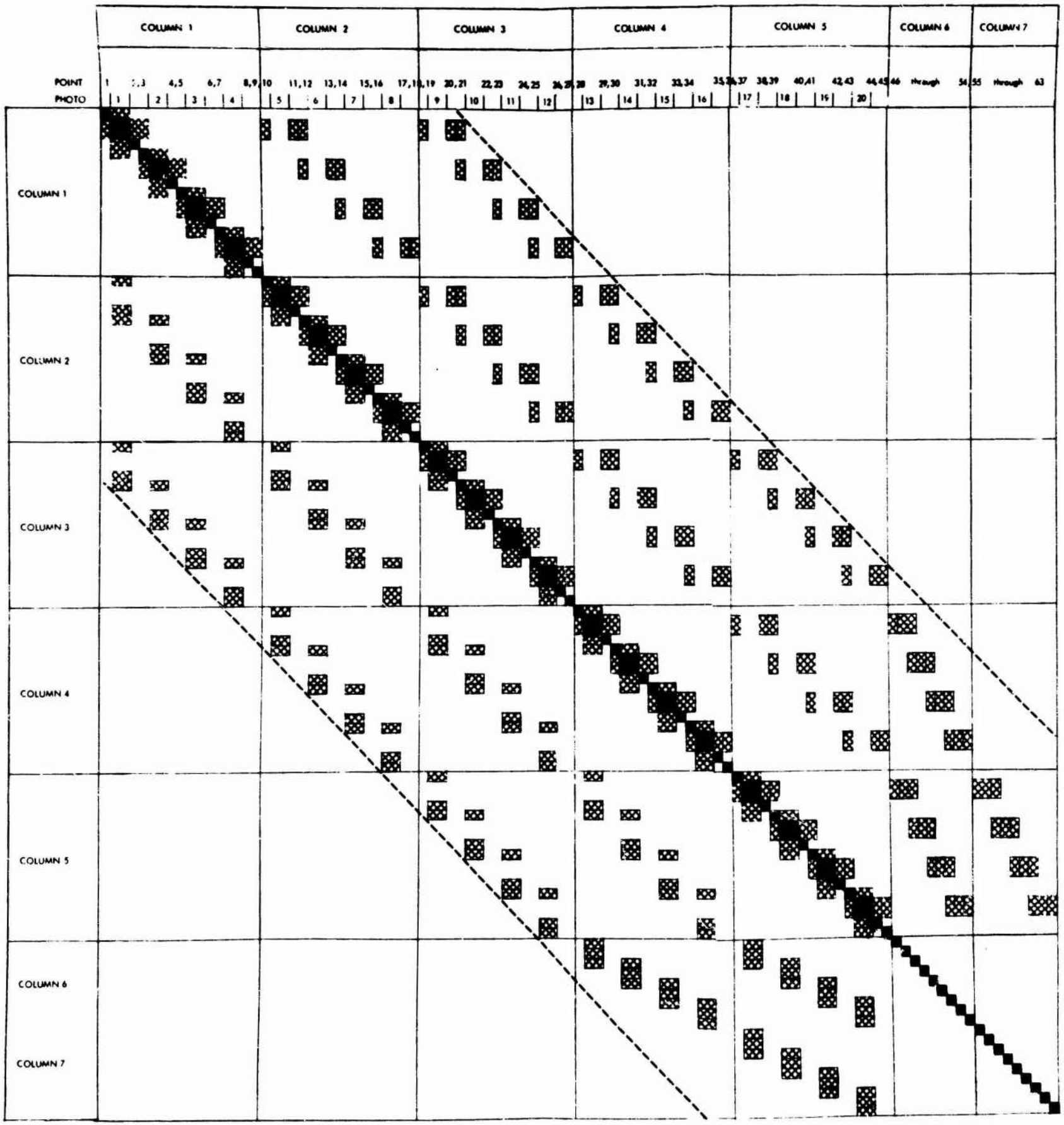

FIGURE 1.5a. EXAMPLE OF INTERTWINED FORM OF COEFFICIENT MATRIX OF NORMAL EQUATIONS NUMBERING OF PHOTOS AND CONTROL POINTS CORRESPONDS TO THAT OF FIGURE 1.3.

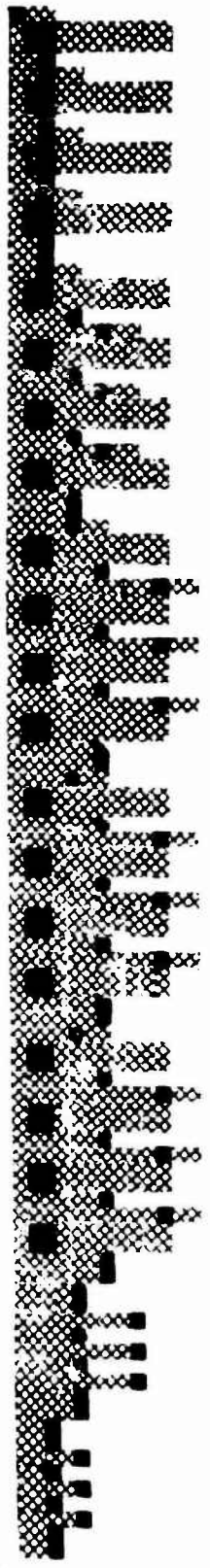

FIGURE 1.5b COLLAPSED FORM OF COEFFICIENT MATRIX OF FIGURE 5a

1.18 OUTLINE OF KEY RESULTS

The results of our initial four months of effort ore summarized in on interim report (Brown, Davis, Johnson, 1963) which is now superceded by this, the final report. By a process of numerical simulation we were able to estoblish in the interim report thot of the three iterative techniques investigated

1. Gauss-Seidel,
2. Gauss-Seidel with Luisternik accelerotion (Faadevo, 1959),
3. Method of Successive Over Reloxotion (Varga, 1962),

the first was far too slow in converging to be considered practicol, and the second blew up numerically. On the other hand, the third provided excellent results, converging to a satisfactory solution for a simuloted 25-photo strip in less thon 10 minutes on on IBM 7094.

One of our most significant findings concerns the effect of obsolute control on the rate of convergence of the iterotive process. A strip hoving only the minimal obsolute control required for determinocy wos found to converge appreciably more slowly than one having a moderate sprinkling of control throughout the strip. With o 41-photo strip generating o system of normal equations of order 633, for instance, odequate convergence wos obtained within 150 iterotions (6 minutes on an IBM 7094) when o pair of fresh absolute control points was introduced on about every fifth phcto. On the other hand, on the order of 600 iterations were required when the same strip was odjusted with absolute control limited to the beginning of the strip (full detalls are given in Section 2). Our simulations to date indicate that the number of iterations required for satisfactory convergence is roughly equol to the order of the normal equotions for the cose of strips with minimal obsolute control; for strips having a moderate level of well-distributed absolute control, the number of iterotions may be as few as one fifth to one tenth of the order of the normal equotions. There is even some indication that once a certain level of obsolute control is attoined, the number of iterations for satisfactory convergence may be only very weakly dependent of the order of the normal equations. If further investigotion should prove this to be the cose, the distinct

possibility emerges that the simultaneous adjustment of a long strip of aerial photography may entail no more than the general order of computational effort as is required for the reconstruction of the strip by means of analytic cantilever extension operating on poirs of photos.

Toward the end of our study we were successful in devising an efficient collapsing algorithm for the normal equations generated by a general, non-uniform block of photography. Our limited numerical simulations with blocks lead us to believe that, in full scale practical application, the rigorous adjustment of large blocks of aerial photography will involve appreciably less computational effort than the adjustment of long strips having comparable numbers of photos and levels of control. To appreciate this, one should view the conventional aerial block as a continuous, folded strip. In such a folded strip, control in the side-overlap is common to subintervals of the strip and serves, therefore, to reduce appreciably the number of unknown control points. The resulring reduction of the order of the normal equations and the bi-directionality of computational transference made possible by side-overlap constraints combine to accelerate the convergence of the iterative solution of the normal equations of the block. It is this that ultimately renders the block computationally more attractive than the strip, even though the logic of the data handling for the block is more complicated.

1.19 CONCLUSIONS

Our central goal of developing a computationally feasible procedure for solving the normal equations for large photogrammetric nets has been successfully attained. In particular, we have removed the primory impediment to the implementation of the rigorous adjustment of large blocks of aerial photography. By virtue of the successful implementation of the concept of the direct formation of the collapsed normal equations the computing time required for the formation of the normal equations for an aerial block becomes strictly proportional to the number of photos in the block rather than increasing as the square of the number of photos as in previous

reductions. With sufficiently large blocks having a sufficient level of absolute control, there is some evidence to suggest that the number of iterative cycles required for adequate convergence of the normal equations may level off to an almost stationary value, little affected by the inclusion of additional photos. If this should bear up under further investigation, it will mean that not only the formation of the normal equations but also their solution will be essentially proportional to the number of photos in adequately controlled aerial blocks of sufficient size. We believe that the simultaneous adjustment of blocks of several thousand photos will prove to be altogether feasible through the implementation of optimal buffering procedures wherein external storage (tape, magnetic disks, etc.) and core storage are both used to maximum advantage. In this regard, we would point out that Varga (1962, p.1) tells of a computer program designed to accomplish the iterative solution of a system of simultaneous equations of order 108,000 generated by the numerical solution of a three dimensional system of partial differential equations. In view of this coupled with our success in applying iterative procedures to the photogrammetric problem, we feel that the time is at hand when the photogrammetrist need no longer be intimidated by the enormous systems of equations arising from the uncompromisingly rigorous adjustment of large blocks of photography.

Our numerical investigations so far have been limited to the realm of classical photogrammetry where auxiliary sensors play no role. Yet, with the development of such integrated mapping configurations as the Air Force USQ-28 system, it is clear that we are at the threshold of a new era in photogrammetry in which auxiliary sensors will become of increasing importance. Anticipating this, we extended the theory of the general photogrammetric adjustment in a nonrestrictive fashion to accommodate information from any conceivable combination of auxiliary sensors with due allowance being made for the likelihood that the output of many such sensors may be subject to significant bias and hence may have to be calibrated within the framework of the over-all adjustment. We are of the opinion that the role of analytical techniques will be increased, rather than diminished, by the implementation of integrated mapping systems exploiting various

arroys of ouxiliory sensors. Just os the introduction of o certoin level of obsolute control serves to accelerate greatly the convergence of the iterotive solution of the normal equotions, so too, we suspect, would the introduction of constroints imposed by ouxiliory sensors. In our future work we expect to determine to what extent this is the case ond to concentrote on the potential contribution to the photogrammetric odjustment of vorious combinations of existing ond proposed ouxiliary sensors.

SECTION 2

NUMERICAL ANALYSIS AND NUMERICAL RESULTS

By

Duane C. Brown
Ronald G. Davis
Frederick C. Johnson

2.01 INTRODUCTION

The development of the theory of the general photogrammetric adjustment and of a specific approach to the solution of the normal equations has been accomplished in Section 1. Our objectives in this section are to provide a detailed account of the steps taken to test and implement this approach and to present and interpret results obtained.

The first part of this section is devoted to an expository treatment of iterative procedures for the solution of simultaneous linear equations with particular emphasis on the Method of Successive Over Relaxation. Following this, we describe the successive stages of our numerical investigation beginning with the simulation of the basic two photo problem and proceeding to simulated six photo strips, twenty-five photo strips and forty-one photo strips (the maximum that can be handled in core of a 32K IBM 7094). Each stage of these strip simulations was designed to answer certain specific questions and each provided unexpected insight into various facets of the general problem. From the simulation of strips, we proceeded to the simulation of small blocks (3x5 photos) and finally to the reduction of a 23 photo strip of actual photography. As we shall see, the results of our numerical studies confirm the validity of the approach developed in Section 1.

2.02 GENERAL BACKGROUND ON ITERATIVE METHODS OF SOLVING LINEAR EQUATIONS

Because of the excessive dimensions of the system of normal equations generated by a sizeable photogrammetric block, direct methods of solving the system (e.g., Gaussian elimination or one of its many variants) are not practical. Unfortunately, such methods tend to collapse due to the excessive amount of round-off error introduced into the solution of large systems by the required machine calculations.

To alleviate the undesirable consequences arising from the round-off error introduced by direct methods of solution, recourse may be made to iterative methods. The advantage of such methods is that the original system of equations or some simple transformation thereof remains unaltered in memory throughout all stages of the calculation of the solution thus adding a great stabilizing factor to the computational process.

The first of the iterative procedures was developed by C. Jacobi (1845). This method was improved in 1874 to give the Gauss-Seidel method. Unfortunately, both of these methods suffer from the fact that the rate of convergence for large systems of equations is often very slow; that is to say, many thousands of iterations are often needed for the iterative procedure to converge to a good approximation to the solution of a sizeable system of equations. Since the required computations were necessarily done by hand when these methods were developed, they were considered impractical and fell into a state of temporary disuse except for occasional applications to geodetic reductions and minor roles in other applied fields.

With the advent of the modern electronic computer, iterative methods were again investigated as a method of solving large systems of linear equations. Although the actual computations involved in the iterative process were no longer formidable,

the prohibitively slow rate of convergence of the Jacobi and Gauss-Seidel methods caused these procedures to be used only on moderately large systems of equations and methods of occelerating the rate of convergence were sought. D. Young (1954) developed the method of Successive Overrelaxation (SOR) which may be viewed as a powerful algorithm for accelerating the rate of convergence of the Gauss-Seidel method. With the development of this method and its extension to the block iterative technique (to be discussed shortly) the solution of large systems of linear equations has become feasible for a large class of important problems including (as we shall see) the adjustment of large photogrammetric nets.

2.03 THEORETICAL DEVELOPMENT OF ITERATIVE METHODS

Let us consider a system of n linear equations in n unknowns:

$$
(1)\qquad \begin{aligned}
a_{11}x_1 + a_{12}x_2 + \cdots + a_{1n}x_n &= b_1 \\
a_{21}x_1 + a_{22}x_2 + \cdots + a_{2n}x_n &= b_2 \\
\vdots \qquad\quad \vdots \qquad\qquad \vdots \qquad &\quad \vdots \\
a_{n1}x_1 + a_{n2}x_2 + \cdots + a_{nn}x_n &= b_n
\end{aligned}
$$

If we set

$$
(2)\qquad A = \begin{bmatrix} a_{11} & \cdots & a_{1n} \\ a_{21} & \cdots & a_{2n} \\ \vdots & & \vdots \\ a_{n1} & \cdots & a_{nn} \end{bmatrix}, \quad x = \begin{bmatrix} x_1 \\ x_2 \\ \vdots \\ x_n \end{bmatrix}, \quad b = \begin{bmatrix} b_1 \\ b_2 \\ \vdots \\ b_n \end{bmatrix}
$$

then the system (1) can be written in matrix notation as

$$(3) \qquad Ax = b \ .$$

If we express the coefficient matrix A as the sum

$$(4) \qquad A = D - E - F$$

where

$$D = \begin{bmatrix} a_{11} & 0 & \cdots & 0 \\ 0 & a_{22} & \cdots & 0 \\ \vdots & \vdots & & \vdots \\ 0 & 0 & \cdots & a_{nn} \end{bmatrix}$$

$$(5) \qquad E = \begin{bmatrix} 0 & 0 & 0 & \cdots & 0 & 0 \\ -a_{21} & 0 & 0 & \cdots & 0 & 0 \\ -a_{31} & -a_{32} & 0 & \cdots & 0 & 0 \\ \vdots & \vdots & \vdots & & \vdots & \vdots \\ -a_{n1} & -a_{n2} & -a_{n3} & \cdots & -a_{n,n-1} & 0 \end{bmatrix}$$

$$F = \begin{bmatrix} 0 & -a_{12} & -a_{13} & \cdots & -a_{1n} \\ 0 & 0 & -a_{23} & \cdots & -a_{2n} \\ 0 & 0 & 0 & \cdots & -a_{3n} \\ \vdots & \vdots & \vdots & & \vdots \\ 0 & 0 & 0 & \cdots & -a_{n-1,n} \\ 0 & 0 & 0 & \cdots & 0 \end{bmatrix}$$

then equation (2) becomes

$$(6) \qquad (D - E - F)\,x = b$$

which may be rewritten as

$$(7) \qquad Dx = (E + F)\,x + b.$$

From this we may immediately write

$$(8) \qquad x = D^{-1}(E + F)\,x + D^{-1}b$$

provided none of the a_{ii} are zero. If any of the a_{ii} were zero, we could rearrange the equations to remove this difficulty.

If we let $x^{(0)}$ be the initial approximation to the solution x of (1), then equation (8) can be used to define the iterative procedure

$$(9) \qquad x^{(k+1)} = D^{-1}(E + F)\,x^{(k)} + D^{-1}b \quad .$$

This is the Jacobi iterative method.

Since D is a diagonal matrix, we have

$$(10) \qquad D^{-1} = \begin{bmatrix} \frac{1}{a_{11}} & 0 & 0 & \cdots & 0 \\ 0 & \frac{1}{a_{22}} & 0 & \cdots & 0 \\ \vdots & \vdots & \vdots & & \vdots \\ 0 & 0 & 0 & \cdots & \frac{1}{a_{nn}} \end{bmatrix}$$

Accordingly, if we let

$$(11) \qquad x^{(k)} = \begin{bmatrix} x_1^{(k)} \\ x_2^{(k)} \\ \vdots \\ x_n^{(k)} \end{bmatrix}$$

we can rewrite (9) in its computational form

$$(12) \qquad x_i^{(k+1)} = -\frac{1}{a_{ii}} \sum_{\substack{j=1 \\ j \neq i}}^{n} a_{ij}\, x_j^{(k)} + \frac{1}{a_{ii}} b_i; \quad 1 \leqq i \leqq n .$$

If equation (6) is rewritten as

$$(13) \qquad (D - E)\, x = F x + b,$$

the immediate result

$$(14) \qquad x = (D - E)^{-1} F x + (D - E)^{-1} b$$

can be used to define the iterative procedure

$$(15) \qquad x^{(k+1)} = (D - E)^{-1} F x^{(k)} + (D - E)^{-1} b .$$

This is the Gauss Seidel iterative method.

We can also rewrite (15) in the more simple computational form

$$(16)\quad x_i^{(k+1)} = -\frac{1}{a_{ii}} \sum_{j=1}^{i-1} a_{ij}\, x_j^{(k+1)} + \sum_{j=i+1}^{n} a_{ij}\, x_j^{(k)} - b_i \quad ; \quad 1 \leq i \leq n \ .$$

It should be noticed that the Gauss-Seidel method offers two advantages over the Jacobi method. The first is that the Jacobi method uses only the components af the k^{th} approximate vector in computing the components of the $(k+1)$st appraximate vector, while the Gauss-Seidel method uses each component of the $(k+1)$st approximate vector immediately in the calculation of the remaining components of the $(k+1)$st vector. In ather words, the Gauss-Seidel method always uses the most recent approximation of the individual components of an iterative vector ta calculate the remaining campanent while the Jacobi method does not.

The second advantage of the Gauss-Seidel method is that, since anly the most recent appraximations are used, the components of the $(k+1)$st appraximate vectar may be stored in the same vectar as those af the k^{th} approximate (as soon as a component af the $(k+1)$st vector is calculated, it replaces a component af the k^{th} vector). The Jacobi method, on the other hand, requires that the k^{th} and $(k+1)$st approximate vectars be stored as separate vectars.

Yaung determined an effective way to accelerate the Gauss-Seidel method by the use of the fallowing device. If $\tilde{x}^{(k+1)}$ represents the $(k+1)$st approximate vector as calculated by the Gauss-Seidel method, then the $(k+1)$st approximatian vector for the method of Successive Overrelaxation is given by

$$(17)\quad x^{(k+1)} = x^{(k)} + \omega(\tilde{x}^{(k+1)} - x^{(k)})$$

where ω is some suitably chosen fixed acceleratian parameter.

Expanding (17) by the replacement of $x^{(k+1)}$ by expression (15), we have

$$(18)\quad x^{(k+1)} = x^{(k)} + \omega\left((D-E)^{-1} F x^{(k)} + (D-E)^{-1} b - x^{(k)} \right)$$

$$= x^{(k)} + \omega(D^{-1}E\, x^{(k+1)} + D^{-1} F x^{(k)} + D^{-1} b - x^{(k)})$$

which gives

$$(19)\quad (I - \omega D^{-1}E)\, x^{(k+1)} = (1-\omega)x^{(k)} + \omega D^{-1} F x^{(k)} + \omega D^{-1} b\ .$$

If we let $L = D^{-1}E$ and $U = D^{-1}F$, we have

$$(20)\quad x^{(k+1)} = (I-\omega L)^{-1} [\,(1-\omega) I + \omega U\,] x^{(k)} + \omega (I-\omega L)^{-1} b.$$

This is the formula for the SOR method.

Returning to (17), we can easily obtain the computational form of the SOR method

$$(21)\quad x_i^{(k+1)} = x_i^{(k)} + \frac{\omega}{a_{ii}} \left(- \sum_{j=1}^{i-1} a_{ij}\, x_j^{(k+1)} - \sum_{j=i+1}^{n} a_{ij}\, x_j^{(k)} + b_i - a_{ii}\, x_i^{(k)}\right).$$

The SOR method possesses all of the advantages of the Gauss-Seidel method while, as will soon be seen, offering a significant increase in the rate of convergence.

2.04 THE BLOCK ITERATIVE METHOD

In the development of the SOR method up to this point each component of the approximate vector has been calculated individually. Such a process is known as a point iterative method. If related groups of components are solved for simultaneously, then the iterative process is known as a block iterative method. Since the elements of orientation of the photographs are naturally related in blocks of order 6 and the coordinates of the ground control points are naturally related in

blocks of order 3, the system of normal equations is highly amenable to block iterative techniques.

Consider again the system of equations

$$A x = b,$$

only now let A be partitioned into submatrices (blocks) in the following manner

$$(21) \quad A = \begin{bmatrix} A_{11} & A_{12} & \cdots & A_{1r} \\ A_{21} & A_{22} & \cdots & A_{2r} \\ \vdots & \vdots & & \vdots \\ A_{r1} & A_{r2} & \cdots & A_{rr} \end{bmatrix}$$

where the A_{ii}'s are square submatrices of A and the A_{ij}'s ($i \neq j$) assume the appropriate dimensions as generated by the diagonal blocks. If A_{ii} has order p and A_{jj} has order q then A_{ij} will have dimensions $p \times q$ and A_{ji} will have dimensions $q \times p$.

In a similar manner let both the x and b vectors be partitioned into subvectors

$$(22) \quad x = \begin{bmatrix} X_1 \\ \vdots \\ X_r \end{bmatrix}, \quad b = \begin{bmatrix} B_1 \\ \vdots \\ B_r \end{bmatrix}$$

If A_{ii} has order p, then both X_i and B_i will have dimensions p x 1. Then, in a manner completely analogous to the development of the point SOR method the computational form of the block SOR method can be obtained.

$$(23) \quad X_i^{(k+1)} = X_i^{(k)} + \omega A_{ii}^{-1} \left(-\sum_{j=1}^{i-1} A_{ij} X_j^{(k+1)} - \sum_{j=i+1}^{n} A_{ij} X_j^{(k)} + B_i - A_{ii} X_i^{(k)} \right) .$$

If all the submatrices of A are single points (have dimensions 1x1), then the block SOR method degenerates into the point SOR method. The theoretical form of the block and point SOR methods are identical (see (20)).

2.05 CONVERGENCE

If we define

$$(24) \quad L_\omega = (I - \omega L)^{-1} ((1-\omega) I + \omega U)$$

then the SOR method becomes

$$(25) \quad x^{(k+1)} = L_\omega x^{(k)} + \omega (I - \omega L)^{-1} D^{-1} b ,$$

and the solution vector x satisifies the identity

$$(26) \quad x = L_\omega x + \omega (I - \omega L)^{-1} D^{-1} b .$$

If we define the error at the k^{th} iteration, $e^{(k)}$, to be the difference between x and $x^{(k)}$, then we have

$$
\begin{aligned}
(27)\quad e^{(k+1)} &= x - x^{(k+1)} \\
&= L_\omega x + \omega(I-\omega L)^{-1}D^{-1} b - (L_\omega x^{(k)} + \omega(I-\omega L)^{-1} D^{-1} b) \\
&= L_\omega x - L_\omega x^{(k)} \\
&= L_\omega (x - x^{(k)}) \\
&= L_\omega e^{(k)}
\end{aligned}
$$

and, therefore,

$$
\begin{aligned}
e^{(1)} &= L_\omega e^{(0)} \\
(28)\quad e^{(2)} &= L_\omega e^{(1)} = L_\omega (L_\omega e^{(0)}) = L_\omega^2 e^{(0)} \\
&\vdots \\
e^{(k)} &= L_\omega^k e^{(0)} \quad .
\end{aligned}
$$

Hence, if the initial error vector $e^{(0)}$ is not equal to the null vector, then it is obvious that the sequence of error vectors

$$e^{(0)}, e^{(1)}, e^{(2)}, \ldots$$

will tend to the null vector if and only if the sequence of matrices

$$L_\omega, L_\omega^2, L_\omega^3, \ldots$$

tends to the null matrix. Any matrix M for which the sequence $M, M^2, M^3, \ldots$ converges to the null matrix is said to be a convergent matrix. It can be shown (Varga, 1962) that an nxn matrix M is convergent if and only if $\rho(M) < 1$ where $\rho(M)$ is called the spectral radius of M and is defined by

$$\rho(M) = \max_{1 \leq i \leq n} |\lambda_i|$$

where the λ_i's are the eigenvalues of M.

Therefore, we have that the sequence of iterative vectors $x^{(0)}, x^{(1)}, x^{(2)}, \ldots$ will converge to the true solution x only if $\rho(L_\omega) < 1$. Varga proves that if the matrix A in the equation

$$A x = b$$

is symmetric and positive definite (as is the case for the coefficient matrix of the normal equations) then $\rho(L_\omega) < 1$ if and only if $0 < \omega < 2$.

Thus, the convergence of the SOR method when applied to the system of normal equations has now been guaranteed provided that ω is chosen such that $0 < \omega < 2$. The question which now arises is the determination of a value for ω which will yield the fastest rate of convergence. In order to be able to develop an explicit formula for an optimal ω, we must be assured that the coefficient matrix A possesses certain additional properties conjointly with symmetry and positive definiteness. Specifically, the coefficient matrix A must be what Varga defines as a consistently ordered 2-cyclic matrix. This is equivalent to Young's definition of a consistently ordered matrix possessing block Property A. Through the use of the ordering vectors (as defined by Varga) associated with the arrangements of the coefficient matrices of the normal equations indicated in Figures 1.2 and 1.4, it can easily be shown that both of these matrices satisfy the additional hypotheses.

If the coefficient matrix is a consistently ordered 2-cyclic matrix, Varga proves that the optimum acceleration parameter ω_b (optimum in the sense that

$\rho(L_{\omega_b}) \leqq \rho(L_\omega)$ for $0 < \omega < 2$) can be explicitly calculated by the formula

$$(29) \qquad \omega_b = \frac{2}{1 + \sqrt{1 - \rho(G)}}$$

where

$$(30) \qquad G = (I - L)^{-1} U .$$

Varga also shows that

$$\rho(L_{\omega_b}) = \omega_b - 1 .$$

Under the above conditions on A, it is also true (Varga) that, if λ is a non-zero eigenvalue of L_ω and if μ satisfies

$$(31) \qquad (\lambda + \omega - 1)^2 = \lambda \omega^2 \mu^2 ,$$

then μ is an eigenvalue of $B = L + U$. Conversely, if μ is an eigenvalue of B and λ satisfies (31), then λ is an eigenvalue of L_ω.

If ω is set equal to 1 in (20) then we have

$$(32) \qquad L_\omega = (I-L)^{-1} U = G$$

and the SOR method reduces to the Gauss-Seidel method.

With $\omega = 1$ and an application of (31), we see that, if μ is an eigenvalue of B, then μ^2 is an eigenvalue of G. Hence, $\rho(G) = \rho^2(B)$ and $\rho(G) < \rho(B)$ since $\rho(G) < 1$.

The rate of convergence R(M) of a matrix M is defined by (Young)

$$(33) \qquad R(M) = -\log(\rho(M)) .$$

Hence, we have $R(G) = 2R(B)$ and, under the previously mentioned conditions, we have that the Gauss-Seidel method (G) converges twice as fast as the Jacobi method ($B = L+U = D^{-1}(E+F)$) . It can also be shown (Varga) that

$$(34) \qquad \lim_{\rho(B)\to 1^-} R(L_{\omega_b}) = 2[R(G)]^{\frac{1}{2}} ,$$

which gives us that

$$(35) \qquad R(L_{\omega_b}) \cong 2[R(G)]^{\frac{1}{2}} > 2R(G).$$

Hence, the SOR method with the optimum acceleration parameter converges approximately twice as fast asymptotically as does the Gauss-Seidel method. It must be emphasized that, in actual practice, the SOR method can and often does offer a much larger increase in the rate of convergence. This is due to the fact that the result in (35) is developed only for the limiting case $\rho(B) \to 1^-$.

The effect of using the block SOR method is to again increase the rate of convergence although no general relationship is known. (For a result restricted to partial differential equations see Arms, Gates and Zondek, 1956). Intuitively, we may view the use of the block SOR method as having the effect of reducing the order of the system of equations thus making the iterative process converge more rapidly.

Rather than attempt to compute $\rho(G)$ explicitly, one can approximate it in the following manner (Young, 1962): Set $\omega = 1$ in formula (21) and perform several iterations while calculating

$$(36) \qquad \rho(G) \cong \frac{\left\| x^{(k+1)} - x^{(k)} \right\|}{\left\| x^{(k)} - x^{(k-1)} \right\|}$$

where

$$(37) \qquad \|x\| \equiv \max_{1 \leq i \leq n} |x_i| \ .$$

2.06 OTHER ITERATIVE METHODS

In the early stages of our study another iterative method, that of Luisternik as described by Faadeva (1959), was investigated. The formula for this method is

$$(38) \qquad x^{(k+1)} = x^{(k+1)} + \frac{1}{1-\mu} \left(\tilde{x}^{(k+1)} - x^{(k)} \right)$$

where $\tilde{x}^{(k+1)}$ is the $(k+1)^{st}$ approximation obtained by the Gauss-Seidel process and μ equals $\rho(G)$ with G defined as in (30).

We would emphasize that our studies have by no means covered all iterative methods worthy of consideration. The fact that other methods were not applied to the photogrammetric problem is in large measure attributable to the very satisfactory results which were obtained with the Method of Successive Over Relaxation. Also some of the iterative methods are highly specialized to apply to matrices generated for the numerical solution of certain systems of partial differential equations and are inherently unsuited

to our problem. The entire field of semi-iterative procedures (Varga) has yet to be applied to the photogrammetric problem. A particularly promising solution referred to as Block Symmetric Successive Over Relaxation (Ehrlich, 1963) came to our attention as we were completing our studies for this report. This is a two step method in which the solution vector proceeds first from the top of the matrix to the bottom in the usual manner but, then, instead recycling to the top again as in normal Successive Over Relaxation, it reverses and proceeds from bottom of the matrix backwards to the top. In some applications the method has been found to yield a substantial improvement in convergence over Block Successive Over Relaxation with no increase in computation. Accordingly, we would strongly recommend that Block Symmetric Successive Over Relaxation receive serious consideration in any future investigations of the photogrammetric application.

Within the past decade or so, the field of iterative techniques for the solution of simultaneous linear equations has become a very fertile area of investigation with new and significant results appearing at frequent intervals. It is our intention to keep abreast of latest developments and to investigate those which would appear to have particular merit in the photogrammetric application. Although we are immensely satisfied with the results obtained so far, we are certain that they can be and will be appreciably improved upon before very long.

2.07 GENERAL APPROACH TO NUMERICAL SIMULATION

Inasmuch as several possible combinations of iterative techniques and arrangements presented themselves at the outset, we decided to confine the initial phase of the study to the application of various approaches to the solution of simulated strips of photography. Both economics and logic dictated such a course of action, for it was clear that if an acceptable solution could not be found for a strip of photography the possibility of developing an acceptable solution for large blocks would be even more remote. On the other hand, success with strips of photos would warrant extension of the approach to embrace blocks.

A process of elimination was carried out in order to determine which specific combination of iterative method and arrangement of normal equations would yield the highest rate of convergence. In order to obtain results which would be as meaningful as possible, it was necessary to generate systems of normal equations similar in general character to those to be expected from actual data. For convenience, we adopted a perfect 9-point pattern of ground control. This assumption in no way compromises the essential validity of the simulation and serves to simplify the data handling. In our initial simulations involving 2-photo, 6-photo and 25-photo strips, the ground points were assumed to lie in the horizontal X-Y plane and to be spaced at 18,000 ft. intervals in both X and Y. Flying height was taken as 40,000 ft. from all photos. This combination of flying height and spacing of control points is appropriate to two thirds forward overlap with a 150 mm (6 inch) lens and a 19 cm (7.5 inch) plate format. In our later simulations involving 41 photo strips and 3x5 blocks, the basic nine point pattern was maintained, but the flying height was raised (in accord with RADC requests) to 50,000 ft. and the spacing of ground control was increased to 30,000 feet (a combination appropriate to 60% forward overlap with a 6 inch lens and a 9x9 inch format). The X axis was considered to be defined by the flight line, along which the middle row of ground control points was also assumed to lie. The x,y plate coordinate axes were taken to be parallel to the X,Y axes, thus rendering the Φ, ω, κ for each photo equal to 0°, 0° and 90° respectively. The general geometry of the simulated photography is illustrated in Fig. 2.1.

The true coordinates of the control points and the true elements of orientation were employed to generate the true plate coordinates of the images of the ground control. Random normal deviates having the standard deviations indicated in Table 2.1 were added to the true elements of orientation and the true coordinates of control.

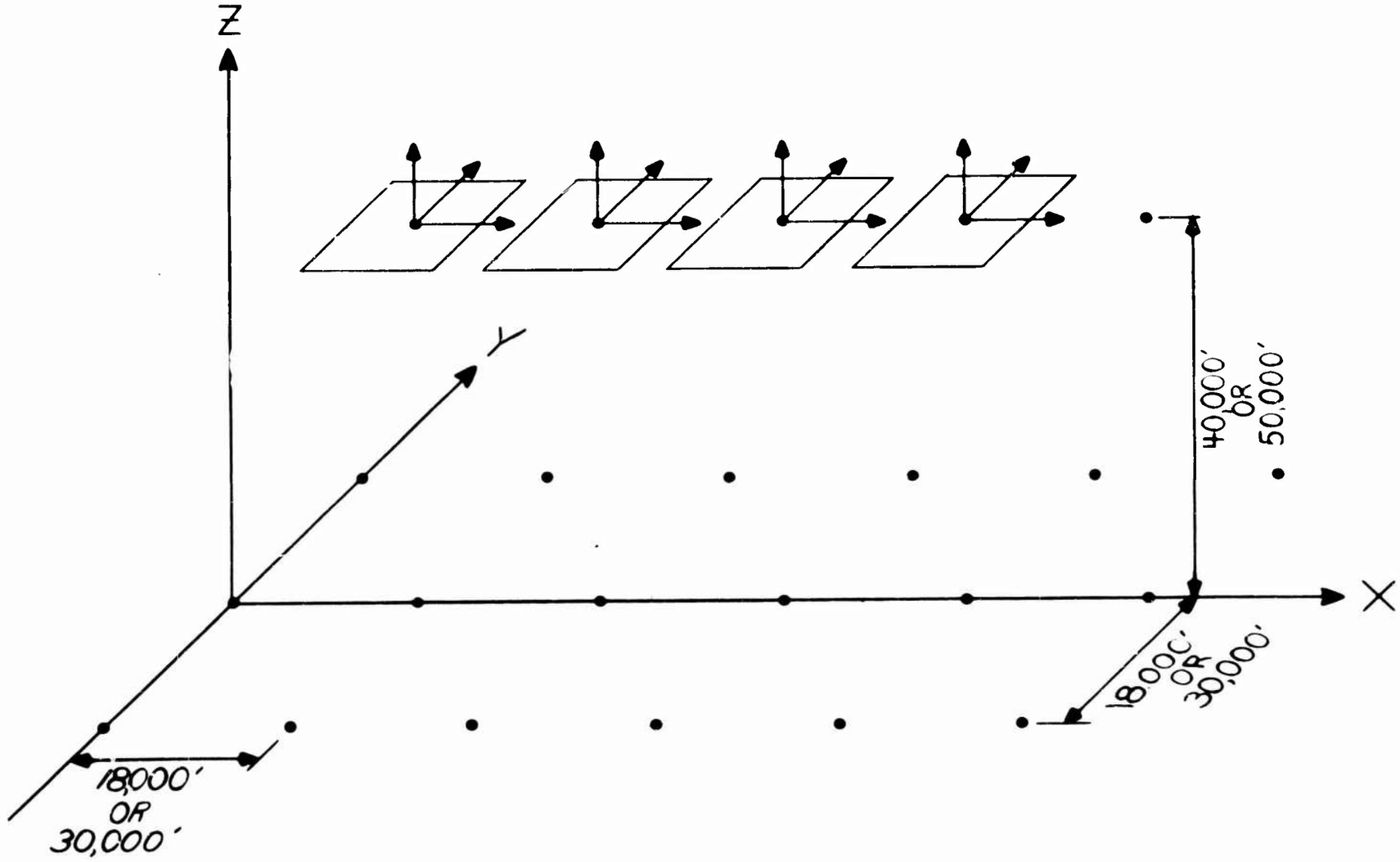

Figure 2.1. Illustrating geometry of aerial photography employed in numerical simulations.

Quantity	STANDARD DEVIATION	
	2-Photo Strip 6-Photo Strip 25-Photo Strip	41-Photo Strip 3x5 Photo Block
$\sigma_{X_c}, \sigma_{Y_c}, \sigma_{Z_c}$	10 ft.	25 ft.
$\sigma_\alpha, \sigma_\omega, \sigma_\kappa$	.0003 radian (1')	.00075 radian (2'.5)
$\sigma_X, \sigma_Y, \sigma_Z$	10 ft.	25 ft.

Table 2.1. Standard deviations of random normal deviates added to true values of elements of orientation and coordinates of control in order to create simulated approximations.

No random normal deviates were applied to those control points which were considered to be absolute in a given simulation. Except for such absolute control points, no constraints were placed on the control points. Neither were constraints placed on the elements of exterior orientation (the elements of interior orientation were, of course, enforced). Accordingly, all pass points and all elements of exterior orientation were allowed unlimited freedom to adjust.

The random deviates having standard deviations as indicated in Table 2.1 lead to fairly close initial approximations by usual standards. Such close approximations were invoked in order to avoid contamination of the essential results by second order effects of the process of linearization by means of Taylor's series. As indicated in Table 2.1, in our later simulations (41-Photo strip and 3x5 block) the errors in the initial approximations were relaxed by a factor of 2.5.

No random errors were applied to the true plate coordinates in any of the simulations, for had this been done the exact solution of the normal equations would not have been known. As it is, the solution of the normal equations should

precisely reproduce the known random deviates which had been added to the true elements of orientation and coordinates of control. This, then, provides the standard needed to gauge the relative effectiveness of various approaches to the solution of the normal equations. One should not lose sight of the fact that the central objective of our entire program of numerical simulation is to determine the feasibility of solving the normal equations by means of certain iterative procedures. Inasmuch as the introduction of random errors in the plate measurements would induce only a second order change in the coefficient matrix of the normal equations and hence would not alter its essential properties pertaining to convergence, it is clear that the assumption of perfect plate measurements in no way compromises the validity of our investigation of iterative solutions.

Four different arrangements of the normal equations were investigated in our simulations of strips. The basic forms of the normal equations are illustrated in Figures 2.2, 2.3, 2.4, 2.5 for the case of a sample 1x5 strip. In the arrangements A and B (Figs 2.2, 2.3) the elements of orientation and the coordinates of control are totally separated. The numbering of control points leading to the form A is indicated in Fig. 2.6 and that leading to the form B is indicated in Fig. 2.7. The arrangements C and D (Figs. 2.4, 2.5) are intertwined forms. Both intertwined forms correspond to the numbering of control points of Fig. 2.7. The C form may be viewed as a special case of the block intertwining of Fig. 1.5. In the D form, an even tighter, and more strongly diagonal arrangement is achieved through a different ordering process. The unknowns for the C and D forms are ordered as follows:

C FORM	D FORM
Point 1	Points 1,2,3,4,5
Photo 1	Photo 1
Points 2,3,4	Points 6,7,8
Photo 2	Photo 2
Points 5,6,7	Points 9,10,11
Photo 3	Photo 3
Points 8,9,10	Points 12,13,14
Photo 4	Photo 4
Points 11, 12, 13	Points 15,16,17
Photo 5	Photo 5
Points 14 through 21	Points 18,19,20,21.

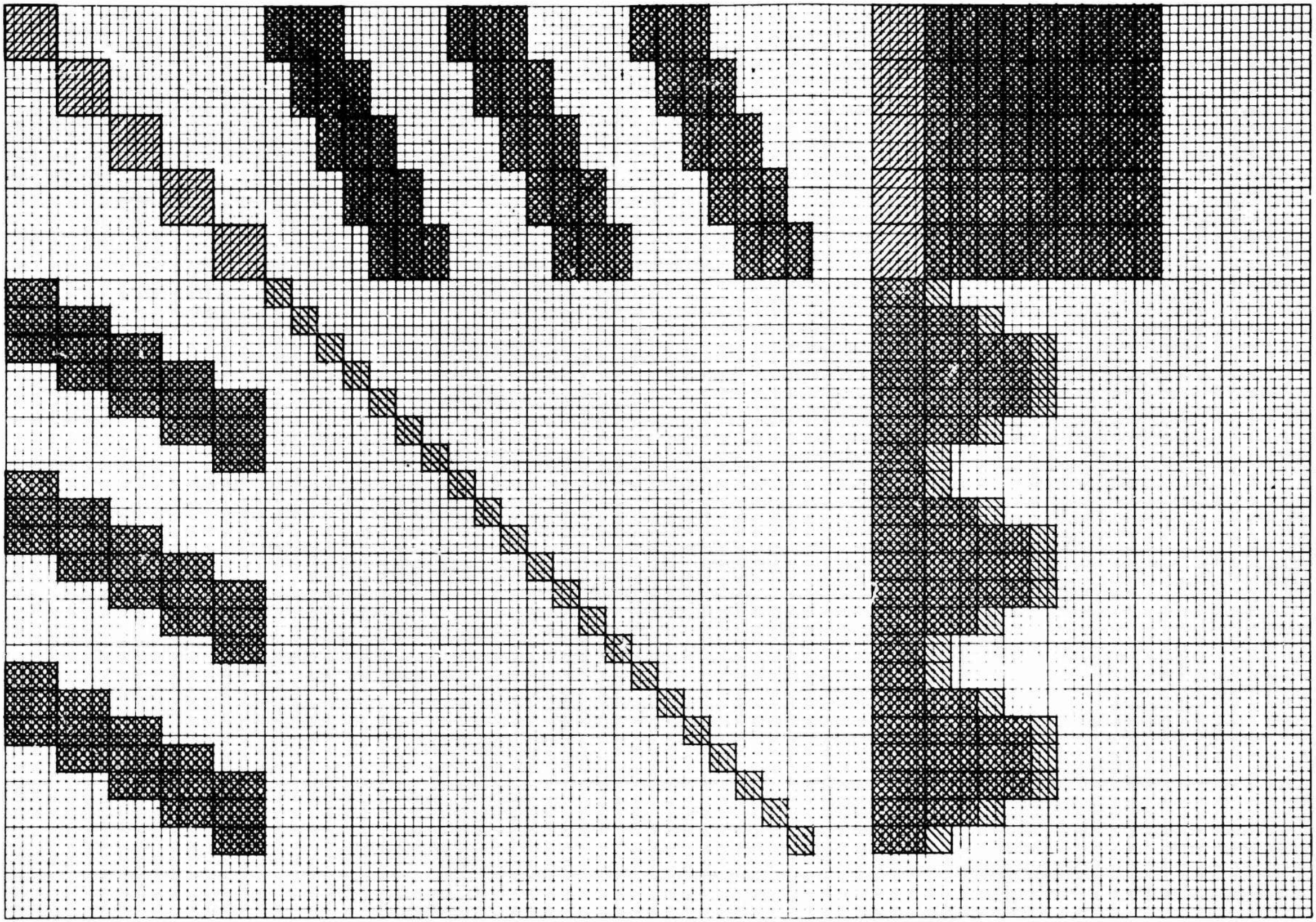

Figure 2.2a. The A form of the coefficient matrix of the general normal equations arising from adjustment of 1x5 strip of photography with photos and control points numbered as in Fig. 2.6.

Figure 2.2b. Collapsed form of normal equations of Fig. 2.2a.

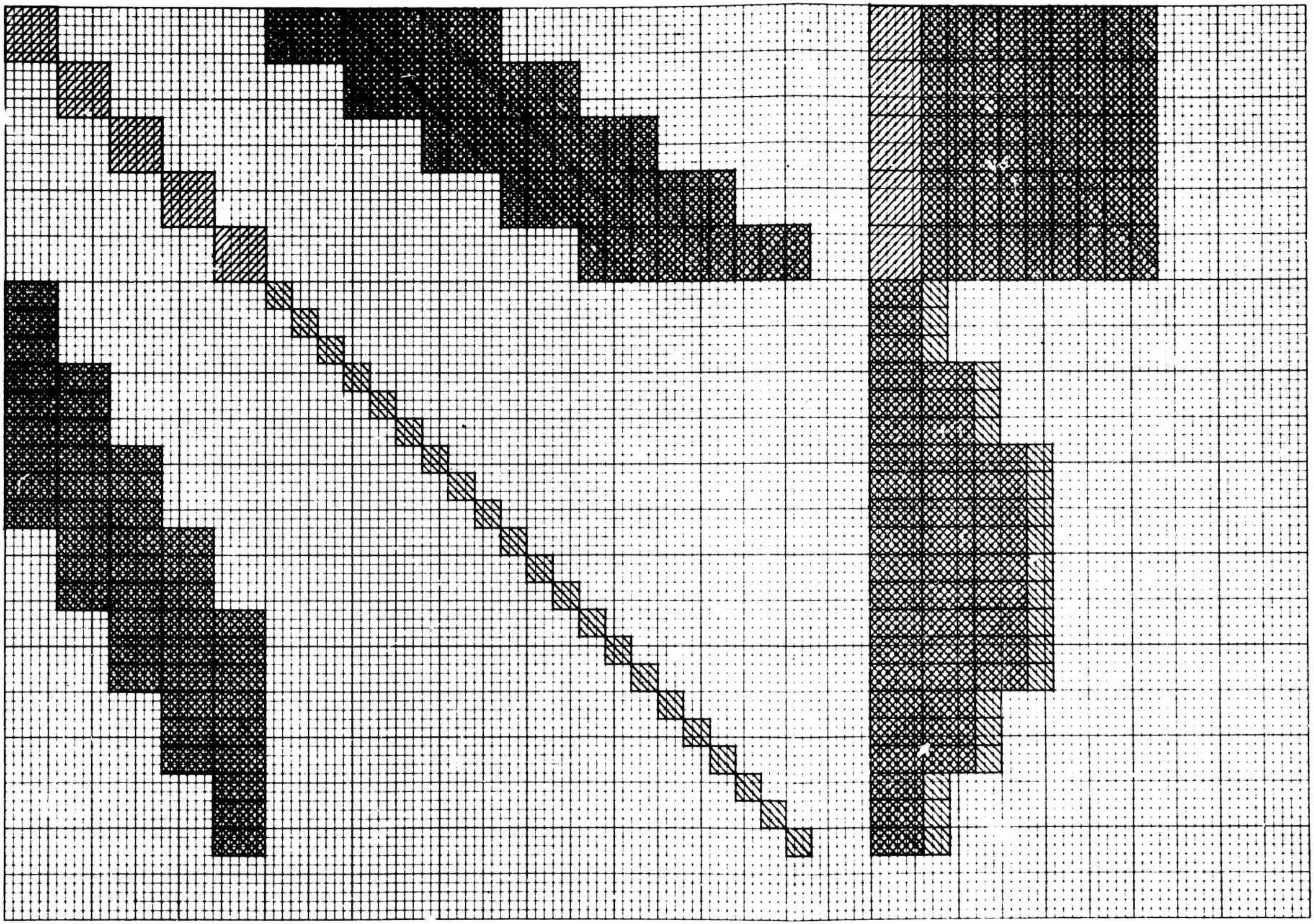

Figure 2.3a. The B form of the coefficient matrix of the general normal equations arising from adjustment of 1x5 strip of photography with photos and control points numbered as in Fig. 2.7.

Figure 2.3b. Collapsed form of normal equations of Fig. 2.3a.

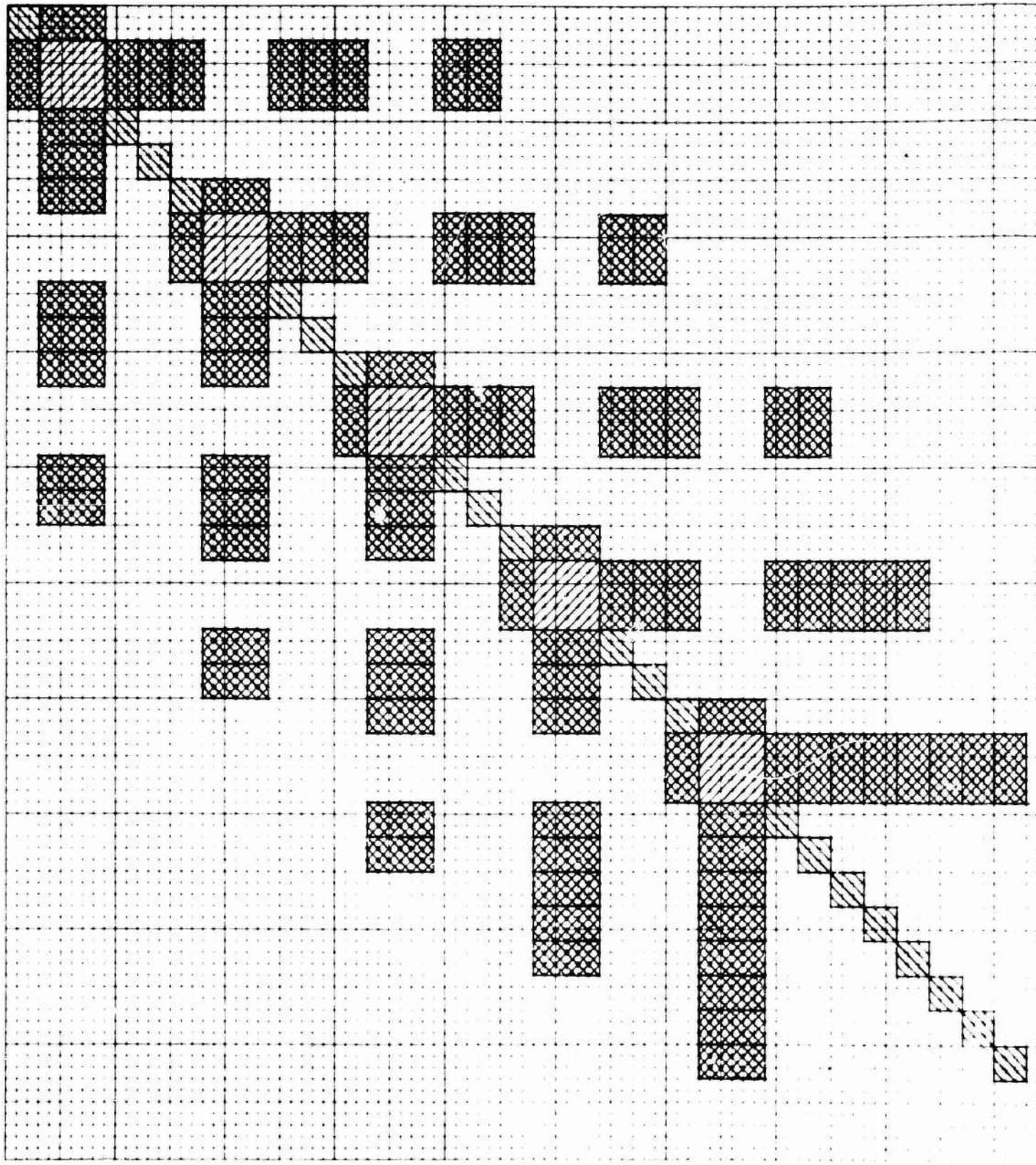

Figure 2.4a. The C (intertwined) form of the coefficient matrix of the general normal equations arising from adjustment of 1x5 strip of photography with photos and control points numbered as in Fig. 2.7.

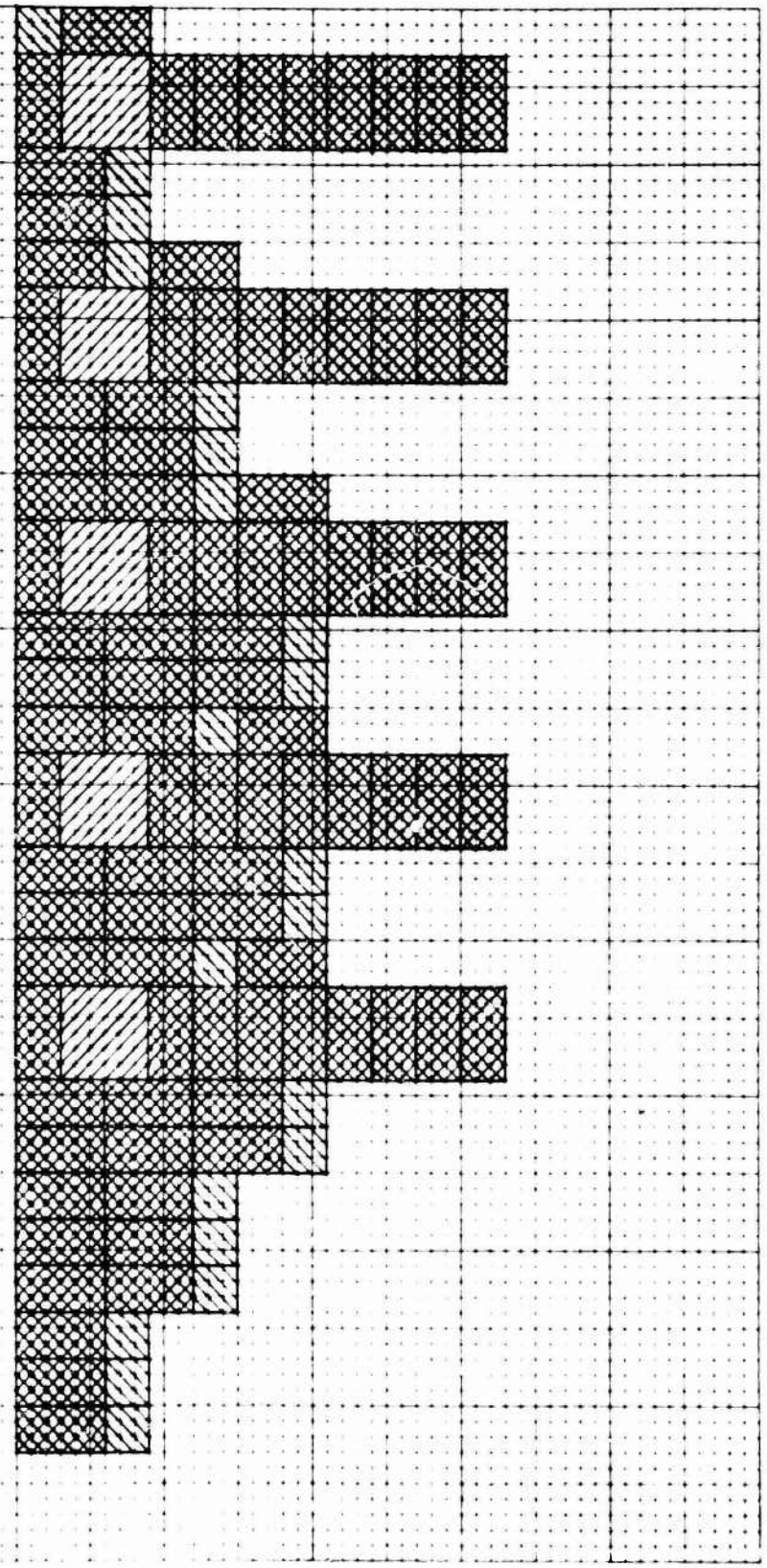

Figure 2.4b. Collapsed form of normal equations of Fig. 2.4a.

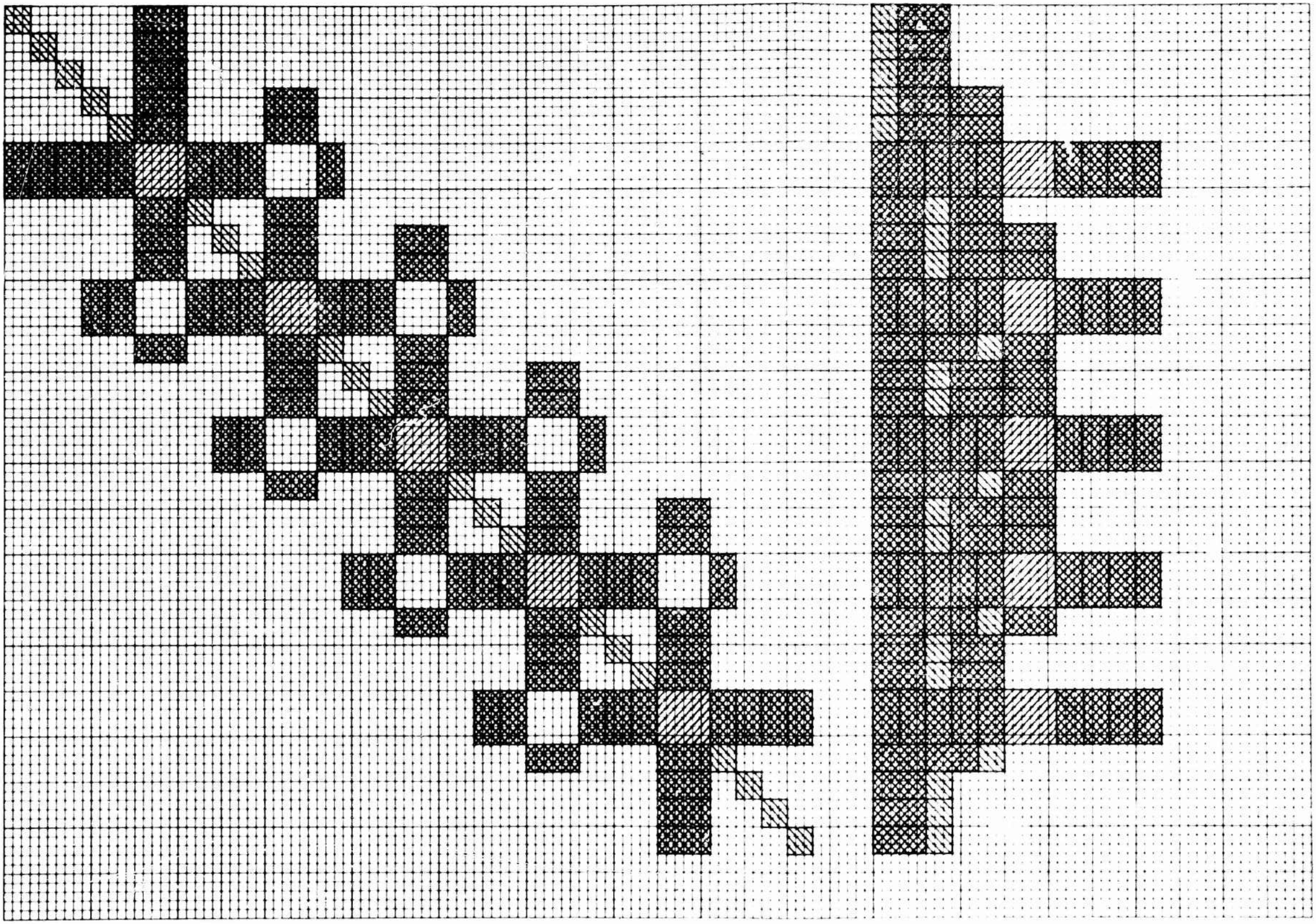

Figure 2.5a. The D (intertwined form of the coefficient matrix of the general normal equations arising from adjustment of 1x5 strip of photography with photos and control points numbered as in Fig. 2.7.

Figure 2.4b. Collapsed form of normal equations of Fig. 2.5a.

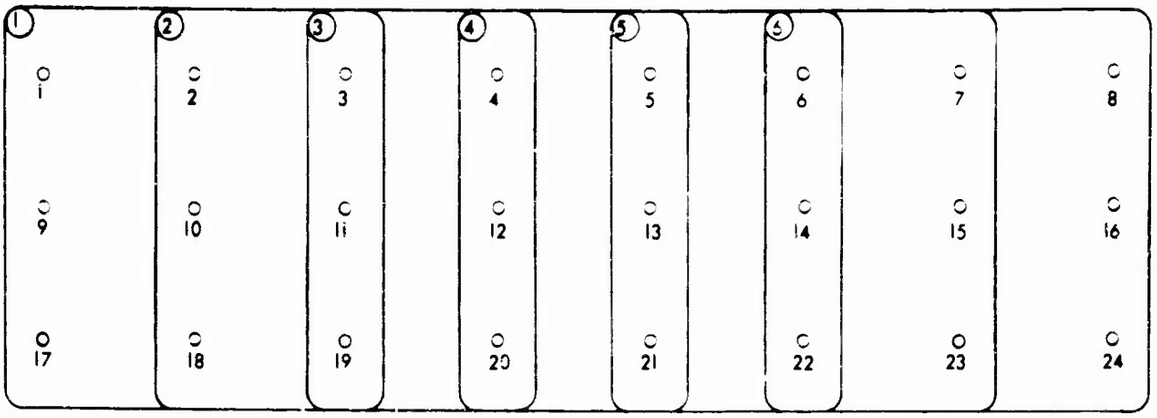

Figure 2.6. General scheme of photo and control point numbering leading to A form of normal equations for strip.

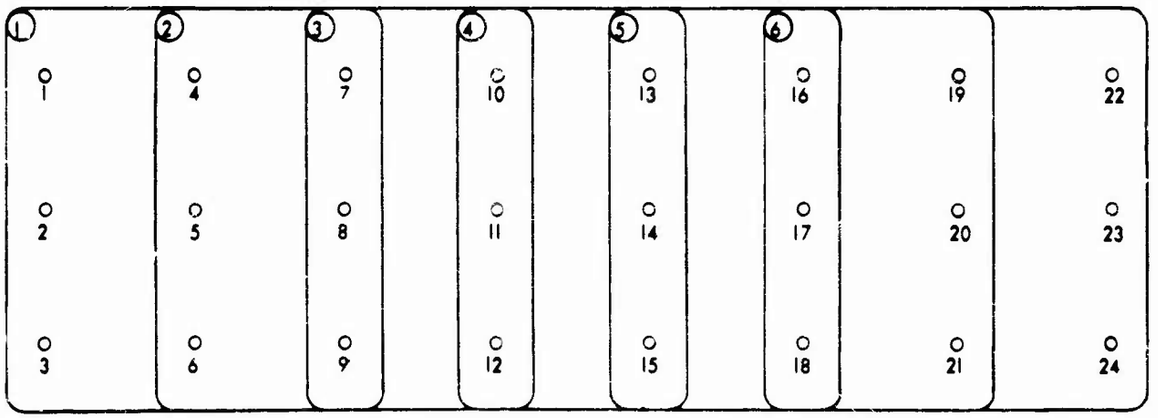

Figure 2.7. General scheme of photo and control point numbering leading to B, C, D forms of normal equations for strip.

In the next several subsections we shall describe the results of our simulations and shall show how each series of simulations answered certain specific questions while raising still others which were in turn answered by subsequent simulations.

2.08 SIMULATIONS OF 2-PHOTO STRIPS USING POINT ITERATIVE METHODS

The basic 2-photo combination is, of course, the fundamental unit for photogrammetric triangulation and is the combination which has traditionally been exploited as the 'building block' for cantilever extension. We concentrated initially on the 2-photo unit mainly in order to become familiar with the 'mechanics' of the various approaches to be applied later to more extensive photogrammetric nets. The four corner points of the first photo were taken as absolute control points. The middle control point of the first column and all three control points of the last column were considered to be known perfectly in Z in order to preserve the basic nine point pattern (since these particular points do not lie in overlap areas, they must be constrained in at least one coordinate in order to be carried in the adjustment; being constrained only in Z, the can have no influence on the results of the adjustment and accordingly may be viewed as dummy control introduced merely for convenience). With a total of 12 control points being carried, the general normal equations for the 2-photo strip become of order 48x48. All four arrangements of the normal equations (A,B,C,D) were generated on an IBM 1620 computer and solutions were attempted by means of the following 'point-iterative' processes

1. Gauss-Seidel,
2. Gauss-Seidel with Luisternik Acceleration,
3. Successive Over Relaxation.

The results for Gauss-Seidel iteration for all four arrangements of the normal equations are summarized in Table 2.2. Those for Successive Over Relaxation are summarized in Table 2.3. The Gauss-Seidel process with Luisternik acceleration was found to diverge for reasons to be discussed later.

Number of Iterations	ARRANGEMENT OF NORMAL EQUATIONS							
	A		B		C		D	
m	S_m	$\rho_m(G)$	S_m	$\rho_m(G)$	S_m	$\rho_m(G)$	S_m	$\rho_m(G)$
5	9.320	.8184	9.320	.3184	8.527	.8062	13.630	.6462
10	4.339	.8523	4.339	.8523	4.485	.9058	5.370	.9063
15	2.210	.8468	2.210	.8468	2.366	.9117	3.016	.9392
20	1.302	.9086	1.302	.9086	1.667	.9267	2.210	.9448
25	.982	.9861	.982	.9861	1.397	.9440	1.808	.9534
30	.839	.9881	.839	.9881	1.231	.9583	1.532	.9593
35	.773	.9890	.773	.9890	1.130	.9932		
40	.699	.9897	.699	.9897				

Table 2.2 Values of convergence parameter S_m and estimated spectral radius $\rho_m(G)$ for every 5 iterations of point-iterative Gauss-Seidel process applied to normal equations for basic 2-photo strip.

Number of Iterations	ARRANGEMENT OF NORMAL EQUATIONS							
	A		B		C		D	
m	S_m	$\rho_m(G)$	S_m	$\rho_m(G)$	S_m	$\rho_m(G)$	S_m	$\rho_m(G)$
5	9.321	.8184	9.321	.8184	10.180	.8088	13.630	.6462
10	6.871	.8531	6.158	.6974	6.657	.8187	8.685	.7293
15	3.164	.9036	3.071	.9050	3.291	.9009	6.367	.8185
20	2.289	.9730	2.478	1.0020	2.836	.9878	4.171	.9147
25	1.855	.9683	2.049	.9718	2.439	.9625	2.714	.9501

Table 2.3. Values of convergence parameter S_m and estimated spectral radius $\rho_m(G)$ for every 5 iterations of point-iterative method of Successive Over Relaxation applied to normal equations for basic 2-photo strip.

In Tables 2.2 and 2.3 the quantity S_m, defined by

$$S_m = \sum_{i=1}^{n} (x_i^{(m)} - x_i^{(m-1)})$$

serves as the criterion for convergence. Here $x_i^{(m)}$ and $x_i^{(m-1)}$ are corresponding components of two successive approximations to the solution vector of the normal equations. The quantity $\rho_m(G)$ denotes the approximation to the spectral radius resulting from the m^{th} iteration. The time required per iteration on the IBM 1620 was 2½ minutes in all cases. It should be pointed out that all operations were performed on the full 48x48 coefficient matrix, for the collapsed form was not employed at this stage of the investigation.

From Table 2.2 we see that the results for the A and B arrangements are identical and are superior in convergnece to those for the C and D arrangements. In comparing Tables 2.2 and 2.3 we see that the point-iterative Gauss-Seidel process actually converges more rapidly than the point-iterative Method of Successive Over Relaxation. This indicates that the Method of Successive Over Relaxation did not realize a good approximation to its optimum acceleration parameter within the span of iterations considered.

The most important finding of the simple 2-photo simulations was the demonstration that the Luisternik acceleration actually leads to divergence. Upon reviewing this result from the theoretical standpoint the reason became obvious. The Luisternik process may actually be viewed as a special case of the Method of Successive Over Relaxation in which the acceleration parameter ω is computed from

$$\omega = \frac{1}{1 - \rho(G)} \quad . \tag{39}$$

As was indicated in Subsection 2.05, the SOR process will converge only for $0 < \omega < 2$. Thus when ω is computed according to the above formula, convergence will result only if $\rho(G) < 0.5$. In the general photogrammetric problem, on the other hand, $\rho(G)$ is generally close to unity. This makes Luisternik's acceleration

coefficient greater than 2 which in turn causes divergence. When $\rho(G) < 0.5$, Luisternik's choice for the acceleration parameter is related to the optimum parameter by the following approximation

$$\omega_{Luisternik} \cong (1 + \rho(G))\, \omega_{Optimum}. \tag{40}$$

Hence even when it leads to convergence the Luisternik acceleration parameter tends to overshoot the optimum acceleration parameter by a factor equal to the spectral radius.

2.09 SIMULATIONS OF 2-PHOTO STRIPS USING BLOCK-ITERATIVE METHODS

Having dismissed the Luisternik method in our initial point-iterative simulations, we proceeded to apply block-iterative methods to the basic 2-photo case. Here, as in all subsequent simulations, we employed an IBM 1620 computer to generate the normal equations and an IBM 7094 to solve them. At this point we decided to concentrate on one non-intertwined form of the normal equations and one intertwined form. The B arrangement was selected for the non-intertwined form because its implementation was considered to be somewhat easier than that of the A form. The D arrangement was selected for the intertwined form because it is more strongly diagonal than the C arrangement.

The method of Block Successive Over Relaxation was applied to both the B and D forms. To serve as a control, the Block Gauss-Seidel process was applied to the B form. The convergence criterion S_m and estimated spectral radius $\rho_m(G)$ were read out at the end of every tenth iteration and are listed in Table 2.4 for the three cases considered.

The results in Table 2.4 demonstrate that the rate of convergence of Block Successive Over Relaxation far exceeds that of the Block Gauss Seidel Process, being on the order of 40 to 50 times faster at 100 iterations. In comparing Tables 2.2 and 2.4 we see that the block-iterative Gauss Seidel process

Number of Iterations	TYPE OF ITERATIVE SOLUTION					
	BLOCK GAUSS-SEIDEL		BLOCK SUCCESSIVE OVER RELAXATION			
	B FORM		B FORM		D FORM	
	S_m	$\rho_m(G)$	S_m	$\rho_m(G)$	S_m	$\rho_m(G)$
10	5.693	.9239	18.34	.9590	8.013	.8978
20	3.098	.9197	1.798	.9268	3.644	.7789
30	1.819	.9254	.5516	.9316	.4887	.7909
40	1.125	.9449	.2690	.9320	.1297	.9523
50	.7198	.9498	.1320	.9311	.0635	.9454
60	.4769	.9522	.0648	.9253	.0357	.9485
70	.3302	.9836	.0318	.9323	.0202	.9373
80	.2413	.9847	.0158	.9042	.0151	.9317
90	.1818	.9826	.0076	.9163	.0065	.9509
100	.1411	.9829	.0039	1.0370	.0037	.9556
110	.1138	.9824	.0019	.9612	.0022	1.049

Table 2.4. Values of convergence parameter S_m and estimated spectral radius $\rho_m(G)$ for 10 iterations of block-iteration Gauss-Seidel Process and block-iterative Method of Successive Over Relaxation applied to normal equations of basic 2-photo strip.

Number of Iterations	ARRANGEMENT OF NORMAL EQUATIONS			
	B FORM		D FORM	
	S_m	$\rho_m(G)$	S_m	$\rho_m(G)$
10	10.68	.8273	25.58	.7706
30	6.186	.9847	5.067	.9716
50	3.049	.9614	3.634	9930
70	1.511	.9770	2.746	.9827
90	.7854	.9760	2.159	.9953
110	.4976	.9651	1.777	.9947
130	.4020	.9793	1.537	.9955
150	.3490	.9910	1.389	.9954
170	.3077	.9948	1.281	.9961
190	.2723	.9975	1.199	.9974
210	.2404	1.002	1.134	.9971

Table 2.5. Values of convergence parameter S_m and estimated spectral radius $\rho_m(G)$ for every 20 iterations of block-iterative Method of Successive Over Relaxation applied to simulated 1x6 strip.

actually tends to converge less rapidly than the point-iterative Gauss-Seidel process. On the other hand in comparing Tables 2.3 and 2.4 we see that precisely the opposite is true with Successive Over Relaxation; here the block-iterative procedures afford a very considerable improvement over point iterative procedures.

The general rate of convergence with Block Successive Over Relaxation is seen from Table 2.4 to be about the same for the B and D arrangements. Certainly, the D arrangement in this case does not provide the hoped for improvement motivating the concept of intertwining.

2.10 SIMULATION OF 6-PHOTO STRIPS

At this point it was thought that the failure of intertwining to offer a significant improvement in convergence might well be attributable to the fact that with such a short strip only a weak measure of relative diagonality is provided by intertwining. For this reason, we decided to continue our investigations of intertwining in further parallel simulations of the B and D arrangements of the normal equations. Accordingly, the original 2-photo strip was extended to a 6-photo strip. This produced a system of normal equations of order 108x108, thus providing the D intertwined form a chance to achieve a fair measure of diagonality.

The results of 210 iterations of the process of Block Successive Over Relaxation are indicated in Table 2.5 for every 20th iteration starting with the 10th. We see that instead of leading to an improvement in convergence, the intertwined form D actually retards convergence to an appreciable degree and at 210 iterations is about five times slower in converging than the B form. Thus the actual effect of intertwining would appear to be just the opposite of what was desired.

In an attempt to account for this result, we investigated from the theoretical standpoint the structural properties characteristic of intertwined forms. As stated in Subsection 2.05, through the use of ordering vectors it can be established that the simple arrangements A and B of the normal equations are consistently ordered 2-cyclic matrices. In a similar manner we have been able to establish that the more complex intertwined arrangements C and D are not 2-cyclic. It follows that formula (29) for estimating the optimum acceleration parameter is not theoretically valid for the intertwined forms. Varga (1962) states that the rate of convergence of Successive Over Relaxation can be extremely sensitive to changes in the acceleration parameter. It is evident from our numerical results that equation (29) does not yield the optimum acceleration parameter for the intertwined arrangements and hence the maximum rate of convergence of Successive Over Relaxation is not achieved with intertwining. Inasmuch as no formula is known for computing the optimum acceleration parameter for matrices which are not consistently ordered 2 cyclic, we decided to abandon further consideration of intertwining in subsequent numerical simulations.

2.11 SIMULATION OF 25-PHOTO STRIPS

The investigations to this point were largely exploratory, serving to suggest avenues meriting more intensive investigation. While the iterative reduction for the 6-photo strip did lead to a satisfactory solution of the normal equations, the over-all computing time was almost tenfold greater than that which would have been required by the direct reduction of Subsection 1.12. Nonetheless, the fact that a satisfactory solution had been obtained at all was considered to be encouraging because the iterative approach was not expected to be computationally superior for such small photogrammetric nets.

Having settled on a single arrangement of the normal equations (the B form) and a single iterative method of solution (Block Successive Over Relaxation) we proceeded to revise the solution to incorporate a collapsing algorithm in order to bypass unnecessary operations on blocks of zero elements. With this successfully accomplished, we tested the resulting version of the reduction on the 6-photo strip and found that the collapsing algorithm speeded the reduction by more than one third. By implementing the collapsing algorithm, we not only speeded the reduction but were also able to handle much larger matrices in core, for storage of blocks of zero elements was no longer required. This set the stage for our next series of simulations which were concerned with 25-photo strips. The 25-photo strip was selected because this was judged to be close to the cross-over point where the iterative approach would possibly emerge as computationally superior. The order of the general normal equations for the 25-photo strip is 393x393.

In the 25-photo simulations the basic nine point pattern was maintained and two levels of control were considered:

(1) four absolute control points at the beginning of the strip and none elsewhere (minimal control case);

(2) four absolute control points at the beginning and another four at the end of the strip and none elsewhere (augmented control case).

Three non-collinear control points (or more precisely 2-1/3 points) actually constitute a minimal control situation; by including a fourth control point in the set, we obtain a practical check through redundancy. Since such a check should, we feel, be considered to be virtually indispensible in practice, we regard a set of four absolute control points as constituting the 'minimal control case'.

Inasmuch as the plate coordinates were completely uncontaminated by random error, the root mean square (rms) error of the residuals of the plate coordinates was adopted as an alternative criterion of convergence. This was

felt to be more meaningful for the problem at hand than our earlier criterion. For a perfect solution, the rms error would, of course, be precisely zero. With real data, on the other hand, the rms error would stabilize at a higher level and a more appropriate criterion would be one based on the change in the rms error per, say, twenty iterations.

The new convergence criterion was computed and read out every 20 iterations until an arbitrary cut-off level of 300 iterations was reached. The results for both cases are listed in Table 2.6. On the surface, the level of 0.38 and 0.35 microns attained by 300 iterations is quite impressive, particularly when considered in the light of normal plate measuring accuracies. However, gauging the convergence criterion in this manner is deceptive for reasons to be brought out in Figs. 2.8a through 2.12b. Here we have presented curves depicting the actual errors in the solutions for the various unknowns of the normal equations. For convenience in making comparisons we have placed in juxtaposition corresponding figures for the 'minimal control case' and the 'augmented control case'. Corresponding figures are given the same number with the suffix 'a' referring to the 'minimal control case' and the suffix 'b' corresponding to the 'augmented control case'.

In comparing Figs. 2.8a and 2.8b we have the first indication of what we shall call the 'pinch' effect of absolute control. The truncation errors in Φ, ω, κ in Fig. 2.8b, unlike those in 2.8a, are reduced almost to zero at the 25th photo. This reflects the effects of the absolute control present at the end of the strip for the 'augmented control case'. Not only does this extra control pinch the truncation error almost to zero at the end of the strip, but it also reduces somewhat the amplitude of the intermediate excursions. The tip (Φ), tilt (ω), and swing (κ) errors are suppressed for the most part to less than 5 seconds of arc by 300 iterations.

The pinch effect is also evident in the comparison of Figs. 2.9a and 2.9b. By the end of 300 iterations, the errors in the values of the coordinates X^c, Y^c, Z^c

Number of Iterations	RMS ERROR (MICRONS)	
	Minimal Control Case	Augmented Control Case
0	183.8	179.4
20	1.87	1.85
40	1.30	1.25
60	1.01	.94
80	.84	.78
100	.73	.68
120	.66	.61
140	.61	.56
160	.57	.51
180	.53	.48
200	.50	.45
220	.47	.43
240	.45	.40
260	.42	.38
280	.40	.37
300	.38	.35

Table 2.6. RMS errors of residuals of plate coordinates after each 20 iterations of solution of normal equations generated by simulated 25-photo strips.

are generally suppressed to less than 3, 5 and 2 ft. respectively, for the 'minimal control case' and to less than 2, 4 and 1 ft. for the 'augmented control case . To place these in proper perspective one should recall that the assumed flying height for these simulations is 40,000 ft. and that the strip is on the order of 60 miles in length. Relative to the measuring errors normally to be expected for such an operation, the errors in the truncation of the iterative process at 300 iterations are acceptably small.

In Figs. 2.10a through 2.12b we have plotted the errors of truncation of the X,Y,Z coordinates along each of the three rows of control points. Not surprisingly, these curves are rather well correlated with the X^c, Y^c, Z^c curves of the exposure stations (Figs. 2.9a and b). Their amplitudes are generally under 3 feet at 300 iterations, although the error in the Y coordinate does become as large

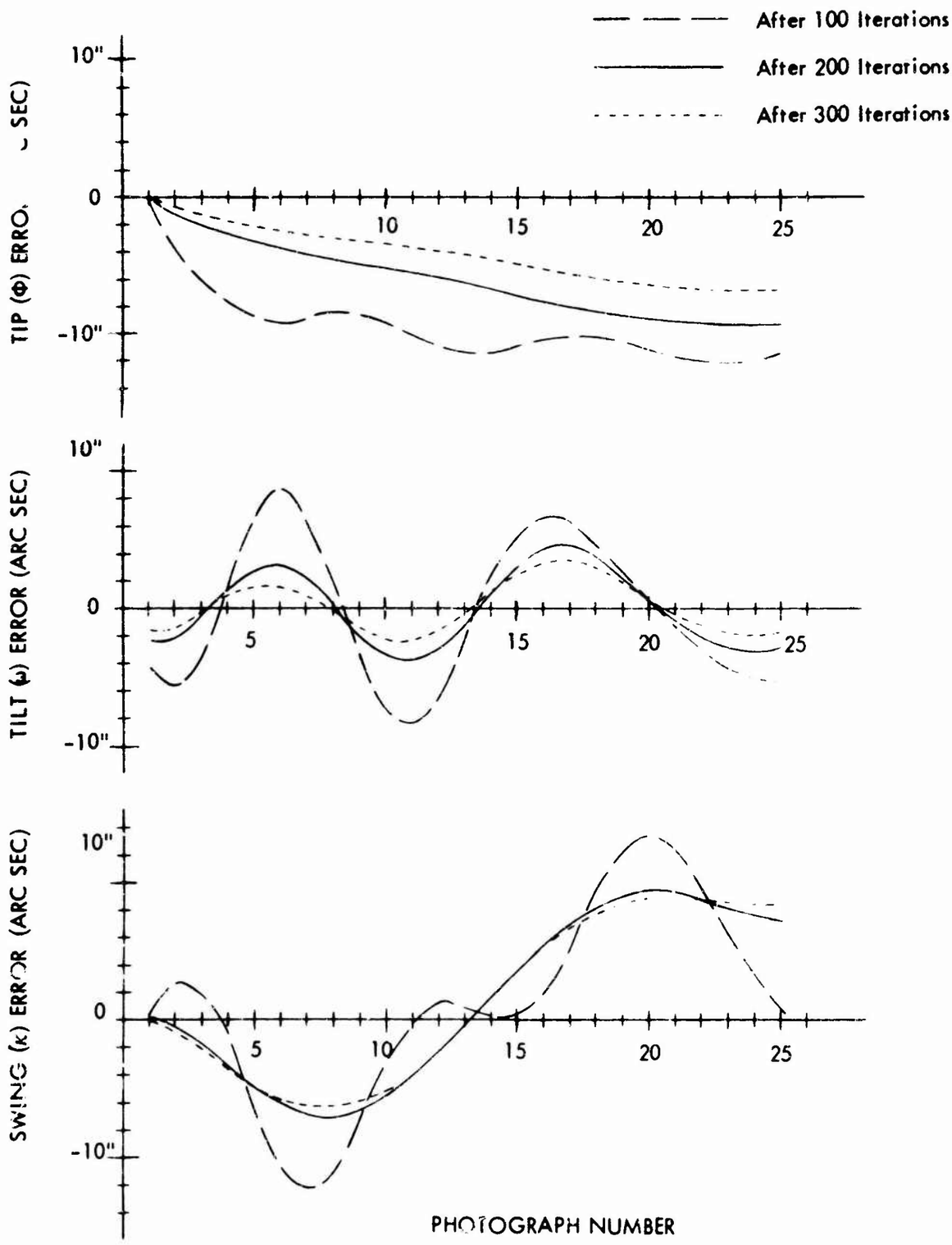

Figure 2.8a. Errors remaining in Φ, ω, κ for 25-photo strip after truncation of iterative solution at 100, 200 and 300 iterations; minimal control case.

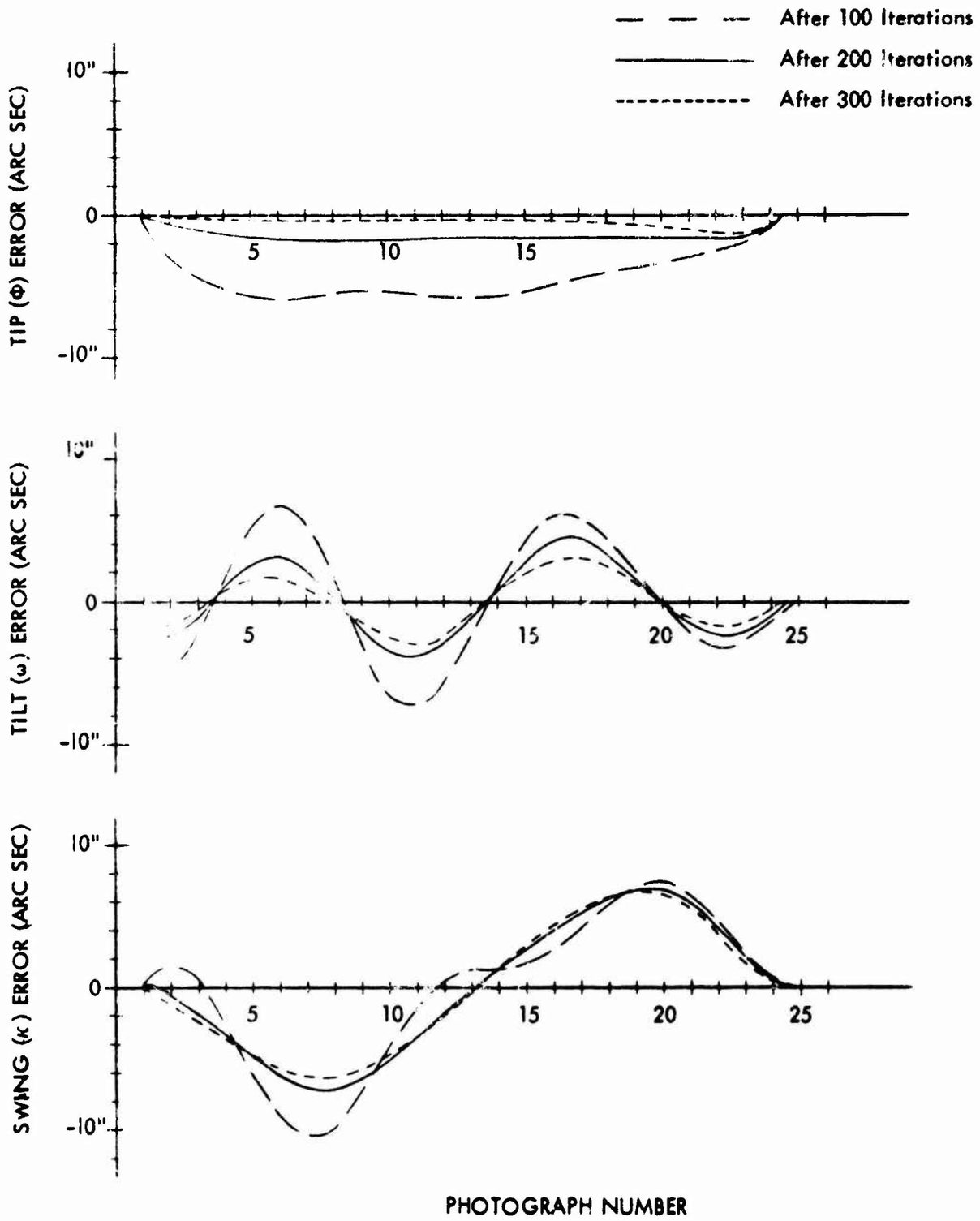

Figure 2.8b. Errors remaining in Φ, ω, κ for 25-photo strip after truncation of iterative solution at 100, 200 and 300 iterations; augmented control case.

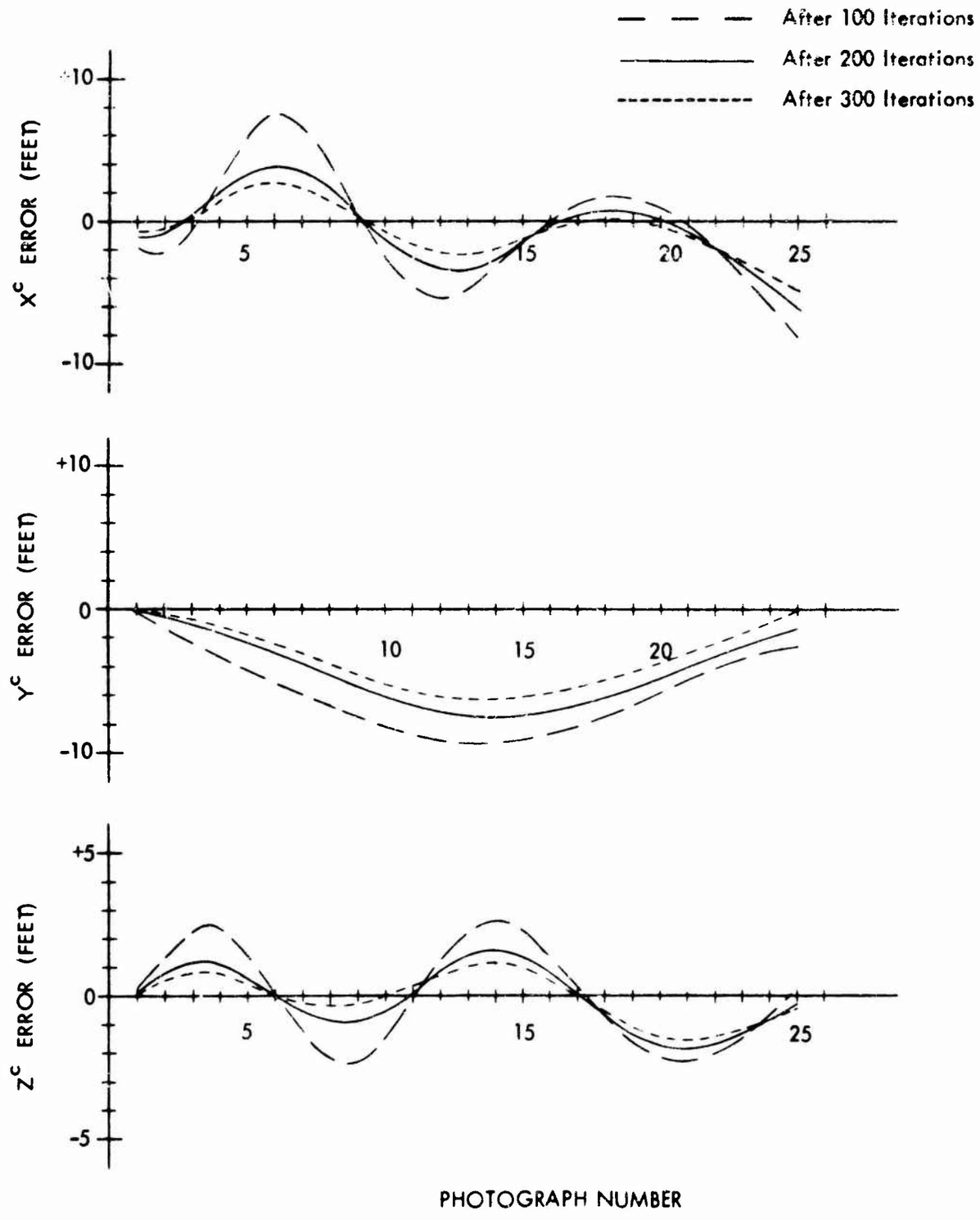

Figure 2.9a. Errors remaining in X^c, Y^c, Z^c for 25-photo strip after truncation of iterative solution at 100, 200 and 300 iterations; minimal control case.

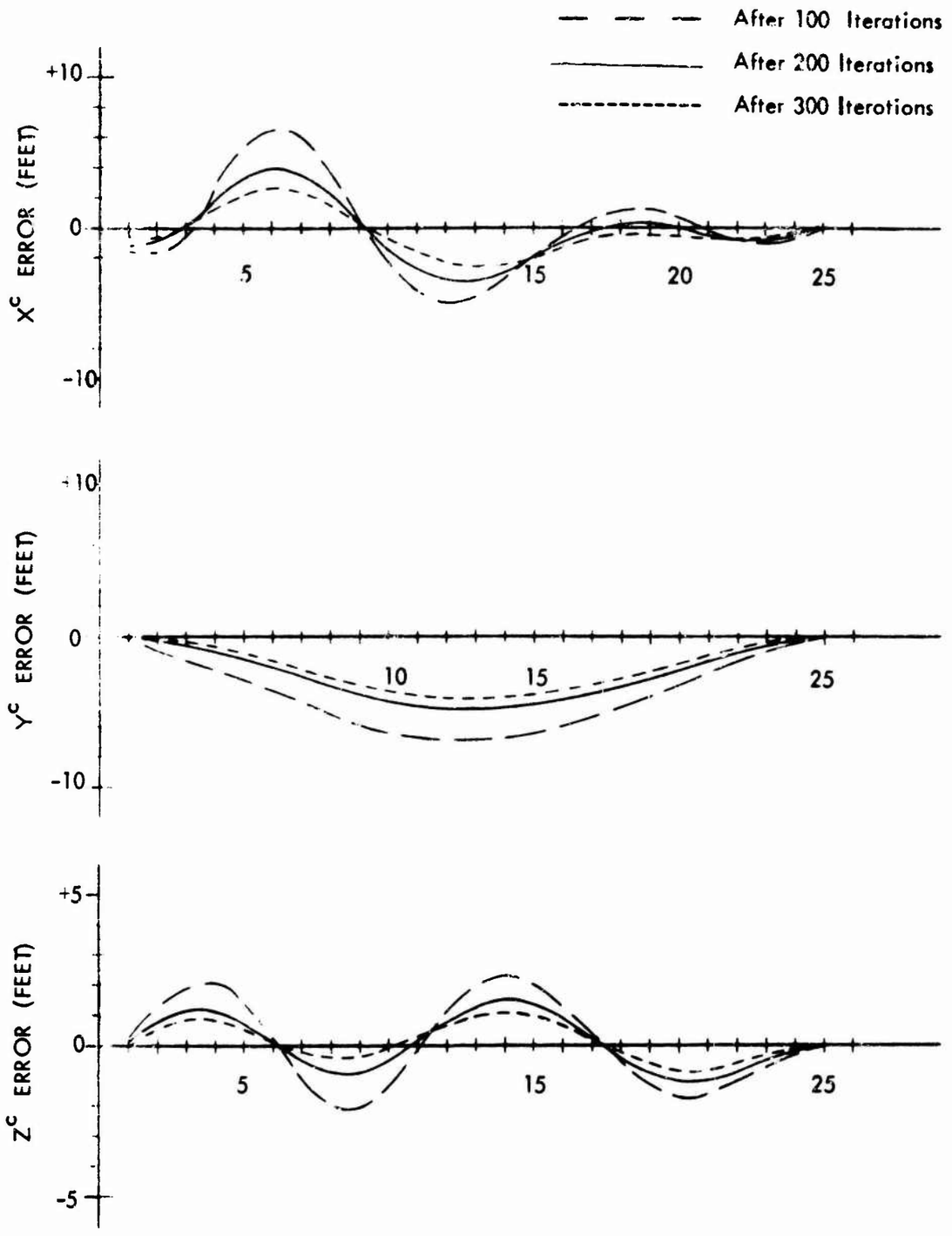

Figure 2.9b. Errors remaining in X^c, Y^c, Z^c for 25-photo strip after truncation of iterative solution at 100, 200 and 300 iterations; augmented control case.

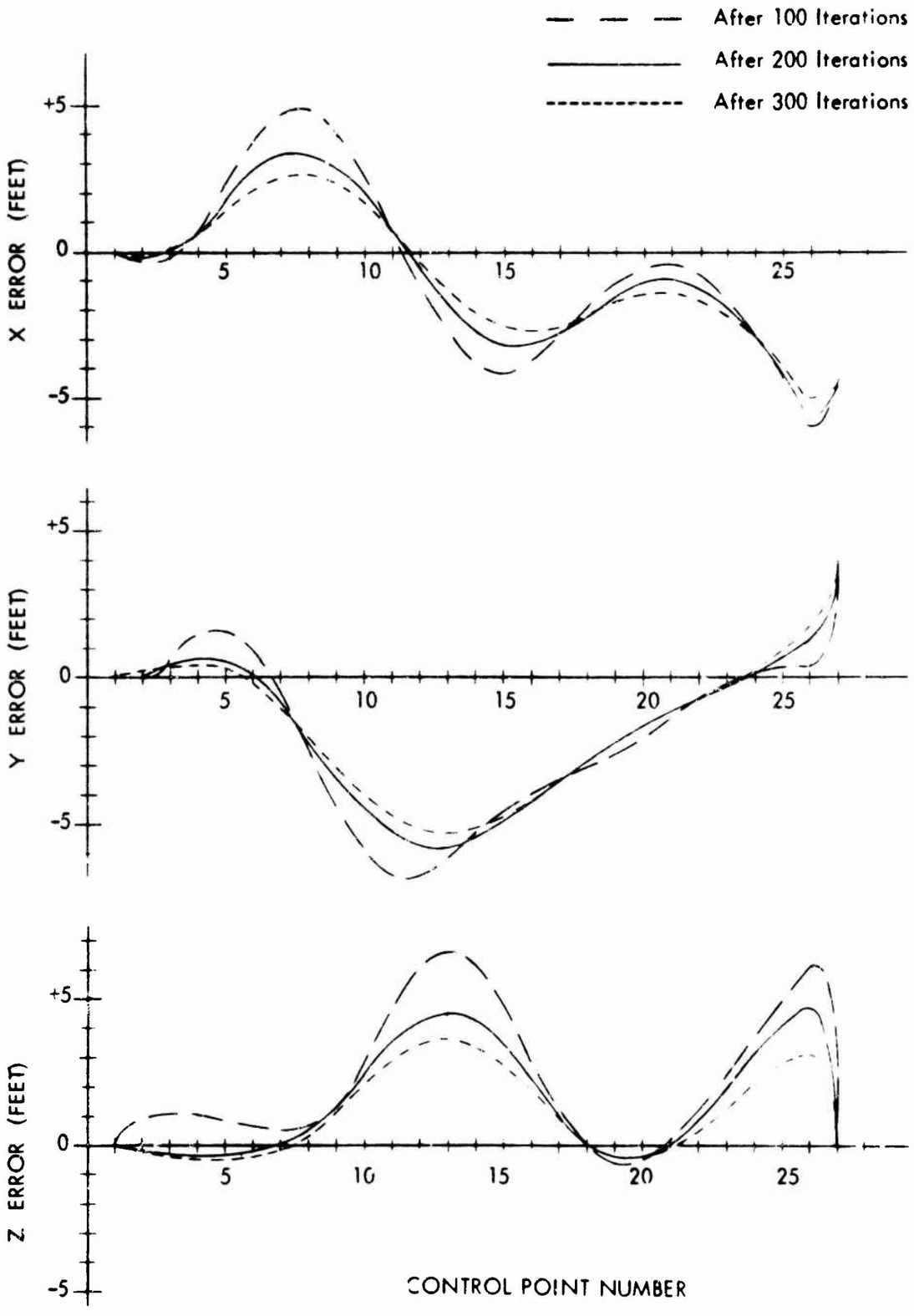

Figure 2.10a. Errors remaining in X,Y,Z of 1st row of control of 25-photo strip after truncation of iterative solution at 100, 200 and 300 iterations; minimal control case.

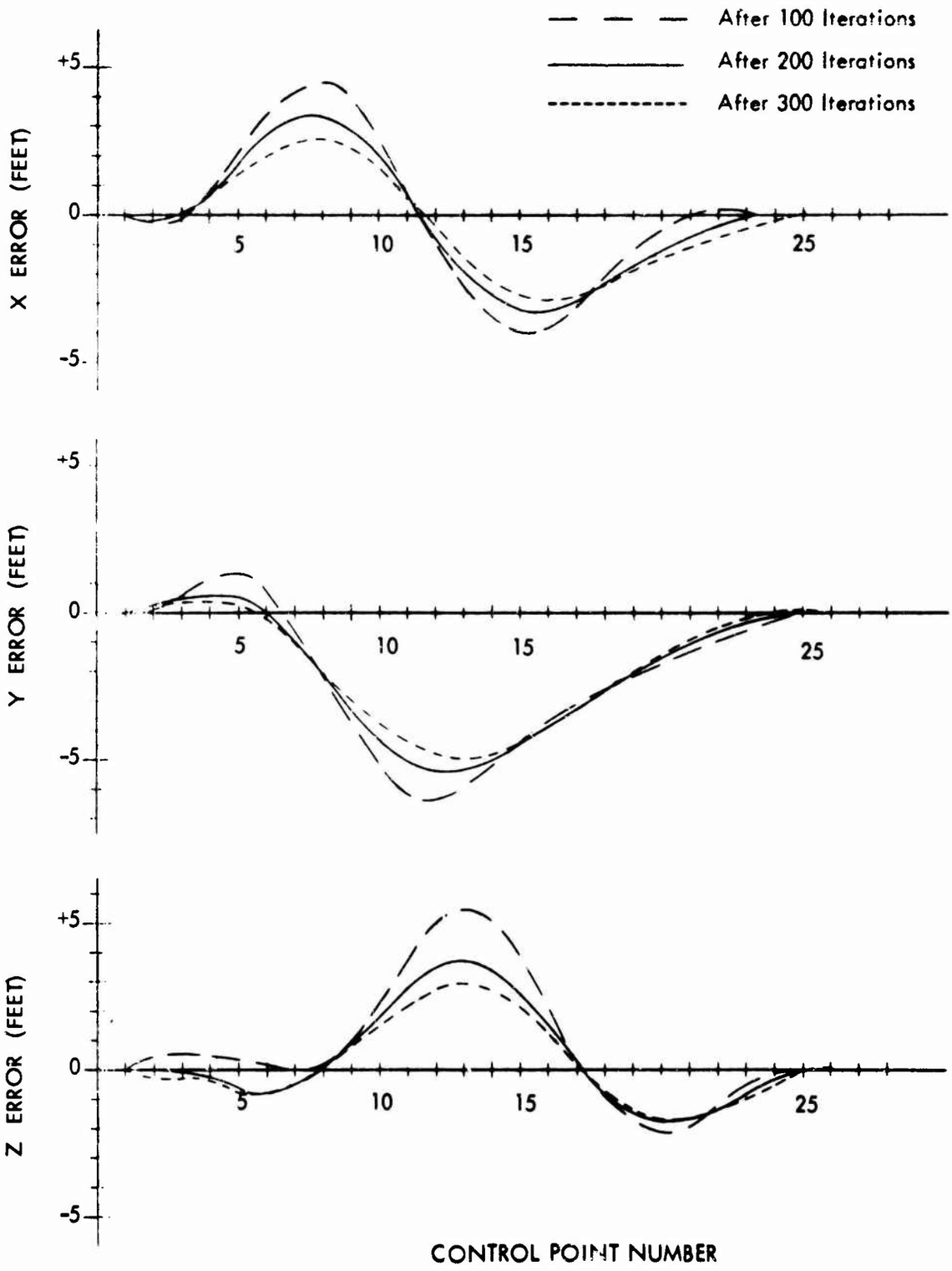

Figure 2.10b. Errors remaining in X, Y, Z of 1st row of control of 25-photo strip after truncation of iterative solution at 100, 200 and 300 iterations; augmented control case.

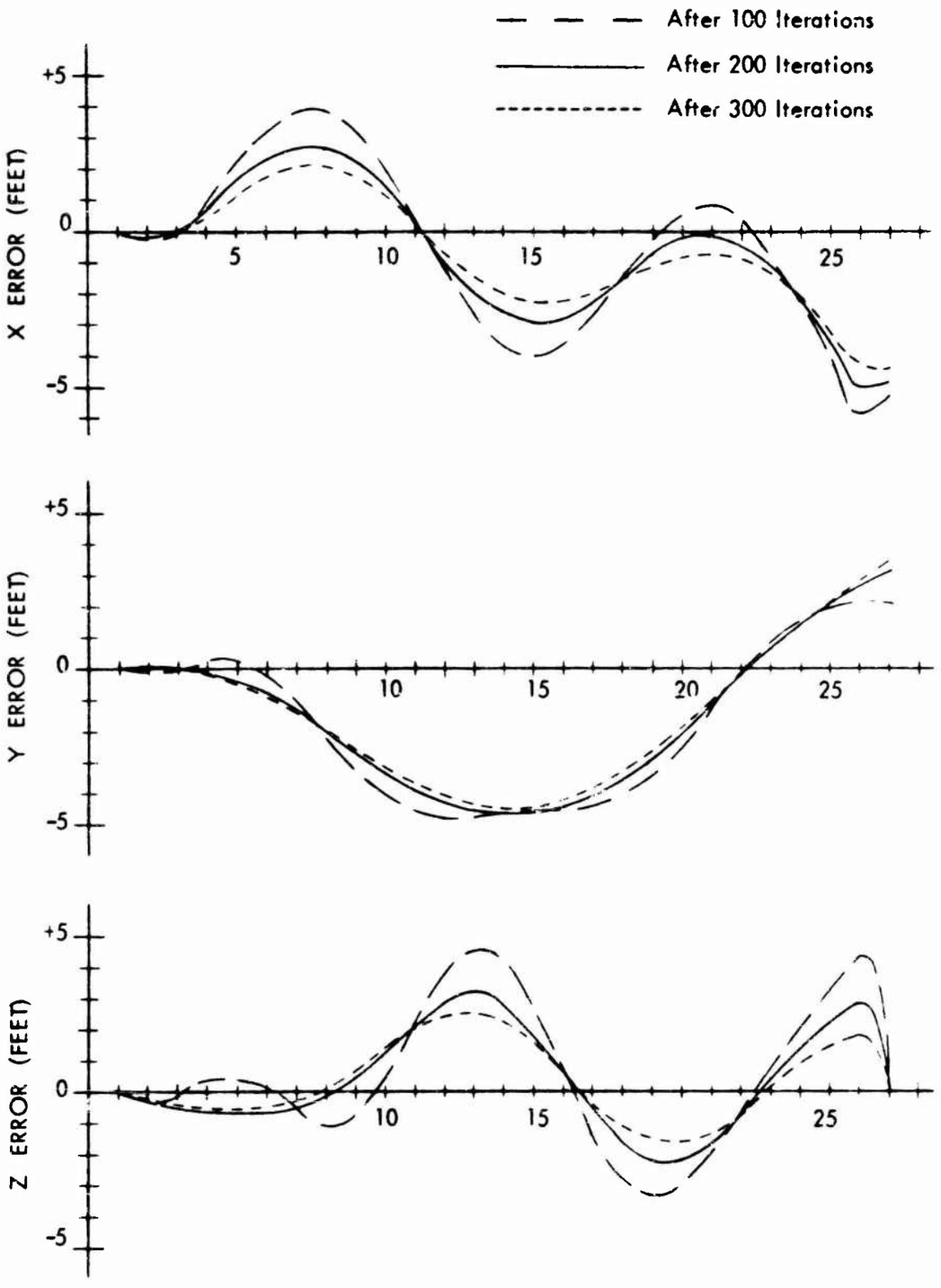

Figure 2.11a. Errors remaining in X,Y,Z of 2nd row of control of 25-photo strip after truncation of iterative solution at 100, 200 and 300 iterations; minimal control case.

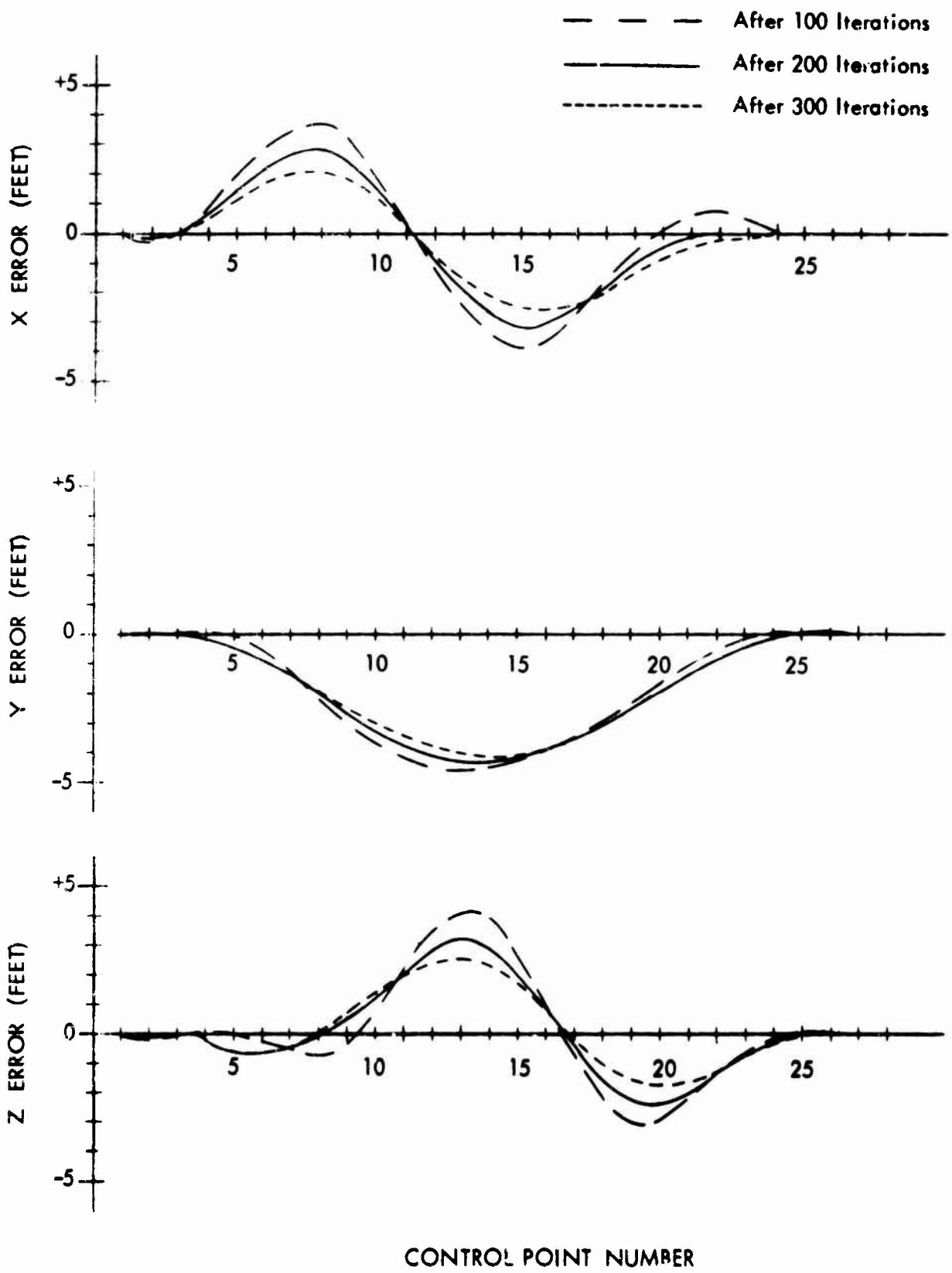

Figure 2.11b. Errors remaining in X,Y,Z of 2nd row of control of 25-photo strip after truncation of iterative solution at 100, 200 and 300 iterations; augmented control case.

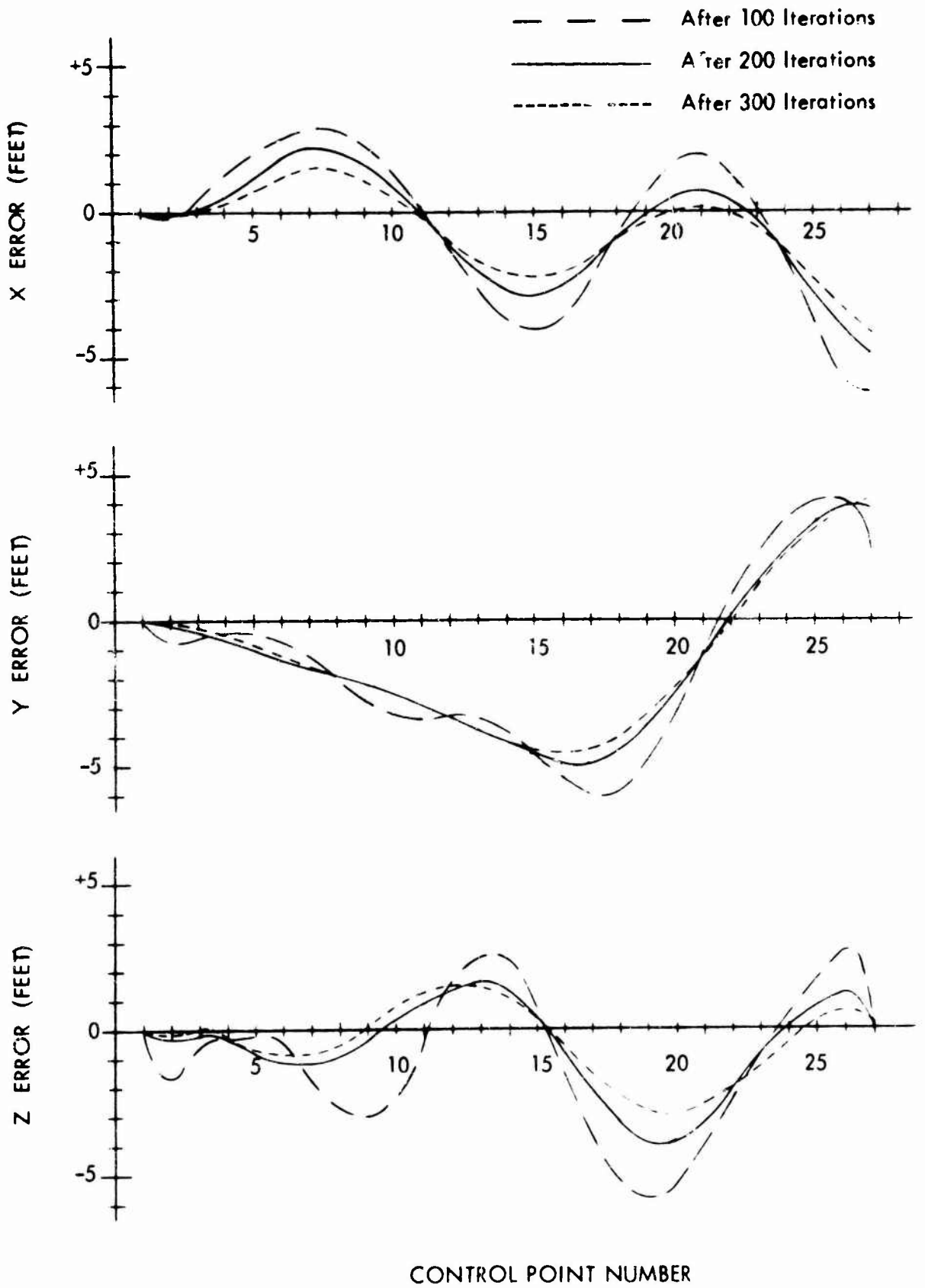

Figure 2.12a. Errors remaining in X, Y, Z of 3rd row of control of 25-photo strip after truncation of iterative solution at 100, 200 and 300 iterations; minimal control case.

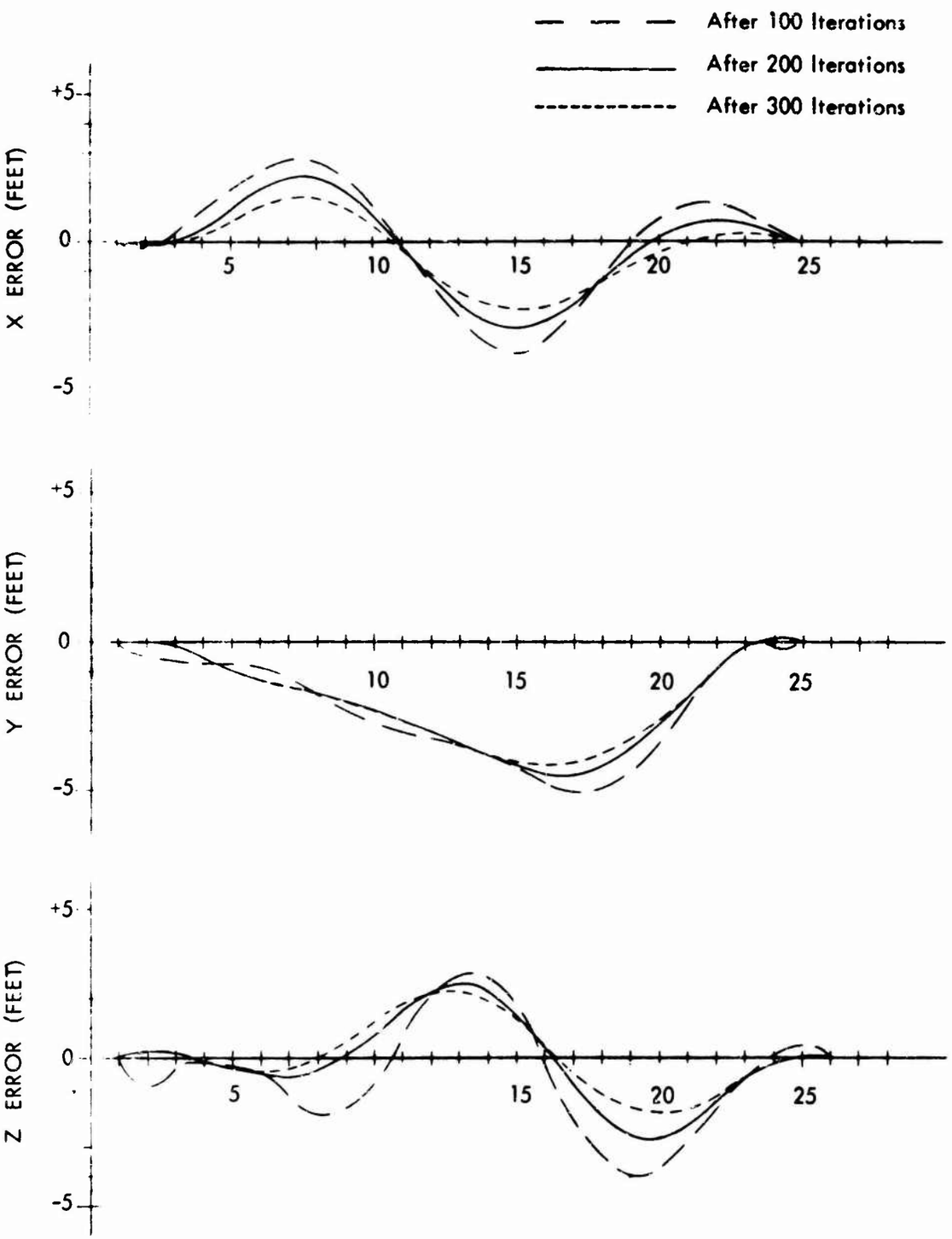

Figure 2.12b. Errors remaining in X, Y, Z of 3rd row of control of 25-photo strip after truncation of iterative solution at 100, 200 and 300 iterations; augmented control case.

as 5 feet at one point (to a great extent, this is a reflection of the truncation error in Y^c). By normal standards, the truncation errors at 300 iterations are acceptably small for the most part. However, further iteration to suppress the maximum error in the Y coordinates to a lower level might be considered advisable.

A remarkable property of the error curves of truncation is that their general characteristics closely resemble those of error curves of measurement. If, for example, one were to add random errors to the plate coordinates and iterate the solution to perfect convergence, the resulting error curves would bear a marked similarity in the domains of spatial frequency and autocorrelation to those curves characteristic of truncation of the iterative process. We believe that a full scale investigation of the autocorrelation and crosscorrelation spectra of error curves of truncation and error curves of measuring would prove most enlightening and would recommend this to future studies.

From the error curves of Figs. 2.8a through 2.12b it is evident why the error remaining in the ground control points (typically 1 to 3 feet and as much as 5 feet) is seemingly inconsistent with the very low mean error of the plate residuals (less than 0.4 microns) attained at 300 iterations. Truncation errors in the elements of orientation of successive photos are seen to be highly correlated. This leads to a gradual and subtle deformation of the model wherein the property of intersection of free rays is preserved to a remarkably high degree. Because of this pronounced serial correlation of errors in orientation, systematic excursions of the model are very poorly reflected by residuals in the plate coordinates. For this reason, adequate convergence is not actually attained with simulated data free of random plate measuring errors until the rms error of the plate coordinates has been suppressed to appreciably less than one micron.

Simulations of the 25-photo strips provided the first really convincing evidence of the feasibility of the iterative approach. The computing time required for 300 iterations on the IBM 7094 was approximately 7 minutes, a value competitive with the direct reduction of a 25-photo strip.

2.12 SIMULATION OF 41-PHOTO STRIPS

Having definitely established the promise of the iterative approach through 25-photo simulations, we proceeded to implement the final stage of our program of simulation on strips, namely, the adjustment of the longest strip which could be handled totally in the memory of a 32K IBM 7094. This was originally computed to be a 48-photo strip for the particular computer we were using. However, we were forced to cut this back to 41 photos after an expansion of the monitor of the computer consumed almost 3000 previously available cells.

In order to gain a more definitive evaluation of the 'pinch' effect of absolute control, we considered five different levels of control throughout the 41-photo strip. These are pictured in Fig. 2.13. In Case 1 (Fig. 2.13a.) five absolute points were established at the beginning of the strip. The four points controlled only in Z do not lie in overlap areas and hence are actually dummy control points introduced solely to preserve the convenient nine point pattern. In Case 2 (Fig. 2.13b.) five additional control points were established at end of the strip. Cases 3, 4 and 5 (Figs. 2.13c., d., e.) correspond to the introduction of additional control at approximately the half, quarter and one-eighth divisions of the strip.

For each of the five cases the rms errors of the residuals of the plate coordinates are listed in Table 2.7 for every 10 iterations to 50 iterations and for every 50 iterations thereafter to 600 iterations. The computing time required for 600 iterations averaged about 24 minutes. In general, the computing time for p iterations of an n photo strip having the basic nine point pattern of control is given very nearly by

$$T\ (\text{min.}) \cong knp$$

where

k = a constant depending on speed of the computer,

$\cong 0.0010$ for an IBM 7094.

Number of Iterations	RMS ERROR (MICRONS)				
	Case 1	Case 2	Case 3	Case 4	Case 5
0	336.0	336.0	336.0	336.0	336.0
10	8.2	7.9	8.0	8.3	8.6
20	5.1	4.9	5.0	5.1	5.2
30	4.0	3.9	3.9	3.9	3.8
40	3.4	3.3	3.3	3.2	2.9
50	3.0	2.9	2.8	2.7	2.3
100	2.0	1.8	1.9	1.7	1.01
150	1.5	1.4	1.5	1.4	.63
200	1.3	1.2	1.3	1.13	.49
250	1.15	1.1	1.2	1.01	.44
300	1.00	1.05	1.10	.92	.43
350	.96	.97	1.00	.81	.42
400	.91	.90	.96	.72	.413
450	.85	.86	.90	.67	.410
500	.81	.83	.84	.62	.407
550	.79	.85	.80	.59	.405
600	.75	.82	.75	.56	.403

Table 2.7. RMS errors of residuals of plate coordinates after various numbers of iterations of solution of normal equations generated by simulated 41-photo strips.

From Table 2.7 we see that the improvement in convergence with increasing control is not very pronounced until Case 5 is reached. Here, the inclusion of but four additional points (one new point per 10 photos) leads to a marked and sudden improvement in convergence. This is perhaps most strikingly illustrated in Figures 2.14 through 2.18 in which the individual errors in the elements of orientation and coordinates of control are plotted after 600 iterations for Cases 1 - 4 and after 200 iterations for Case 5. The errors in the X,Y coordinates of control are for the most part suppressed to less than one foot in Case 5 and those for the Z coordinate are generally suppressed to less than 3 feet. The results for Case 5 after 200 iterations are actually superior to the results for Case 4 after 600 iterations. It should be pointed out that because of a quirk in the program not discovered until very recently, the full value of the acceleration parameter for Block Successive

○ Relative Control Point

◀ Absolute Control Point

● Control Point Constrained in Z

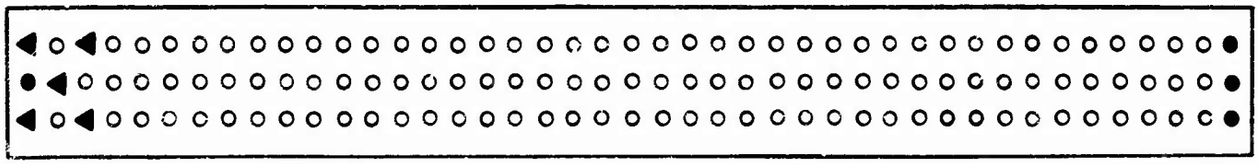

Figure 2.13a. Case 1

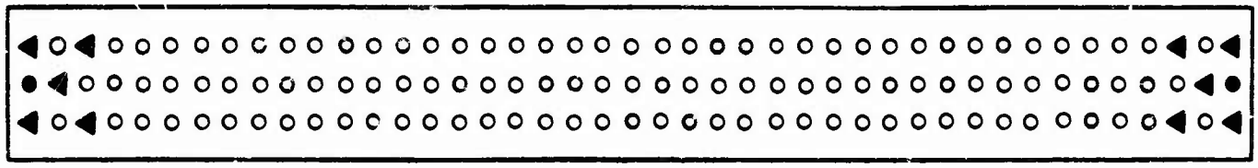

Figure 2.13b. Case 2

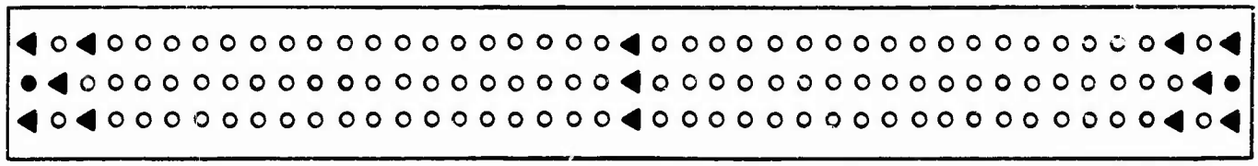

Figure 2.13c. Case 3

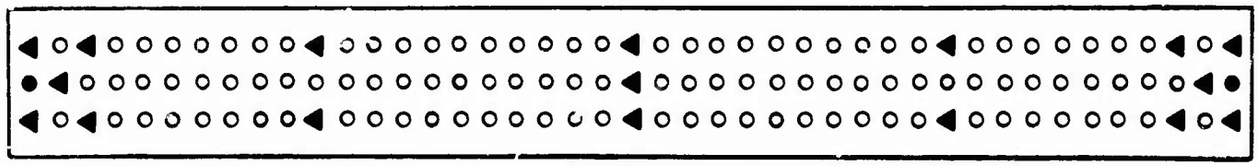

Figure 2.13d. Case 4

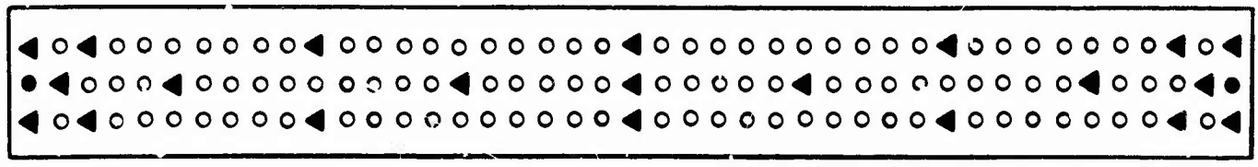

Figure 2.13 e. Case 5

Figure 2.13. Illustrating different levels of control considered in simulations of 41-photo strip.

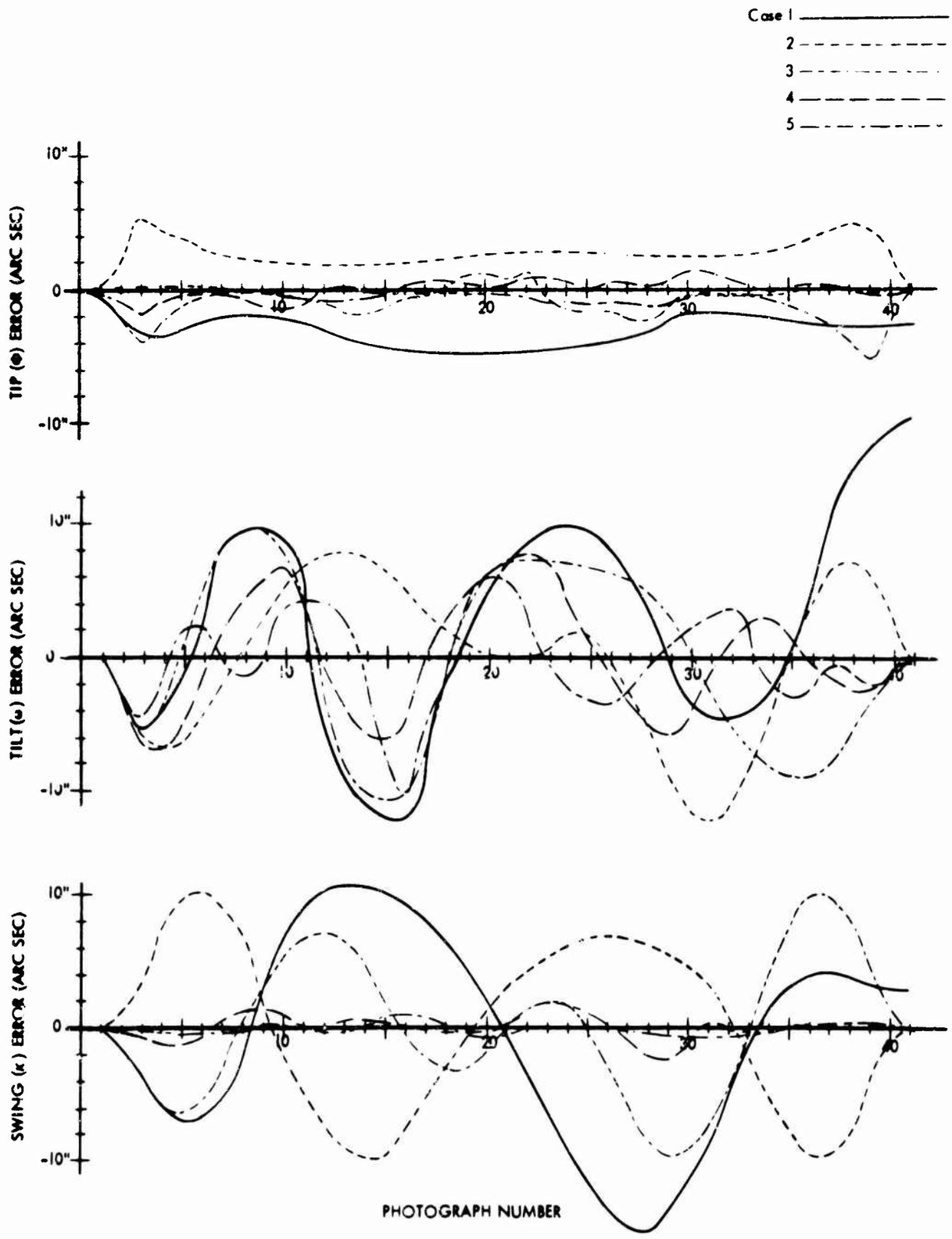

Figure 2.14. Errors remaining in Φ, ω, κ after truncation of iterative solution of normal equations at 000 iterations for case of 41-photo strip with 5 different levels of control.

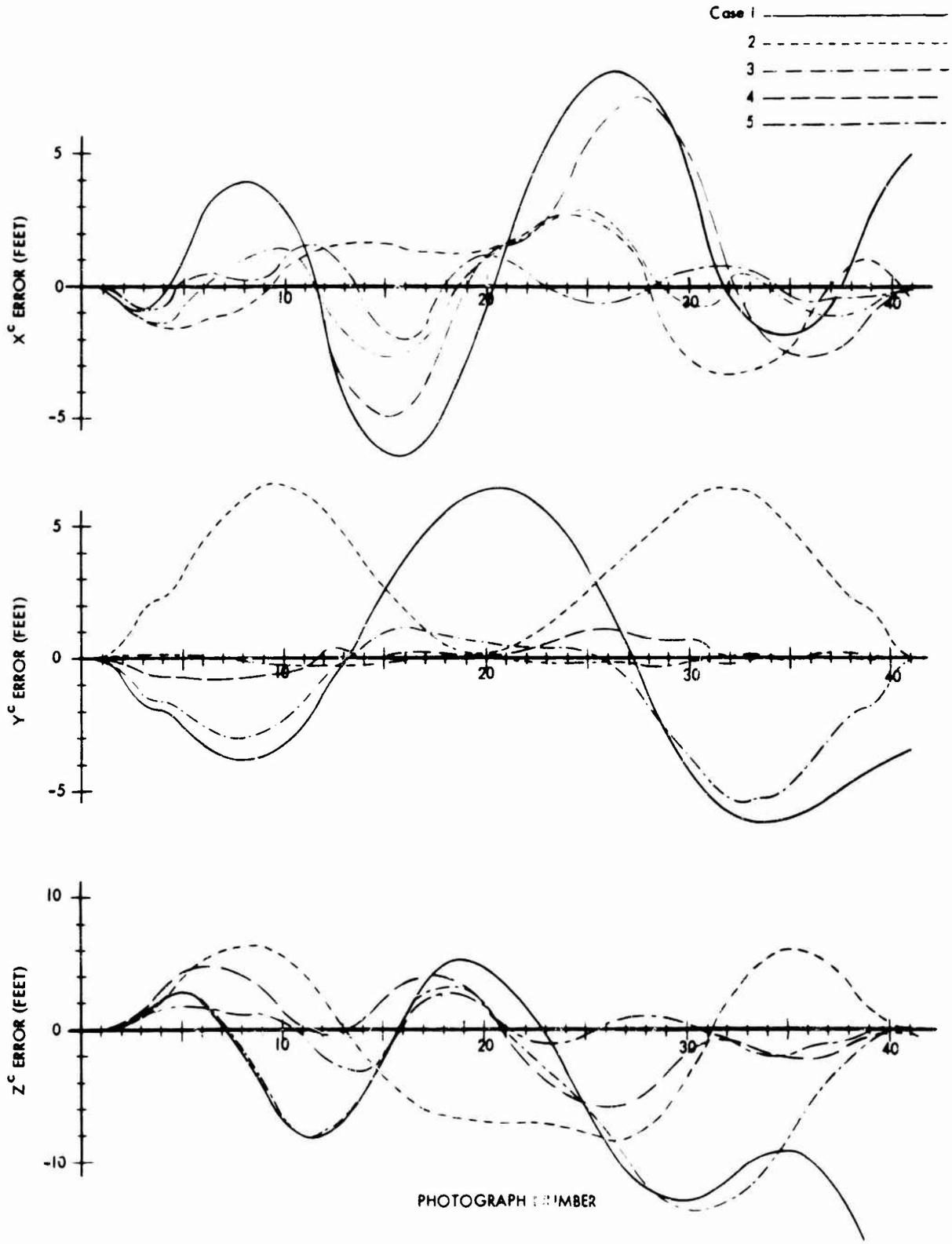

Figure 2.15. Errors remaining in X^C, Y^C, Z^C after truncation of iterative solution of normal equations at 600 iterations for case of 41-photo strip with 5 different levels of control.

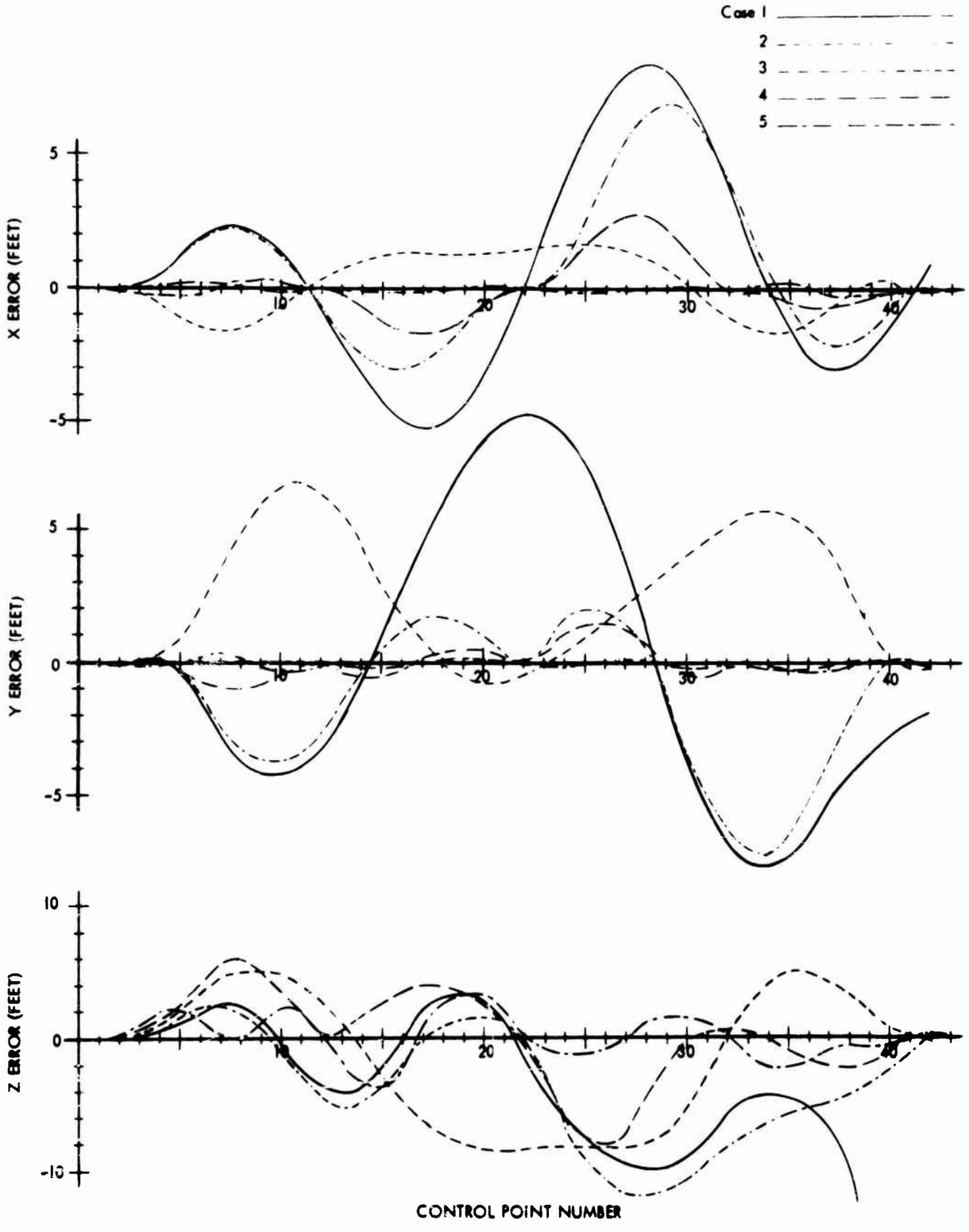

Figure 2.16. Errors remaining in X, Y, Z of 1st row of control after truncation of iterative solution of normal equations at 600 iterations for case of 41-photo strip with 5 different levels of control.

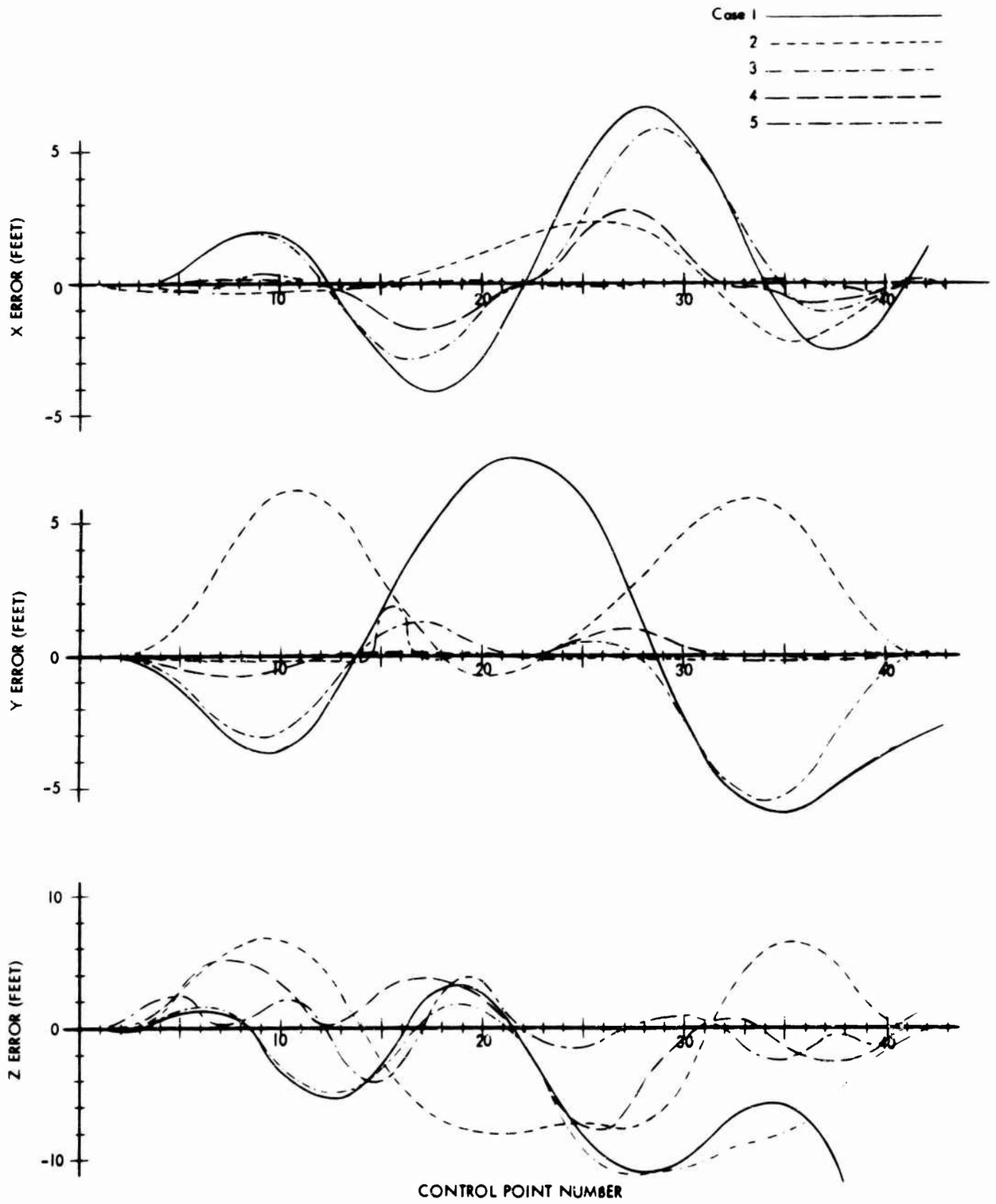

Figure 2.17. Errors remaining in X, Y, Z of 2nd row of control after truncation of iterative solution of normal equations at 600 iterations for case of 41-photo strip with 5 different levels of control.

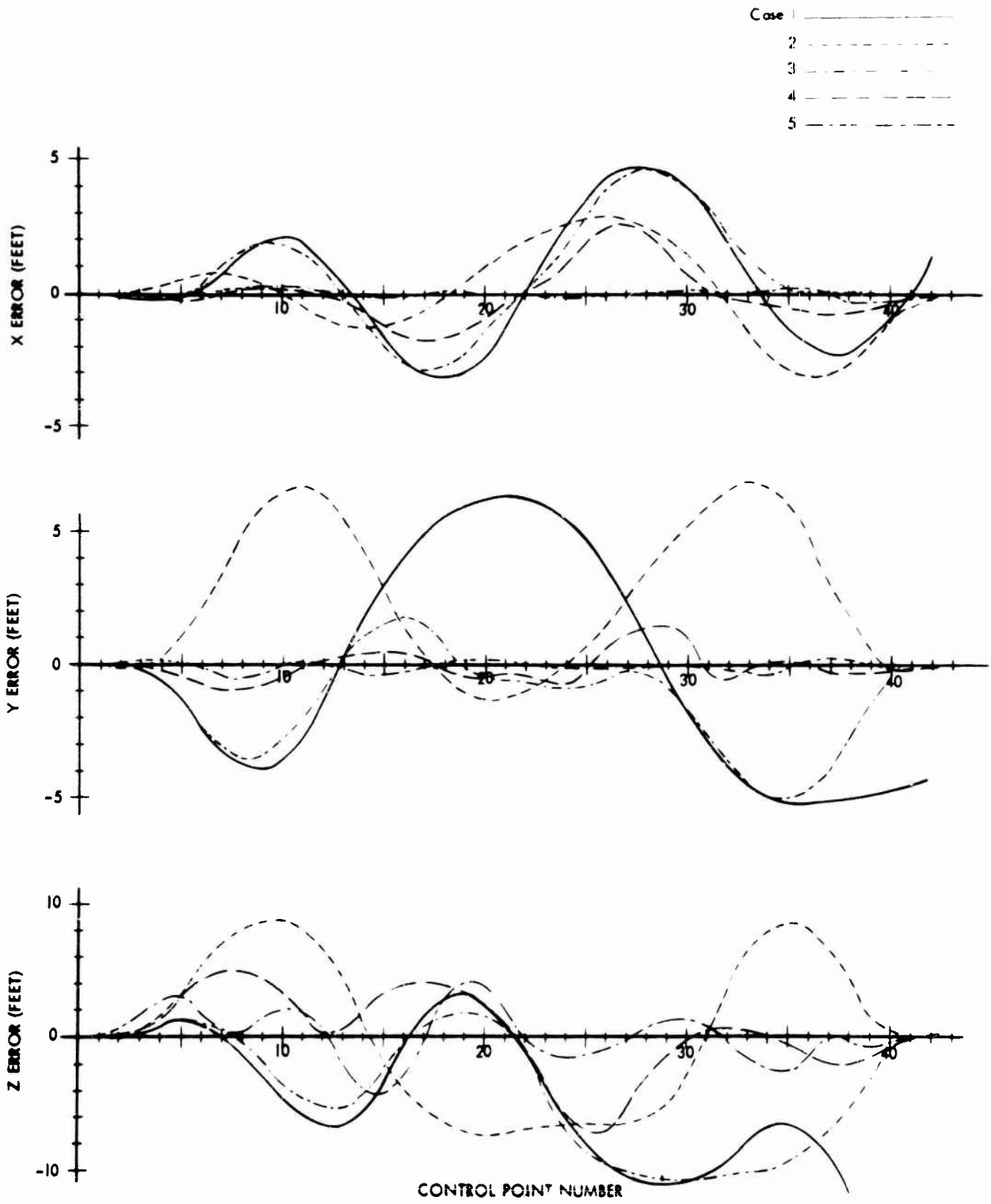

Figure 2.18. Errors remaining in X Y Z of 3rd row of control after truncation of iterative solution of normal equations at 600 iterations for case of 41-photo strip with 5 different levels of control (results for Case 5 are after 200 iterations).

Over-Relaxation was not actually realized in the simulations of the 41-photo strip (the results for the 25-photo strip, on the other hand, were not affected by this difficulty which has now been corrected). For this reason, the results in Table 2.7 and Figs. 2.14 through 2.18 may be regarded as a conservative indication of the power of the iterative method.

Figs. 2.14 through 2.18 fully confirm the existence of the pinch effect of absolute control first suggested by the results of the 25-photo simulations. They also provide some insight into the possible reason for the sudden improvement in convergence which is realized once a certain level of control is established. All simulations performed so far suggest that error in truncation of the iterative process for the minimally controlled strip has a natural fundamental spatial frequency of about one cycle per 12 photos. Therefore, the pinch effect exerted by control introduced at any multiple of the half cycle (6 photos) has a tendency to be in phase with this fundamental spatial frequency and hence does not exert nearly as strong an influence on convergence as control deliberately distributed to be out of phase with the fundamental frequency. By this reasoning, control introduced at the quarter cycle mark (i.e., centered on every third photo) should be especially effective in accelerating convergence. Fresh control introduced at the center of every fourth to fifth photo would likewise significantly disturb the natural frequency of the system and should therefore also exert a marked influence on rate of convergence. Clearly the topic of optimal distribution of limited absolute control is one warranting further investigation in future studies. Here, a power spectrum and autocorrelation analysis of the truncation error of the iterative process as applied to extremely long strips (at least 150 photos) would be of particular value.

Perhaps the most important single finding of the 41-photo simulation is that once a certain minimal level of well-distributed control is attained the convergence of the iterative process is greatly improved. This minimal level would appear to entail the introduction of fresh control on at least every fifth photo.

2.13 SIMULATION OF 3x5 BLOCKS

Because of the success of the iterative approach in applications to photogrammetric strips, we proceeded to implement the approach for photogrammetric blocks. This necessitated the development of a more complex collapsing algorithm and development of a more comprehensive computer program. The resulting IBM 7094 program was tested on the pair of simulated 3x5 blocks pictured in Figs. 2.19a and 2.19b. The block with the greater level of absolute control (Fig. 2.19a) was reduced first. The cutoff level for iterations was set at 200 iterations or an rms error of 0.5 microns, whichever came first. The rms error was set to be computed every 50 iterations. As it turned out the solution converged to 0.16 microns by the end of the first 50 iterations. Hence no intermediate readout was obtained for this case. The errors in the X and Y coordinates of the control points were suppressed to less than 0.2 ft. at 50 iterations. The errors in the Z coordinates, on the other hand, were, in some instances, appreciably larger, growing to as much as one foot. The time required for the solution (50 iterations) was under one minute.

Because the extraordinarily rapid rate of convergence experienced with the initial 3x5 block had not been anticipated, details on the nature of the convergence were not obtained. To remedy this, the second block (Fig. 2.19b) was generated with a lesser number (four) absolute control points and results were read out every 10 iterations for a total of 120 iterations. The rms errors of the residuals of the plate coordinates listed in Table 2.8 would seem to indicate that extremely rapid convergence was obtained. On the other hand, the errors in the elements of orientation (Table 2.9) and the coordinates of control (Table 2.10), while generally acceptably small by normal standards, are quite large in some

● Partially Absolute in Z

○ Relative

▲ Absolute

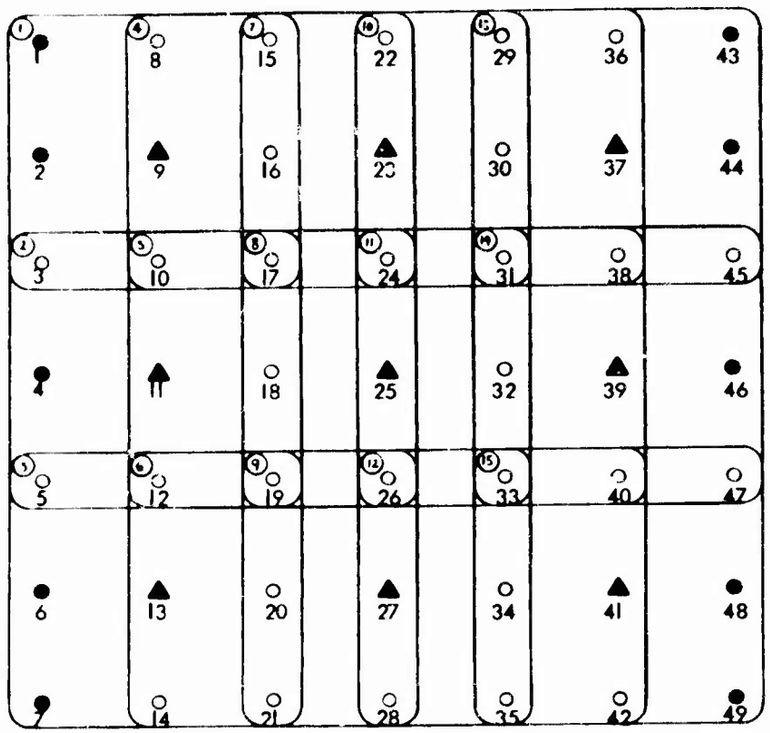

Figure 2.19a. Illustroting 3x5 block employed in numerical simulations (case of 9 absolute control points).

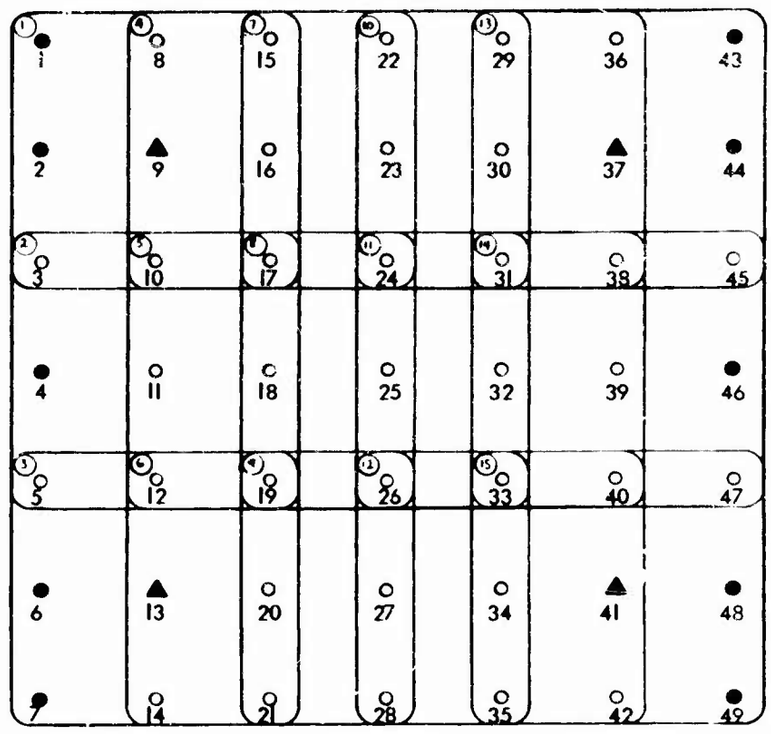

Figure 2.19b. Illustrating 3x5 black emplayed in numerical simulations (case of 4 absolute control points).

Number of Iterations	RMS Error (Microns)
0	155.0
10	2.7
20	1.1
30	.70
40	.49
50	.37
60	.29
70	.24
80	.20
90	.17
100	.14
110	.13
120	.11

Table 2.8. Convergence of iterative solution of 3x5 block with four absolute control points.

Photo Number	$\Delta\Phi$ (sec)	$\Delta\omega$ (sec)	$\Delta\kappa$ (sec)	ΔX^c (ft)	ΔY^c (ft)	ΔZ^c (ft)
1	- 1.1	1.4	6.4	.35	- .26	- .06
2	-11.0	1.6	4.9	.39	-2.40	-1.81
3	23.3	1.6	6.0	.36	5.65	- .02
4	- .9	.9	6.0	.20	-0.12	- .19
5	-11.3	1.1	5.4	.28	-2.55	2.01
6	23.5	1.1	5.8	.29	5.74	- .20
7	- 1.0	.1	5.6	.05	- .11	- .23
8	-11.4	.1	5.6	.04	-2.55	-2.05
9	23.5	.2	5.6	.07	5.76	- .29
10	- .9	- .7	5.2	-.14	- .13	- .21
11	-11.5	- .7	5.8	-.15	-2.57	-2.03
12	23.5	- .8	5.4	-.16	5.76	- .24
13	- 1.0	-1.3	4.8	-.30	- .24	- .10
14	-11.3	-1.2	6.3	-.27	-2.43	-1.89
15	23.2	-1.1	5.0	-.23	5.63	- .12

Table 2.9. Errors in elements of orientation after 120 iterations of solution of normal equations of simulated 3x5 block having four absolute control points.

	POINT NO.	ΔX(ft.)	ΔY(ft.)	ΔZ(ft.)
Column 1	1	-.31	.10	.00
	2	-.11	-.12	.00
	3	.35	.12	.43
	4	.96	.37	.00
	5	-.29	.15	-3.50
	6	-.16	-.06	.00
	7	-2.13	-2.24	.00
Column 2	8	.12	.06	.02
	9	.00	.10	.00
	10	.13	.12	.00
	11	.00	.02	-1.82
	12	-.10	.14	-3.50
	13	.00	.00	.00
	14	.05	.02	3.39
Column 3	15	-.06	.19	-.20
	16	.00	.11	-.26
	17	.05	.14	-.30
	18	.02	.18	-2.03
	19	-.02	.13	-3.75
	20	.00	.06	-.30
	21	.03	.06	3.18
Column 4	22	.01	.23	-.30
	23	.00	.01	-.04
	24	.01	.16	-.38
	25	.00	.02	-2.12
	26	.03	.13	-3.84
	27	.00	.00	-.38
	28	.03	.08	3.09
Column 5	29	.08	.17	-.20
	30	.03	.11	-.26
	31	-.03	.15	-.30
	32	.02	.20	-2.05
	33	.06	.14	-3.79
	34	.03	.07	-.32
	35	.00	.08	3.15
Column 6	36	.13	.06	-.03
	37	.00	.00	.00
	38	-.11	.14	-.02
	39	.00	.28	-1.92
	40	.14	.16	-3.74
	41	.00	.00	.00
	42	-.05	.09	3.40
Column 7	43	.28	.03	.00
	44	.07	-.12	.00
	45	-.05	.14	.37
	46	-1.01	.40	.00
	47	.36	.16	-3.75
	48	.06	-.08	.00
	49	2.01	-2.14	.00

Table 2.10. Errors in coordinates of control points after 120 iterations of solution of normal equations generated by simulated 3x5 block.

instances (e.g., a value of almost minus four feet for ΔZ of point 26). Such errors are seemingly inconsistent with the extremely low rms error of 0.11μ attained at 120 iterations. The explanation, we believe, lies in an inherent instability of the system of normal equations. To appreciate this, one should contemplate Fig. 2.19b. Taken by themselves the three horizontal strips forming the block are individually indeterminate. The first and third strips are indeterminate in tip (Φ), for the entire model can rotate about the line joining the two absolute control points in each of these strips. The middle strip is, of course, completely indeterminate because it contains no absolute control. By virtue of relative control in the side overlaps, determinacy is achieved when the three strips are treated as an integral block. However, there is a basic weakness of the linkage between the first and third strips, for closures of rays to the points in the side overlaps are not strongly affected by small biases in the tip angles of strips 1 and 3. Indeed, if the control points in the side overlaps were measured only on those pairs of photos having the same Y coordinates as the control points themselves, the block would degenerate to indeterminacy, for intersection of rays in the side overlap would then be perfectly preserved under any Φ rotation whatever of strips 1 and 3. The general tendency towards instability of the particular block under discussion would be strongly damped, we believe, if a single point in each of the side overlaps was an absolute control point. A particularly good choice would be points 24 and 26 of Fig. 2.19b.

The order of the normal equations generated by the 3x5 block is 237x237. The form of the normal equations employed in the simulation is indicated in Fig. 2.20. For whatever academic interest they may hold, we have presented in Figs. 2.21 and 2.22 two intertwined forms of the normal equations for the 3x5 block. These were developed before the theoretical shortcomings of the concept of intertwining had been appreciated.

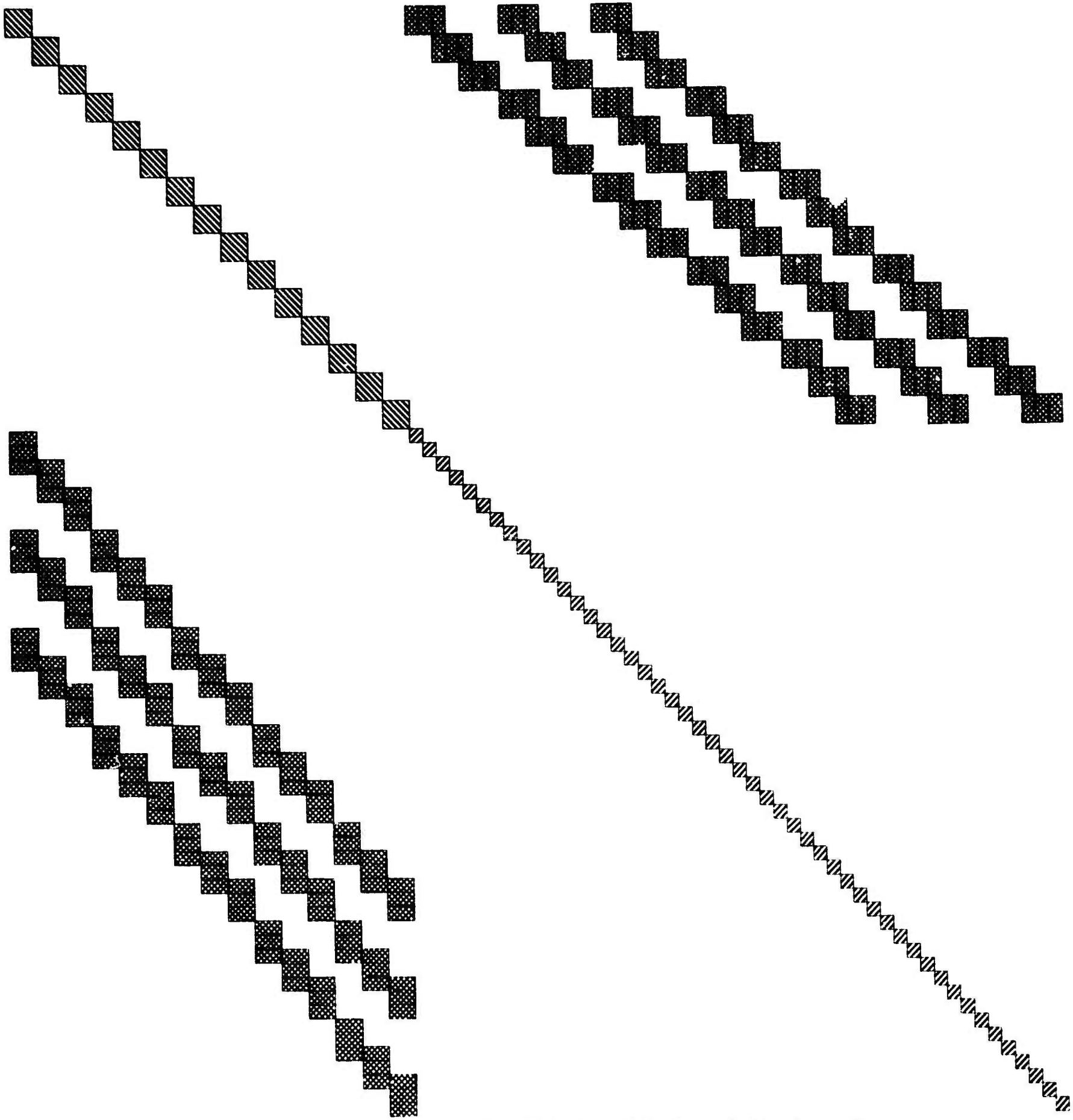

Figure 2.20a. Form of normal equations employed in numerical simulation of iterative solution of normal equations of 3x5 block.

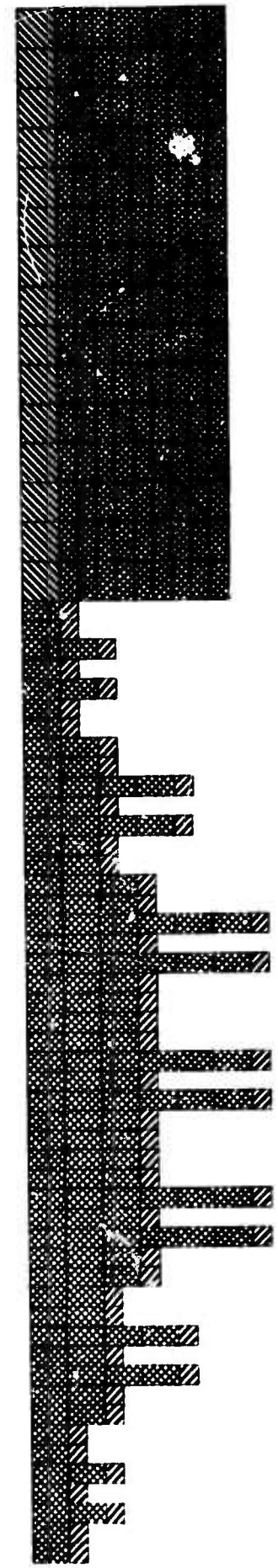

Figure 2.20b. Collapsed form of coefficient matrix of Fig. 2.20a.

Figure 2.21a. Illustrating one possible intertwined form of general normal equations for 3x5 block employed in numerical simulations.

Figure 2.21b. Collapsed form of coefficient matrix of Fig. 2.21a.

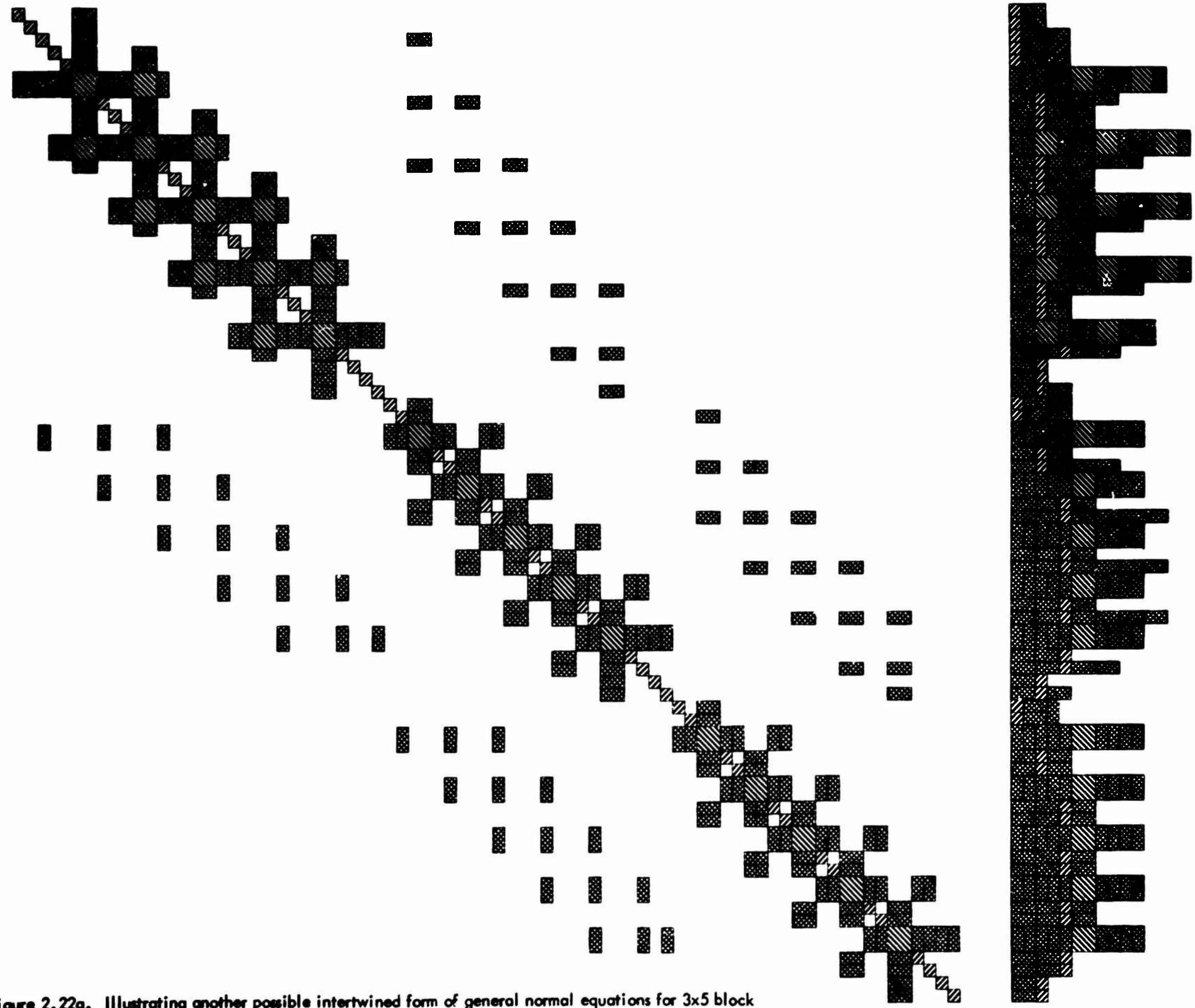

Figure 2.22a. Illustrating another possible intertwined form of general normal equations for 3x5 block employed in numerical simulations

Figure 2.22b. Collapsed form of coefficient matrix of Fig. 2.22a.

Our limited simulations of photogrammetric blocks indicate that the rate of convergence of the iterative solution is several times faster for a compact block than for a strip of comparable number of photos and level of control. Thus the iterative approach is even more attractive for large blocks than for long strips.

Unfortunately, time did not permit a more extensive investigation of the block within the framework of the present study. This will be remedied in future work. Our IBM 7094 routine for block adjustment is designed to handle in core any block of dimensions of n photos by p photos where $nxp \leqq 45$ for $n, p \geqq 2$. When buffering techniques are implemented as outlined in Subsection 2.15, it will be possible to adjust blocks of virtually unlimited dimensions.

2.14 ADJUSTMENT OF 23-PHOTO STRIP OF ACTUAL PHOTOGRAPHY

The various routines developed during the course of the investigation were designed expressly for simulated data and were intended primarily as tools for analysis and studies of feasibility of iterative solutions of the normal equations arising from the adjustment of large photogrammetric nets. In order to process real data a number of auxiliary routines had to be written, most notable of which was a routine for cantilever extension designed to obtain sharp initial approximations for elements of orientation and coordinates of control and also to pre-edit the observational material. With such auxiliary routines and with appropriate modifications of the routines for simulation we were able to process real data in a rather awkward fashion. As in our simulations, an IBM 1620 computer was employed for all preliminary reductions of real data including the preliminary cantilever extension and the formation of the collapsed system of normal equations. The solution of the normal equations was accomplished on an IBM 7094 computer.

The photography employed in our study was taken over the Annex to the Phoenix test range and was supplied to us by Army Map Service through RADC. The photography was supplied as diapositive plates and was generally of very good quality. Flying height was nominally 10,000 feet above the average terrain. The aerial camera employed a calibrated 6 inch Planigon lens; the photo format was 9x9 inches. A layout of the strip and its absolute control is provided in Fig. 2.23. A total of 24 absolute control points in 6 groups of 3 were included in the strip. Unfortunately, practically all of this control fell outside of triple overlap areas and thus could not be accommodated by our adaptation of the simulation routines. Because of this shortcoming of the routine, we elected to adjust the strip with a minimal array of four absolute control points. These consisted of three points across the center of Photo 1 (XY-3, XY-4, XY-5 of Fig. 2.23) and a single point near the center of Photo 4 (ZB-4 of Fig. 2.23). The images of these points were of excellent quality. (The first three were signalized by special ground targets.) A nine point pattern of relative control was selected such that each point lay in a triple overlap area (except at the ends of the strip). The plates were measured on our Mann 422 G comparator which had been calibrated to one micron. The plate readings were referred to the calibrated principal point and were corrected for distortion. The calibrated principal distance was altered by a precalculated amount in order to compensate for atmospheric refraction (compensation for refraction in this manner is admissible for nearly vertical photography over all but very rugged terrain).

The output of a special, analytical least squares cantilever extension operating on single pairs of photos at a time served as initial approximations for the linearization of the observational equations for the rigorous, simultaneous adjustment of the strip. The iterative solution was set to compute the mean error of the plate residuals every fifth iteration and to stop when the difference between successive mean errors was less than 0.01 microns or when a maximum of 250 iterations was reached. As can be seen from Table 2.11, the criterion

Number of Iterations	Mean Error (Microns)	Difference (Microns)
0	21.57	11.96
1	9.61	.70
2	8.91	.41
3	8.50	.30
4	8.20	.21
5	7.99	.88
10	7.11	.12
15	6.99	.027
20	6.963	.009
25	6.954	

Table 2.11. Successive mean errors of plate coordinate residuals from iterative solution of normal equations arising from adjustment of 23-photo strip of actual photography.

for convergence was satisfied by only 25 iterations, a total computing time of less than 40 seconds for the effective solution of a system of equations of order 363x363. We attribute this remarkably rapid convergence to the excellent approximations obtained from the preliminary cantilever extension.

The final mean error of 6.96μ is a substantial improvement over the 21.57μ resulting from the preliminary cantilever extension. The individual residuals for each point on each photo are provided in Table 2.12. These are seen to be highly random throughout the strip. From the standpoint of internal consistency the results of the adjustment are most satisfactory.

Despite the substantial improvement in the mean error, the adjusted values of the relative control points generally differed from the cantilever approximations by less than a foot with only a few differing by as much as 2.5 feet. The largest adjustment to the angular elements of orientation was 40 seconds of arc and most were well under 20 seconds of arc; the largest displacement in the positions of the

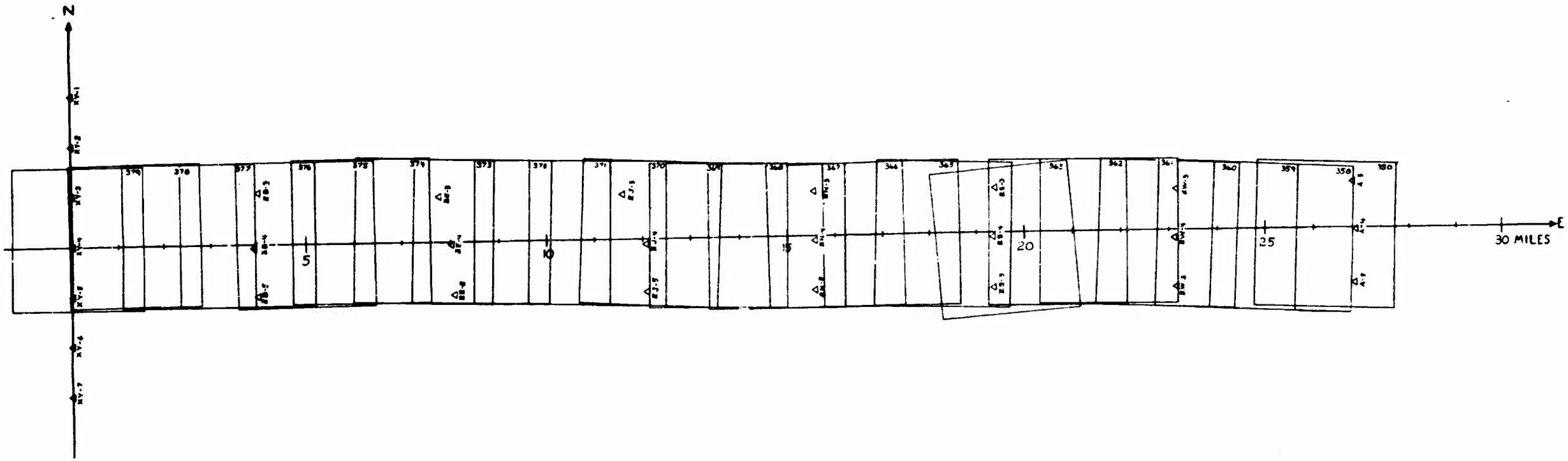

Figure 2.23. Layout of 23-photo strip of actual photography reduced by methods developed in present study.

Photo No.	1		2		3		4		5		6		7		8		9		10		11		12		13		14		15		16		17		18		19		20		21		22		23	
Residuals	x	y	x	y	x	y	x	y	x	y	x	y	x	y	x	y	x	y	x	y	x	y	x	y	x	y	x	y	x	y	x	y	x	y	x	y	x	y	x	y	x	y	x	y
Point No.																																														
1	6.4μ	4.5μ	10.4μ	-8.5μ																																										
2	-3.4	-2.6	-15.3	-7.5																																										
3*	3.6	4.0	3.8	0.9																																										
4	-2.4	-2.8	4.8	1.8																																										
5	0.5	-1.6	-1.0	-2.8																																										
6	1.4	-2.2	-3.8	1.9																																										
7			1.3	3.4	-2.4	-2.3	1.2μ	-1.6μ																																					
8			-1.1	0.4	2.3	-0.8	-1.1	0.4																																					
9			-0.2	2.1	0.3	-1.2	-0.3	-1.0	-0.4μ	-0.1μ																																			
10					-0.3	-2.7	0.9	2.8	2.8	-2.8																																			
11					2.4	4.0	-4.7	0.7	-1.8	0.6																																			
12					-2.0	-1.7	3.7	1.0	1.7	-1.0	-1.4μ	1.6μ																																	
13							-0.8	-0.5	-3.1	3.7	1.6	-1.1																																	
14							1.6	-2.5	0.8	-1.2	-0.4	1.2																																	
15							-0.5	0.2	0.9	2.4	-1.8	-3.9	1.4μ	-1.6μ																															
16									-0.8	-2.6	1.6	4.5	-0.7	1.7																															
17									-0.1	1.6	0.3	-3.1	-0.1	1.7																															
18											-2.8	0.2	-4.6	8.7	2.3μ	-4.9μ																													
19											2.4	0.5	5.5	-8.8	-2.5	8.7																													
20											0.4	0.4	-0.2	5.5	0.1	-5.8																													
21											0.6	0.6	-4.0	-4.0	4.1	9.0																													
22													-1.9	1.2	4.0	-13.3	-1.8μ	-4.7μ																									
23													-2.8	-3.4	-7.3	6.4	-1.7	12.3																									
24													3.8		-2.3	0.9	3.5	-2.9																									
25															2.6	2.5	4.8	-1.3	-2.2μ	0.4μ																							
26															-0.3	1.3	-4.9	-1.2	2.4	-1.0																							
27																	0.6	-2.6	-0.5	1.5																							
28																	0.1	4.2	0.2	-2.6	-0.1μ	-1.5μ																					
29																	-0.7	-5.9	1.3	2.7	-0.6	3.2																					
30																	0.6	3.0	-1.4	-2.8	0.5	-0.1																					
31																			1.4	-0.5	-2.7	-1.3	1.4μ	1.7μ																			
32																			-0.7	2.9	1.4	1.0	-0.8	-3.8																			
33																			-0.6	-0.4	0.9	-1.2	-0.6	1.5																			
34																					1.3	-0.5	-2.7	-0.5	1.4μ	0.8μ																	
35																					-0.1	0.6	-0.1	-2.1	0.0	1.4																	
36																					-1.2	-0.4	2.2	-0.4	-1.2	0.7																	
37																							3.8	-2.3	-7.8	4.0	3.9μ	-2.3μ															
38																							-2.6	8.8	5.2	-5.0	-2.7	-3.8															
39																							-1.1	-3.3	2.0	8.1	-1.0	-4.9															
40																									-2.2	-5.4	4.0	4.5	-1.9μ	0.6μ													
41																									-1.4	-0.3	2.4	-3.3	-1.2	3.5													
42																									3.4	-5.3	-6.8	5.0	3.4	0.2													
43																											1.0	3.9	-2.0	-4.7	1.0μ	0.7μ											
44																											-1.9	-3.4	3.6	5.0	-1.8	-1.4											
45																											1.0	4.1	-1.8	-4.7	0.9	0.6											
46																													0.0	-0.1	-0.2	0.1	0.1μ	0.0μ							
47																													0.8	-0.4	-1.5	0.7	0.7	-0.2							
48																													-0.9	0.3	1.7	-0.4	-1.0	0.0							
49																															0.0	-1.1	-0.3	0.5	0.1μ	0.0μ					
50																															1.2	1.9	-2.5	0.0	1.1	-1.8					
51																															-1.4	-1.1	2.5	0.5	-1.4	0.5					
52																																	1.9	-0.6	-3.8	2.7	1.7μ	-1.9μ			
53																																	-2.5	1.0	5.3	-1.1	-2.6	0.2			
54																																	0.6	-1.0	-1.2	3.1	0.4	-2.2			
55																																			-1.7	-0.7	3.6	0.7	-1.8μ	0.0μ	
56																																			1.0	-2.6	-1.6	-0.9	0.8	3.6	
57																																			1.2	-0.7	-2.0	1.1	0.9	-0.5	
58																																					1.7	0.5	-3.4	-1.9	
59																																					-1.2	2.7	2.0	0.8	
60																																					-0.5	-0.1	1.1	-1.0	
61																																							-0.3	-0.8	
62																																							1.8	0.5	
63																																							-1.5	-0.9	
64																																									1.4	-2.0	
65																																									-0.4	5.8	
66																																									-1.0	-2.6	
67																																											
68																																											
69																																											

* Absolute Control Point

Table 2.12. Plate coordinate residuals resulting from adjustment of 23-photo strip of actual photography. Mean error = 6.96μ.

exposure stations was nearly 3 feet. In view of this, the cantilever extension in its own right provides a quite satisfactory result. We would not expect such good agreement to exist, however, if a liberal sprinkling of absolute control were carried in the simultaneous adjustment of the strip.

Needless to say, much more extensive experience with real data is required before the full potential of the photogrammetric solution developed in this report can be definitively evaluated. In order to handle real data in volume, it will be necessary to develop programs expressly designed for large scale production. This is an entirely straightforward task and is one fully justified by the results obtained in the present study.

2.15 COMPUTER TECHNIQUES

The maximum coefficient matrix generated during the course of our simulations is the 633-order matrix associated with the normal equations for the 41-photo strip. This constitutes the largest coefficient matrix which, together with the iterative program, can be stored in the main memory of the IBM 7094 computer. However, this by no means represents the limit for the theoretical capability of the SOR technique, nor is it a limit for the order of the normal equations which can be solved using somewhat more advanced programming techniques that are currently available. In fact, on o computer with a 32K main memory it would be possible to generate and solve systems of normal equations of order approximately 10,000 with very little loss of efficiency. Since further research in this field anticipates the use of the CDC 1604 computer at RADC, we will limit our discussion of advanced techniques to software which is currently available for this machine.

The almost unlimited capability of the iterative program can be realized through the use of the most advanced version of FORTRAN, FORTRAN-63, available for the 1604 computer in conjunction with auxiliary storage devices

such as high-speed, high-density magnetic tapes or a magnetic disk or drum, and with the buffering facility that the 1604 possesses for the transfer of data from an auxiliary storage unit to the main memory of the computer.

Instead of storing the entire coefficient matrix of the normal equations in the main memory of the computer, the data would be stored in binary form on an auxiliary storage unit (storage of the data in binary form permits a higher rate of data transfer than if the information were stored in the standard BCD form). The only information which at all times remains available to the iterative program in the main memory of the 1604 is the constant vector b and the iterative vector $X^{(m)}$ (as in (9)). To initiate the iterative process, the first row of blocks of the coefficient matrix, consisting of the 6x6 $\hat{N}$ submatrix for the first photograph and the nine 6x3 $\bar{N}$ submatrices associated with it, are transferred into the main memory of the computer from the auxiliary storage unit, and then the first block of the new iterative vector is computed in standard fashion. While this calculation is being performed the second row of blocks of the coefficient matrix is buffered into memory by means of the BUFFER IN statement available in FORTRAN-63. The advantage of the BUFFER IN statement as the instrument of data transfer from auxiliary storage to main memory is that as soon as the transfer has been initiated, control is returned to the iterative program. This then permits the computation of the first block of the iterative vector and the transfer of the second block row of data from auxiliary storage to main memory to occur simultaneously. The second block row of data is then used to compute the second block of the iterative vector while the third block row of the coefficient matrix is being buffered into the main memory. Thus, through successive applications of the above procedure it is possible to compute the entire iterative vector even though at any one time only two block rows of the coefficient matrix are in the main memory of the computer.

The only possibly significant loss of time through the implementation of this procedure would occur if magnetic tape were used as the means of auxiliary storage. In this case, a delay would occur at the end of each iteration to permit

the tape containing the coefficient matrix to be rewound. Of course, this problem would not present itself if a random access device were available for use as auxiliary storage of the coefficient matrix.

The delay caused by the rewind of the data tape could be eliminated if sufficient tape drives were available to permit the coefficient matrix to be stored on two or more magnetic tapes. In this case, at the completion of one iteration an alternate tape would be used for the computation of the succeeding iteration while the original tape were being rewound. A more sophisticated procedure could be put into use should the Block Successive Symmetric Over Relaxation iterative technique prove feasible. As previously stated in Subsection 2.06, this method alternates a forward and a backward iteration which thus eliminates the tape rewind completely since at the end of each forward iteration the coefficient matrix must be entered into memory in a reverse order to perform the backward iteration. In fact, should the computer be equipped with the CDC 607 tape drive, which has a backward read capability, all superfluous motion of the tape would be eliminated, for tape motion would occur only during the actual process of data transfer.

From the foregoing it is clear that through the use of optimal buffering techniques, essentially no time need be wasted because of limitations of core memory. We believe that a comprehensive reduction of a general photogrammetric block leading to normal equations involving as many as 10,000 unknowns could readily be accommodated by a computer having an internal memory equivalent to 32K words, preferably of 36 binary bits or greater (total word length for the CDC 1604 is 48 bits).

REFERENCES

Arms, R.J., Gates, L.D., Zondek, B., "A Method of Block Iteration", J. Soc. Indust. Appl. Math. 4, 220-229 (1956).

Brown, D.C., "A Matrix Treatment of the General Problem of Least Squares Considering Correlated Observations", Ballistic Research Laboratories Report No. 937 (May 1955).

Brown, D.C., "A Solution to the General Problem of Multiple Station Analytical Stereotriangulation", RCA Data Reduction Technical Report No. 43 (February 1958).

Brown, D.C., "Photogrammetric Flare Triangulation - A New Geodetic Tool", RCA Data Reduction Technical Report No. 46 (December 1958).

Brown, D.C., "Results of Geodetic Photogrammetry I", RCA Data Reduction Technical Report No. 54 (October 1959).

Brown, D.C., "Results in Geodetic Photogrammetry II", RCA Data Reduction Technical Report No. 65 (September 1960).

Brown, D.C., "Introduction to Orbital Constraints Into Adjustment of Satellite Photogrammetric Net", Unpublished Report (1960).

Brown, D.C., Davis, R.G., Johnson, F.C., "Photogrammetric Mathematical Targeting Research (Interim Report) Rome Air Development Center Report No. RADC-TR-63-476 (August 1963).

Case, James B., "The Utilization of Constraints in Analytical Photogrammetry", Photogrammetric Engineering, Vol. XXVII, No. 5 (December 1961).

Dodge, H.F., "Analytical Aerotriangulation by the Direct Geodetic Restraint Method", Photogrammetric Engineering, Vol. XXV, No. 4 (September 1959).

Dowdy, J.M., McClure, K.W., "Advanced Analytical Triangulation Techniques", Rome Air Development Center TR 62-253 (July 1962).

Doyle, Frederick J., "The Historical Development of Analytical Photogrammetry", Photogrammetric Engineering, Vol. XXX, No. 2, 259-265 (March 1964).

Ehrlich, L.W., "The Block Symmetric Successive Overrelaxation Method", unpublished Ph.D. dissertation, The University of Texas, Austin, Texas (1963).

Elassal, Atef A., "Analytical Aerial Triangulation through Simultaneous Relative Orientation of Multiple Cameras", University of Illinois Ph.D. Dissertation (1963).

Faddeeva, V.N., "Computational Methods of Linear Algebra", Dover Publications, Inc., New York 14, New York (1959).

Harris, W.D., Tewinkel, G.C., Whitten, C.A., "Analytic Aerotriangulation", Technical Bulletin No. 21, U.S. Coast and Geodetic Survey (July 1962).

Jacobi, C.G.J., "Uber eine Neue Auflosungsart der bei der Methode der kleinsten Quadrate vorkommenden linearen Gleichungen", Asts. Nachr. 22, No. 523, 297-306 (1845).

Liusternik, L.A., "Remarks on the Numerical Solution of Boundary Value Problems for Laplace's Equation and the Calculation of Characteristic Values by the Method of Nets", (Russian) Trudy Martem. Inst. Im., V.A. Steklova, 20: 49-64 (1947).

Matos, Robert A., "Analytical Triangulation with Small or Large Computers" Photogrammetric Engineering, Vol. XXIX, No. 2 (March 1963).

Mikhail, Edward M., "Use of Triplets for Analytical Aerotriangulation", Photogrammetric Engineering, Vol. XXVIII, No. 4, 625-632 (September 1962).

Mikhail, Edward M., "Use of Two-Directional Triplets in a Sub-Block Approach for Analytical Aerotriangulation" Photogrammetric Engineering, Vol. XXIX No. 6, 1014-1024 (November 1963).

Schmid, H., "A General Analytical Solution to Problem of Photogrammetry", Ballistic Research Laboratories Report No. 1065 (July 1959).

Schut, G.H., "Development of Programs for Strip and Block Adjustment at The National Research Council of Canada", Photogrammetric Engineering, Vol. XXX, No. 2, 283-291 (March 1964).

Seidel, L., "Uber ein Verfahren die Gleichungen, auf Welche die Methode der kleinsten Quadrate fuhrt, sowie lineare Gleichungen uberhaupt, durch successive Annaherung dufzulosen", Abhandl. bayer, Akad. Wiss., Math-physik. Kl., 11: 81-108 (1874).

Todd, J., "Survey of Numerical Analysis", McGraw-Hill, New York, New York (1962).

Varga, R.S., "Matrix Iterative Analysis", Prentice-Hall, Inc., Englewood Cliffs, New Jersey (1962).

Young, D.M., "Iterative Methods for Solving Partial Differential Equations for Elliptic Type", Trans. Amer. Math. Soc., 76, 92-111 (1954).

Young, D.M., "On the Numerical Solution of Partial Differential Equations by Finite Difference Methods", Notes of 20 lectures at the National Science of Advanced Topics in the Computer Sciences, University of North Carolina (1962).

UNCLASSIFIED

Security Classification

DOCUMENT CONTROL DATA - R&D

(Security classification of title, body of abstract and indexing annotation must be entered when the overall report is classified)

1. ORIGINATING ACTIVITY *(Corporate author)*

Geo Space Corporation
Milbourne, Fla

2a. REPORT SECURITY CLASSIFICATION

UNCLASSIFIED

2b GROUP

N/A

3 REPORT TITLE

The Practical and Rigorous Adjustment of Large Photogrammetric Nets

4. DESCRIPTIVE NOTES *(Type of report and inclusive dates)*

None

5. AUTHOR(S) *(Last name, first name, initial)*

Duane C. Brown
Ronald G. Davis
Frederick C. Johnson

6. REPORT DATE	7a. TOTAL NO. OF PAGES	7b. NO. OF REFS
October 1964	157	28

8a. CONTRACT OR GRANT NO.	9a. ORIGINATOR'S REPORT NUMBER(S)
AF30(602)-3007	RADC TDR-64-353
b. PROJECT NO 5569	
c.	9b. OTHER REPORT NO(S) *(Any other numbers that may be assigned this report)* N/A
d. 556902 (Task No)	

10. AVAILABILITY/LIMITATION NOTICES

Qualified requestors may obtain copies of this report from DDC.
Release to OTS is authorized.

11. SUPPLEMENTARY NOTES	12. SPONSORING MILITARY ACTIVITY
None	RADC

13 ABSTRACT

The problem of the rigorous simultaneous adjustment of large photogrammetric blocks is reviewed and extensions to an earlier theory are developed. Various matrix iterative approaches to the solution of the very large systems of normal equations characteristic of sizeable photogrammetric nets are investigated. The Method of Block Successive Over Relazation is found to yield a practical and most satisfactory solution to this problem. Results of an extensive series of numerical simulations are reported. The successful application of the approach to a 23-photo strip of actual photography provides final confirmation of the validity and effectiveness of the solution.

DD FORM 1 JAN 64 1473

UNCLASSIFIED

Security Classification

UNCALSSIFIED

Security Classification

14 KEY WORDS	LINK A		LINK B		LINK C	
	ROLE	WT	ROLE	WT	ROLE	WT
a. Contrd Extension						
b. Adjustment of Control Extension						
c. Mathematical Adjustment of Photogrammetric Control						
d. Photogrammetric Analytical Triangulation						

INSTRUCTIONS

1. **ORIGINATING ACTIVITY**: Enter the name and address of the contractor, subcontractor, grantee, Department of Defense activity or other organization *(corporate author)* issuing the report.

2a. **REPORT SECURITY CLASSIFICATION**: Enter the overall security classification of the report. Indicate whether "Restricted Data" is included. Marking is to be in accordance with appropriate security regulations.

2b. **GROUP**: Automatic downgrading is specified in DoD Directive 5200.10 and Armed Forces Industrial Manual. Enter the group number. Also, when applicable, show that optional markings have been used for Group 3 and Group 4 as authorized.

3. **REPORT TITLE**: Enter the complete report title in all capital letters. Titles in all cases should be unclassified. If a meaningful title cannot be selected without classification, show title classification in all capitals in parenthesis immediately following the title.

4. **DESCRIPTIVE NOTES**: If appropriate, enter the type of report, e.g., interim, progress, summary, annual, or final. Give the inclusive dates when a specific reporting period is covered.

5. **AUTHOR(S)**: Enter the name(s) of author(s) as shown on or in the report. Enter last name, first name, middle initial. If military, show rank and branch of service. The name of the principal author is an absolute minimum requirement.

6. **REPORT DATE**: Enter the date of the report as day, month, year, or month, year. If more than one date appears on the report, use date of publication.

7a. **TOTAL NUMBER OF PAGES**: The total page count should follow normal pagination procedures, i.e., enter the number of pages containing information.

7b. **NUMBER OF REFERENCES**: Enter the total number of references cited in the report.

8a. **CONTRACT OR GRANT NUMBER**: If appropriate, enter the applicable number of the contract or grant under which the report was written.

8b, 8c, & 8d. **PROJECT NUMBER**: Enter the appropriate military department identification, such as project number, subproject number, system numbers, task number, etc.

9a. **ORIGINATOR'S REPORT NUMBER(S)**: Enter the official report number by which the document will be identified and controlled by the originating activity. This number must be unique to this report.

9b. **OTHER REPORT NUMBER(S)**: If the report has been assigned any other report numbers *(either by the originator or by the sponsor)*, also enter this number(s).

10. **AVAILABILITY/LIMITATION NOTICES**: Enter any limitations on further dissemination of the report, other than those imposed by security classification, using standard statements such as:

(1) "Qualified requesters may obtain copies of this report from DDC."

(2) "Foreign announcement and dissemination of this report by DDC is not authorized."

(3) "U. S. Government agencies may obtain copies of this report directly from DDC. Other qualified DDC users shall request through

_____."

(4) "U. S. military agencies may obtain copies of this report directly from DDC. Other qualified users shall request through

_____."

(5) "All distribution of this report is controlled. Qualified DDC users shall request through

_____."

If the report has been furnished to the Office of Technical Services, Department of Commerce, for sale to the public, indicate this fact and enter the price, if known.

11. **SUPPLEMENTARY NOTES**: Use for additional explanatory notes.

12. **SPONSORING MILITARY ACTIVITY**: Enter the name of the departmental project office or laboratory sponsoring *(paying for)* the research and development. Include address.

13. **ABSTRACT**: Enter an abstract giving a brief and factual summary of the document indicative of the report, even though it may also appear elsewhere in the body of the technical report. If additional space is required, a continuation sheet shall be attached.

It is highly desirable that the abstract of classified reports be unclassified. Each paragraph of the abstract shall end with an indication of the military security classification of the information in the paragraph, represented as *(TS)*, *(S)*, *(C)*, or *(U)*.

There is no limitation on the length of the abstract. However, the suggested length is from 150 to 225 words.

14. **KEY WORDS**: Key words are technically meaningful terms or short phrases that characterize a report and may be used as index entries for cataloging the report. Key words must be selected so that no security classification is required. Identifiers, such as equipment model designation, trade name, military project code name, geographic location, may be used as key words but will be followed by an indication of technical context. The assignment of links, rules, and weights is optional.

UNCLASSIFIED

Security Classification